Springer Oceanography

Chongwei Zheng
Chongyin Li
Hailang Wu
Min Wang

21st Century Maritime Silk Road: Construction of Remote Islands and Reefs

Springer

Springer Oceanography

The Springer Oceanography series seeks to publish a broad portfolio of scientific books, aiming at researchers, students, and everyone interested in marine sciences. The series includes peer-reviewed monographs, edited volumes, textbooks, and conference proceedings. It covers the entire area of oceanography including, but not limited to, Coastal Sciences, Biological/Chemical/Geological/Physical Oceanography, Paleoceanography, and related subjects.

More information about this series at http://www.springer.com/series/10175

Chongwei Zheng • Chongyin Li • Hailang Wu • Min Wang

21st Century Maritime Silk Road: Construction of Remote Islands and Reefs

Springer

Chongwei Zheng
College of Meteorology and Oceanography
National University of Defense Technology
Nanjing, China

Hailang Wu
No. 91937 of PLA
Zhoushan, China

Chongyin Li
State Key Laboratory of Numerical Modeling for Atmospheric Sciences and Geophysical Fluid Dynamics (LASG), Institute of Atmospheric Physics, Chinese Academy of Sciences
Beijing, China

Min Wang
College of Meteorology and Oceanography
National University of Defense Technolog
Nanjing, China

ISSN 2365-7677 ISSN 2365-7685 (electronic)
Springer Oceanography
ISBN 978-981-10-8113-2 ISBN 978-981-10-8114-9 (eBook)
https://doi.org/10.1007/978-981-10-8114-9

Library of Congress Control Number: 2018948211

This Springer imprint is published by the registered company Springer Nature Singapore Pte Ltd.
The registered company address is: 152 Beach Road, #21-01/04 Gateway East, Singapore 189721, Singapore

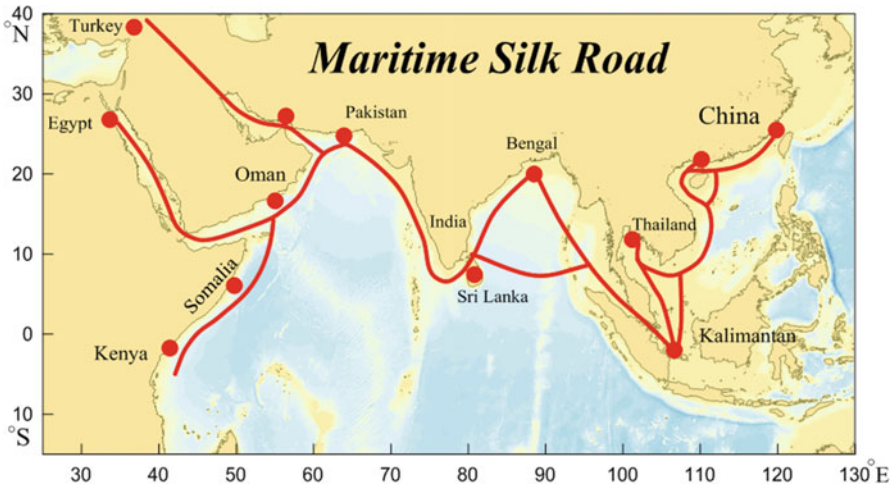

Series Publications on the 21st-Century Maritime Silk Road

(I) 21st Century Maritime Silk Road: A Peaceful Way Forward
(II) 21st Century Maritime Silk Road: Construction of Remote Islands and Reefs
(III) 21st Century Maritime Silk Road: Wave Energy Resource Evaluation
(IV) 21st Century Maritime Silk Road: Wind Energy Resource Evaluation
(V) 21st Century Maritime Silk Road: Location Choice of Marine New Energy
(VI) 21st Century Maritime Silk Road: Long-Term Trends of Oceanic Parameters
(VII) 21st Century Maritime Silk Road: Threat and Characteristics of Swell
(VIII) 21st Century Maritime Silk Road: Early Warning of Wave Disasters

Preface

The Belt and Road Initiative (Silk Road Economic Belt and 21st Century Maritime Silk Road) highlights the continuation theme, peace, and development of China. It brings an important opportunity to both the revival of the Chinese nation and the common prosperity of the human being. At present, comparing with the significant progress that has been made in the Silk Road Economic Belt, the construction of the 21st Century Maritime Silk Road (shorten as "Maritime Silk Road" here after) is relatively lagged behind. The Maritime Silk Road mainly involves the South China Sea and the northern Indian Ocean. The South China Sea is well known as the second Persian Gulf. Meanwhile, the Indian Ocean has always been regarded as the world sea power center and marine lifeline. It is not hard to find the importance of the Maritime Silk Road. However, challenges and opportunities often coexist. The Maritime Silk Road has a long route, covers a wide scope area, and involves multiple nations. It confronted with lots of difficulties such as the complicated marine environment characteristics, weaknesses in infrastructures, difficulty in ocean replenishment, frequent trade friction, differences in the culture, instability of the political situation, continuous security conflicts, and so on. In addition, the scarcity of the ocean data, weak fundamental research, and lack of support of the systematic theory greatly increase the difficulty of the construction of the Maritime Silk Road.

The marine key points that usually based on the important remote islands and reefs are the pivotal support for human society to step into the deep sea. Rational construction of important remote islands and reefs will make positive contribution to cope with the above difficulties that confronted the Maritime Silk Road. A series of remote islands and reefs with stable and efficient function on the South China Sea and the northern Indian Ocean will contribute to enhance the capabilities of ocean-going voyage, integrated supply, ship maintenance, marine observation, humanitarian assistance, medical aid, etc., thus to make the Maritime Silk Road to be the main artery of the international economy and energy. In this book, the necessity and difficulties of the construction of marine key points are firstly presented, such as the rational selection and risk evaluation of the key point, urgent demand of electricity

and fresh water, fragility of the ecological environment, terrible survival and medical condition, complicacy dispute on marine rights and interests, and then corresponding countermeasures are provided.

The remote islands and reefs are usually far from the mainland, which have a particularly urgent demand for electricity and freshwater resources. And this has seriously restricted marine development and utilization activities in the deep sea for a long time. In the era of high electrification, most equipments cannot function or even be paralyzed without electricity. Human beings cannot survive without fresh water. The electricity on the remote islands and reefs usually relies on a diesel that is primarily on shipping supplies, and fresh water also depends primarily on shipping supplies. Obtaining these supplies is especially challenging under bad sea conditions. In addition, the ecosystem of the remote islands and reefs is fragile. The diesel power generation usually results in significant pollution. Once the ecosystem of the remote islands and reefs is damaged, it is difficult to repair. All these difficulties have seriously restricted the economic development in the deep sea. Rational utilizing the clean, renewable, nonpolluting marine new energy (wave energy, offshore wind energy, etc.) to develop wave power generation, offshore wind power generation, and seawater desalination according to local conditions will satisfy the electric energy requirements, to prominently enhance the survival and sustainable capacities of the remote islands and reefs, thus to ensure the healthy development of the Maritime Silk Road. There is an obvious need for "resource evaluation and planning in advance" in energy development. Due to the data scarcity and technical difficulties, the research on the wave energy and offshore wind energy of the South China Sea and the northern Indian Ocean is still scarce until now, especially on the marine key points, which is urgently needed.

The book focuses on coping with the electricity and freshwater shortage of the important remote islands and reefs, thus to provide technical support for the marine key points on the Maritime Silk Road to overcome the energy dilemmas. According to the urgent demand of electricity and fresh water, a systematic evaluation on the wind energy and wave energy of a series of marine key points on the Maritime Silk Road is carried out for the first time at home and abroad. And the Gwadar Port, remote islands and reefs of the South China Sea, etc. are selected as case studies. The wind and wave energy analysis systematically includes the value size of the wind/wave power density, available rate of energy (effective wind speed occurrence and effective wave height occurrence), richness of energy (energy level occurrence), coming direction of energy (co-occurrence of energy direction and power density, shorten as "wind/wave energy rose"), long-term trends of wind/wave energy resources, long-term prediction of energy, etc., thus to provide reference for the choice of power plants location, feasibility verification of wave power generation and wind power generation, daily operation, and long-term plan of wave/wind power generation. Several important marine key points of the Maritime Silk Road are selected as the case study (such as the Gwadar port, a remote island in the South China Sea), to realize the electricity and freshwater self-sufficiency of these marine key points and thus to improve their viability.

Understanding the marine environment characteristics is a prerequisite for the safe and efficient marine construction. For example, a storm surge in the Bay of Bengal in 1970 caused more than 300,000 deaths. A strong wave of about 6 m caused by the storm surge in 1991 in the Chittagong caused about 140, 000 deaths. However, relatively weak basic research and scarce marine data seriously restrict the analysis of marine characteristic of the remote islands and reefs of the Maritime Silk Road and urgently need to be addressed. To promote the safe and efficient implementation of the remote islands and reefs construction, disaster prevention and reduction, prolong the life of the electric generator, and so on, we also analyzed the marine environment of the marine key points on the Maritime Silk Road, systematically including the monthly variation of wind speed and significant wave height, wind class occurrence, wave class occurrence, characteristics of strong wind (co-occurrence of wind speed and wind direction), characteristics of strong wave (co-occurrence of significant wave height and wave direction), extreme wind speed and extreme wave height with different return periods, and long-term trend of wind speed and wave height. In addition, the runway is one of the most important parts of the remote islands and reefs construction. We select a remote island as the assumed object of study to statistically analyze the wind climate characteristics under the demand of runway design, mainly including the wind rose (co-occurrence of wind direction and wind speed), gale occurrence, occurrence of gust wind speed above 10.8 m/s, gust index, and so on, to provide scientific reference for the decision-making of runway design of remote islands and reefs.

The evaluation and utilization of wind/wave energy resources will make contribution to realize the electricity and freshwater self-sufficiency of the important remote islands and reefs; the analysis of marine environment is benefit for the safe and efficient construction of the important remote islands and reefs. We hope the method and scheme formed in this book can be popularized in the construction of remote islands and reefs in global oceans, especially the Maritime Silk Road, to enhance the capability of marine development and utilization.

Nanjing, China — Chongwei Zheng
Beijing, China — Chongyin Li
Zhoushan, China — Hailang Wu
Nanjing, China — Min Wang

Acknowledgments

This work was supported by the Open Research Fund of State Key Laboratory of Estuarine and Coastal Research (Grant No. SKLEC-KF201707), the National Natural Science Foundation of China (No. 41490642, No. 41775165), the Key Laboratory of Renewable Energy, and Chinese Academy of Sciences (No. Y707k31001). All the authors would like to thank ECMWF for providing the ERA-Interim wind and wave data and ERA-40 wave reanalysis and thank the PO.DAAC for providing the cross-calibrated, multi-platform (CCMP) wind data.

Contents

About the Authors

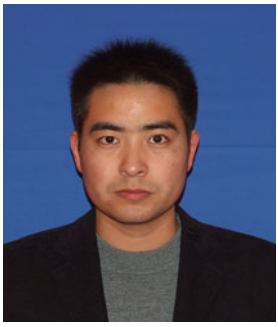

Chongwei Zheng is the creator and organizer of Marine Resources and Environment Research Group on the Maritime Silk Road. His research fields cover major areas in physical oceanography, wind and wave energy resource evaluation, wave climate, and climate change. He has published more than 90 papers in many peer-reviewed journals as the first author, including more than 30 papers indexed by SCI or EI (five papers published in the SCI Top Journals and one paper was listed as the "Essential Science Indicators" highly cited paper), as well as more than 40 papers published in Chinese core periodicals. He has published five books as the first author. He is the invited reviewer of more than 30 high-impact journals.

Chongyin Li is academician of Chinese Academy of Sciences (CAS) and well-known scientist in atmospheric science and climate dynamics. After graduation from the Department of Applied Geophysics, University of Science and Technology of China in 1963, he has been engaged in atmospheric science research all along in the Institute of Atmospheric Physics (IAP), CAS. He was vice chairman of Academic Committee at the IAP, chairman of Dynamical Meteorology Committee, vice president of the Chinese Meteorology Society, and chairman of Chinese Committee of the WCRP. He was member of International Commission for Dynamical Meteorology, member of the CLIVAR Scientific Steering Group, member of Asian-Australian Monsoon Panel, and member of the ICCL. Prof. C. Li has

achieved systematic achievements in the frontier fields of atmospheric science, such as in the dynamics of atmospheric low-frequency oscillation (including MJO) and the ENSO cycle dynamics. Particularly, the CISK wave theory of tropical atmospheric intraseasonal oscillation (MJO) indicated the ENSO is exactly the cycle of subsurface ocean temperature anomalies in the tropical Pacific driven by zonal wind anomalies over the equatorial center-western Pacific, which mainly results from anomalous East Asian winter monsoon.

Hailang Wu born in November 1983, majors in the dynamic analysis on fluid-solid coupling of floating structure. He graduated from PLA University of Science and Technology in June 2006 with a major in physical oceanography. In June 2011, he received the master's degree in physical oceanography. In June 2016, he received the doctor's degree in bridge and tunnel engineering. The academic achievements have been published on high-level journals, including four SCI/EI index and more than six Chinese core papers.

Wang Min graduated in 2005 with a bachelor of automation degree from Northeast Petroleum University and also received the M.S. degree in control theory and control engineering from Hohai University in 2008. She is currently an associate professor and Ph.D. student at National University of Defense Technology. Her research fields cover major areas in remote sensing image processing, physical oceanography, and atmosphere detection. She has published more than 30 papers in many peer-reviewed journals as the first author and authorized more than 20 patents as the first inventor. She has won one award for science and technology at the provincial and ministerial level.

Chapter 1
Necessity, Difficulties and Countermeasures of Remote Islands and Reefs Construction

1.1 Necessity and Function of Marine Key Points

The marine key points that usually based on the important remote islands and reefs are the pivotal support for human society to step into the deep sea. The world sea powers particularly focus on the preset of the key points. Take the United States (US) as an example, the Hawaii Islands which locates on the center of the north Pacific Ocean is an important relay station for the north Pacific strategy of the US; Also, Diego Garcia which locates on the center of the Indian Ocean is forged as the key point of the US on the Indian Ocean, as shown in Fig. 1.1. Similarly, a serial of remote islands and reefs with stable and efficient function on the South China Sea and northern Indian Ocean will make positive contribution to enhance the capabilities of oceangoing voyage, integrated supplies, ship maintenance, marine observation, anti-piracy escort, anti-terrorism cruises, humanitarian assistance, medical aid, etc., to improve the navigation capability, marine construction capability, sea power maintenance capability, etc., thus to make positive contribution to help the Maritime Silk Road become a new link of human friendship and development. At present, there are a lot of discussions about the importance of remote islands and reefs during the construction process of the Maritime Silk Road, however, the real scientific research on solving the key science and technology is rare, which is urgently needed. The following functions of important remote islands and reefs should be researched and evaluated deeply: integrated supplies, ship maintenance, marine observation, humanitarian assistance, maritime search and rescue, medical aid, anti-piracy, etc., as shown in Fig. 1.2.

Integrated Supplies and Ship Maintenance The Maritime Silk Road mainly involves in the South China Sea and the northern Indian Ocean. It has a long route and wide range, so, the ocean supplies is always a difficult problem when the ship is carrying out ocean mission. A serial of important remote islands and reefs with stable and efficient function on the route of the Maritime Silk Road can make positive contribution to navigation, integrated supplies (fresh water, food and other

C. Zheng et al., *21st Century Maritime Silk Road: Construction of Remote Islands and Reefs*, Springer Oceanography, https://doi.org/10.1007/978-981-10-8114-9_1

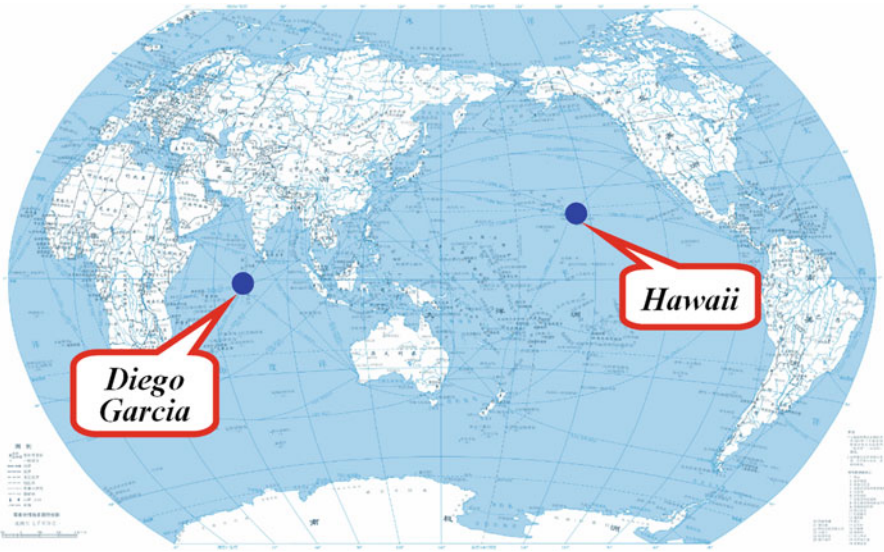

Fig. 1.1 Two typical key points of the United States: Hawaii Island and Diego Garcia. Note: The left point in the Indian Ocean represents the Diego Garcia, the right point in the Pacific Ocean represents the Hawaii. The world map is available at http://www.city8.com/map/1004.html

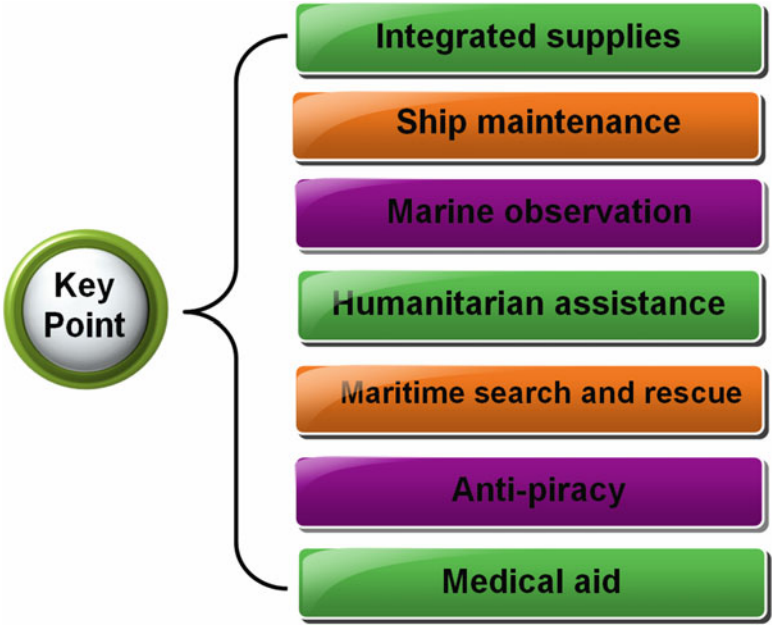

Fig. 1.2 Function prospect of the marine key points

commodity), ship maintenance, marine observation, humanitarian assistance, medical aid, etc. for the cargo ships, thus to enhance the ship's ability of ocean navigation significantly. In return, the oceangoing vessels which usually have a large tonnage, can carry a variety of materials and equipments to support the remote islands and reefs, resulting in a win-win situation, thus to achieve a virtuous circle of mutual assistance for big cargo and important remote islands and reefs. The equipment maintenance of ship is also a difficult problem in the process of ship navigation. If these important remote islands and reefs are equipped with commonly used equipment, parts and given them the function of ship maintenance, they will play a positive and useful contribution.

Humanitarian Assistance and Medical Aid The humanitarian assistance is an important part of the maritime activities. In November 1970, a storm surge occurred in the Bay of Bengal, resulting in more than 300,000 people were killed and more than 1,000,000 people homeless. And the Bay of Bengal is one of the key areas of the Maritime Silk Road. Malaysia Airline 370, many countries have invested a lot of man power, material resources, financial resources, but with little success. If the important remote islands and reefs are existed and equipped with rescue equipments, professional rescue personnel on the Maritime Silk Road, we can deal with the maritime disaster and carry out the humanitarian assistance according to the circumstances in the first place and first time. Meanwhile, combine with ocean monitoring data on these key nodes, the humanitarian assistance is bound to be more effective. In addition, In the process of ocean navigation, the medical aid conditions on the ships are very limited. Allocating some medical staff on the important remote islands and reefs can solve the problem of medical aid.

Marine Monitoring and Observation Based on the important remote islands and reefs, we can establish the land-based and sea-based marine environmental observation station, combining with other observation platform to form the all-weather and stereoscopic observation network to enhance the ability of marine monitoring. The system can not only provide strong information support, improve the ability of real-time observation of the marine environment, but also make a useful contribution to disaster prevention and reduction, early warning of ocean disasters, maritime search and rescue, etc. In addition, towards the deep blue, we must fully grasp the characteristics of the marine environment (Li 2000; Li and Mu 2001a, b; Li et al. 2003, 2004a, b, 2008a, b, 2016) and establish a large and abundant marine database, which is an important basis for the studying, utilizing of the ocean. The world ocean powers attach great importance to marine data. The most important factor in the construction of marine database is the marine observation data. The understanding of ocean numerical and dynamic mechanism can not be separated from the support of marine observation data. The few and scattered of the marine stations and the problem of the data timeliness hinder the development of the marine science. The establishent of marine environmental observation station will make positive contribution to the construction of marine big data.

Anti–terrorism Peacekeeping and Marine Rights Protecting Construction of important remote islands and reefs will make positive contribution for the integrated supplies, ship maintenance, marine monitoring, humanitarian assistance, medical aid, etc., for the Chinese Navy in many international peace affairs. Yemen evacuation, Libya evacuation and anti-piracy campaign in the Gulf of Aden highlight the important role of the Chinese Navy in peacekeeping and anti-terrorism.

1.2 Difficulties and Countermeasures of Marine Key Points Construction

1.2.1 Rational Selection of the Marine Key Points

The marine key points that based on the important remote islands and reefs are the pivotal support for human society to step into the deep sea. The number of marine key points lies in essential and refinement, not in abundance, such as the Hawaii and Diego Garcia that have obvious advantage in the Pacific Ocean and Indian Ocean separately. Construction a series of marine key points along the Maritime Silk Road will make positive contribute to improve the oceangoing voyage capacity, marine development capacity, life quality of residents, tourism, etc. However, challenges and opportunities often coexist. The rational selection of key point is a worldwide difficulty for a long time. In the process of rational selection of the key point, it is necessary to systematically consider the ability to radiate to the periphery on the integrated supply, humanitarian assistance, medical aid, ship maintenance, marine observation, disaster warning, etc., with a combination of common ground of economy, culture and so on along the countries and regions of the Maritime Silk Road.

1.2.2 Risk Evaluation of the Marine Key Points

The Maritime Silk Road, involving a large number of countries, a wide range, and long distances, faces a series of significant difficulties, such as the challenging natural environment, scarcity of freshwater and electricity resources, different cultural and political bases, complex maritime rights disputes, and constant state of conflict, etc., which greatly increase the difficulty of constructing the Maritime Silk Road. As a result, it is necessary to deeply assess the above risk factors by using the expert scoring, network analytic hierarchy process, fuzzy logic reasoning method, etc., to quantitatively evaluate the political risk, security risk, economic risk of the marine key points. Then we can employ the fuzzy clustering analysis method, projection pursuit method and so on to carry out the risk classification of the

surrounding waters of the important remote islands and reefs, thus to scientific referece for the safe and efficient construction of the marine key points.

1.2.3 Insufficiency of Electricity and Fresh Water

There are many islands and reefs exist in the South China Sea and nothern Indian Ocean. Rational exploitation and utilization of these islands and reefs is the key step. Forging them as the support point that capable of integrated replenishment, ship maintenance, information collection, marine monitoring, humanitarian assistance, medical aid and other function will sigificantly strengthen the navigation capability, marine construction capability, sea power maintenance capability of countries and regions along the Maritime Silk Road. However, these islands and reefs are usually far away from the mainland. The insufficient fresh water and electricity and the fragility of ecosystem seriously restrict the facilities and the personnel activities on the remote islands and reefs. For a long time, it is a worldwide problem. In the era of high electrification, most equipment cannot function or is even paralyzed without electricity. Human beings cannot survive without freshwater. The common method to solve the problem is using the ships transport the diesel and fresh water to support the daily operation of the remote islands and reefs. Obtaining these supplies is especially challenging under poor sea conditions. All these difficulties have seriously restricted economic development in the deep sea. Zheng and Li (2011, 2015a, b, c) and Zheng et al. (2016a, 2017a, b) have emphasized that in accordance with local conditions, utilizing and developing the rich, environmental friendly new energy resources on the important nodes, such as the wave power generation, wind power generation, wind-wave combined power generation, sea-water desalination, etc. will effectively improve the survival and sustainable ability of the remote islands and reefs and also protect the fragile ecological environment, and also provide energy for oil plarform, buoy, offshore beacon,marine park, and so on (as shown in Fig. 1.3), thus to contribute to the healthy development of the Maritime Silk Road. However, all these must be based on the full grasp of the characteristics of the resources.

1.2.4 Fragility of the Ecological Environment

The traditional method to solve the electric energy shortage of the remote islands and reefs is utilizing the diesel to generate the electric power, which may easily cause the pollution and destroy the ecology of the reefs. Once the ecosystem of remote islands and reefs is damaged, it is difficult to repair. In addition, the supplies is especially challenging under poor sea conditions. According to the local conditions, rational utilizing the wind power and wave power generation can effectively protect the fragile ecology around the reefs. In addition, the using of the wind power should be

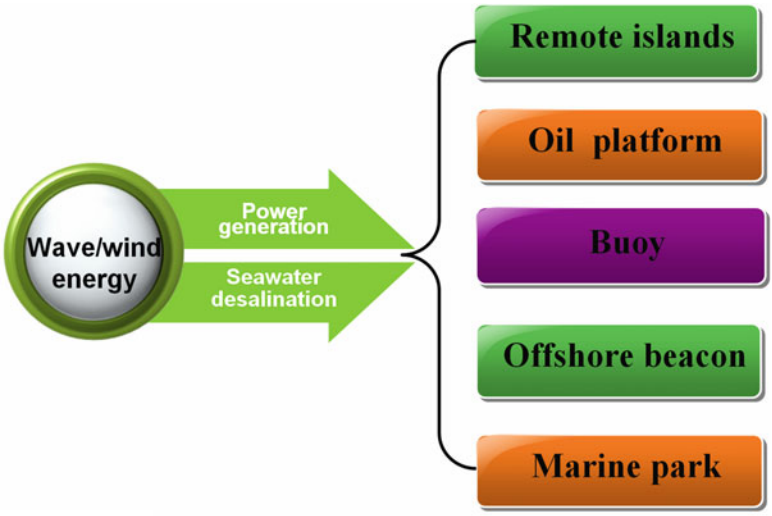

Fig. 1.3 Function prospect of wave energy and offshore wind energy

cautious. Some scholars believe during the working of the wind turbines, the reproduction and the survival of the marine organisms will be affected. Under that situation, the wave power should be fully consideration.

1.2.5 Terrible Survival and Medical Condition

The remote islands and reefs are usually far from the mainland, with poor living conditions and poor medical conditions. How to improve living and medical conditions is a problem. Remote islands with integrated supplies function can provide electricity and freshwater for ships engaged in ocean-going navigation. In turn, ocean-going freighters are usually large tonnage and can carry a variety of daily necessities and medical items for remote islands to achieve a virtuous circle of mutual assistance. In addition, important islands often require personnel to be stationed. Long-term resident will affect the mental state and work efficiency of staff. And therefore it is necessary to establish a reasonable rotation mechanism to ensure the effective operation of strategic support.

1.2.6 Complicacy Dispute on Marine Rights and Interests

The Maritime Silk Road mainly includes the South China Sea and the northern Indian Ocean. Since ancient times, the South China Sea has been part of China's

territorial waters. However, under the instigation of some outside countries, some countries continue to stir up disputes in the South China Sea, which obviously increasing the challenges facing the Maritime Silk Road initiative. In recent years, China has carried out reasonable and legitimate construction on islands and reefs in the own territorial waters, which was unlawfully disturbed and deemed unjustified by some countries. This requires us to create favorable publicity in the international community, so that more countries and regions can understand the truth. The promotional materials and supporting materials should be concise and clear, but not long-winded. For example, all the official maps of the countries of the world agree that the South China Sea belongs to China. However, some countries have been tampering with the truth in recent years. A comparison of the earlier official maps with the altered maps shows the truth that the South China Sea belongs to China at a glance. In the Indian Ocean, India has always regarded itself as the leading country. Anti-piracy escorts in the Indian Ocean launched by other countries and the Maritime Silk Road initiative were regarded as a threat by India (Ye 2016). Therefore, it is particularly important to strengthen regional cooperation and guide the countries and regions involved to participate in the construction of the Maritime Silk Road.

1.3 Structure of This Book

An understanding of the characteristics of the marine environment is a prerequisite for the safety and efficiency of marine construction, while knowledge of the characteristics of marine energy is the basis of reasonable and efficient energy utilization (Zheng et al. 2013a, b, 2014a, b, c, 2015a, b, c, d, 2016b, c, d, e, 2017c, 2018; Zheng and Pan 2014; Zheng and Li 2017a, b). This book focuses on the construction of key points that based on the remote islands and reefs in the Maritime Silk Road. Firstly, we analyze the necessity of the construction of the key points, look forward the function of these marine key points including integrated supply, ship maintenance, information collection, marine monitoring, humanitarian assistance, medical aid and marine rights protecting. Then we discuss the difficulties of the construction of remote islands and reefs and provide corresponding countermeasures. According to the urgent demand of electricity and freshwater, we focus on the wave energy and offshore wind energy evaluation of the important remote islands and reefs of the Maritime Silk Road, to provide reference for the choice of power plants location, daily operation and long term plan of wave/wind power generation. Several important marine key points of the Maritime Silk Road are selected as the case study, to help the remote islands and reefs realizing the electricity and freshwater self-sufficiency, thus to improve their viability. This book also presents the marine characteristics (especially the hazardous elements) under the demands of island runway construction, marine new energy development and so on, to promote the safe and efficient implementation of the remote islands and reefs construction. In the end, we give details of the wind energy rose (co-occurrence of wind direction and

wind power density) in each month of Gwadar port and the wind rose (co-occurrence of wind direction and wind speed), wave rose (co-occurrence of wave direction and significant wave height), wind energy rose and wave energy rose (co-occurrence of wave direction and wave power density) in each month of the Sri Lanka waters in the Appendix, to provide detail scientific reference for the marine energy development, disaster prevention and reduction, etc. of the key remote islands and reefs.

References

Li CY (2000) Introduction to climate dynamics. China Meteorological Press, Beijing
Li CY, Mu MQ (2001a) The dipole in the equatorial Indian Ocean and its impacts on climate. Chin J Atmos Sci 25(4):1–10
Li CY, Mu MQ (2001b) The influence of the Indian Ocean dipole on atmospheric circulation and climate. Adv Atmos Sci 18(5):1–16
Li CY, Long ZX, Mu MQ (2003) Atmospheric intraseasonal oscillation and its important effect. Chin J Atmos Sci 27(4):1–16
Li CY, He JH, Zhu JH (2004a) A review of decadal/Interdecadal climate variation studies in China. Adv Atmos Sci 21(3):1–10
Li CY, Wang ZT, Lin SZ (2004b) The relationship between East Asian summer monsoon activity and northward jump of the upper westerly jet location. Chin J Atmos Sci 28(5):1–9
Li CY, Mu M, Zhou GQ (2008a) Mechanism and prediction studies of the ENSO. Chin J Atmos Sci 32(4):761–781
Li CY, Gu W, Pan J (2008b) Mei-yu, Arctic oscillation and stratospheric circulation anomalies. Chin J Geophys 51(6):1–12
Li CY, Lin J, Yuan Y, Pan J, Jia XL, Chen X (2016) Frontier issues in current MJO studies. J Trop Meteorol 32(6):1–18
Ye K (2016) The establish of the strategy pivot countries of 21st century maritime silk road. Master's dissertation of East China Normal University
Zheng CW, Li XQ (2011) Wave energy resources assessment in the China Sea during the last 22 years by using WAVEWATCH-III wave model. Period Ocean Univ China 41(11):5–12
Zheng CW, Li CY (2015a) Development of the islands and reefs in the South China Sea: wind power and wave power generation. Period Ocean Univ China 45(9):7–14
Zheng CW, Li CY (2015b) Development of the islands and reefs in the South China Sea: wind climate and wave climate analysis. Period Ocean Univ China 45(9):1–6
Zheng CW, Li CY (2015c) Variation of the wave energy and significant wave height in the China Sea and adjacent waters. Renew Sust Energ Rev 43:381–387
Zheng CW, Li CY (2017a) Analysis of temporal and spatial characteristics of waves in the Indian Ocean based on ERA-40 wave reanalysis. Appl Ocean Res 63:217–228
Zheng CW, Li CY (2017b) Propagation characteristic and intraseasonal oscillation of the swell energy of the Indian Ocean. Appl Energy 197:342–353
Zheng CW, Pan J (2014) Assessment of the global ocean wind energy resource. Renew Sust Energ Rev 33:382–391
Zheng CW, Lin G, Shao LT (2013a) Frequency of Rough Sea and Its Long-term Trend Analysis in the China Sea from 1988 to 2010. J Xiamen Univ (Nat Sci) 52(3):395–399
Zheng CW, Su Q, Liu TJ (2013b) Wave energy resources assessment and dominant area evaluation in the China Sea from 1988 to 2010. Acta Oceanol Sin 35(3):104–111
Zheng CW, Pan J, Huang G (2014a) Forecasting of the China Sea ditching probability using WW3 wave model. J Beijing Univ Aeronaut Astronaut 40(3):314–320

Zheng CW, Shao LT, Li G et al (2014b) Analysis of influence on the security of sea skimming caused by a typhoon wave. J Harbin Eng Univ 35(3):301–306
Zheng CW, Zhou L, Song S et al (2014c) Simulation of the wave field caused by 1307 Typhoon "Soulik". J Xiamen Univ (Natural Science) 53(2):257–262
Zheng CW, Pan J, Sun W et al (2015a) Strategic of the ocean environment of the 21st century maritime silk road. Ocean Dev Manag 32(7):4–9
Zheng CW, Li XQ, Gao ZS et al (2015b) Strategic of the 21st century maritime silk road: wind climate analysis. Ocean Dev Manag 32(8):4–11
Zheng CW, Fu M, Rui ZF et al (2015c) Strategic of the 21st century maritime silk road: wave climate analysis. Ocean Dev Manag 32(10):1–7
Zheng CW, Gao ZS, Zhang Y et al (2015d) Strategic of the 21st century maritime silk road: extreme wind speed and extreme wave height. Ocean Dev Manag 32(11):4–8
Zheng CW, Li CY, Yang Y, Chen X (2016a) Analysis of wind energy resource in the Pakistan's Gwadar Port. J Xiamen Univ (Natural Science Edition) 55(2):210–215
Zheng CW, Sun W, Li X et al (2016b) Strategic of the 21st century maritime silk road: important route, crucial node and port feature. Ocean Dev Manag 33(1):4–13
Zheng CW, Li X, Chen X et al (2016c) Strategic of the 21st century maritime silk road: geography and climate characteristic. Ocean Dev Manag 33(2):3–10
Zheng CW, Li X, Chen X et al (2016d) Strategic of the 21st century maritime silk road: marine resources and development status. Ocean Dev Manag 33(3):3–8
Zheng CW, Li CY, Pan J et al (2016e) An overview of global ocean wind energy resources evaluations. Renew Sust Energ Rev 53:1240–1251
Zheng CW, Gao Y, Chen X (2017a) Climatic long term trend and prediction of the wind energy resource in the Gwadar Port. Acta Sci Nat Univ Pekin 53(4):617–626
Zheng CW, Sun W, Chen X et al (2017b) Strategic of the 21st century maritime silk road: construction of integrated application platform. Ocean Dev Manag 34(2):52–57
Zheng CW, Wang Q, Li CY (2017c) An overview of medium- to long-term predictions of global wave energy resources. Renew Sust Energ Rev 79:1492–1502
Zheng CW, Xiao ZN, Zhou W, Chan XB, Chen X (2018) 21st century maritime silk road: a peaceful way forward. Springer, Singapore

Chapter 2
Wave and Wind Energy Boost the Marine Key Points Construction

The marine key points that based on the remote islands and reefs are the important support for human society to step into the deep sea. However, the dilemma of the electricity, insufficiency of the fresh water, fragility of the ecological environment, etc. cause the construction of remote islands and reefs become a worldwide challenge. Rational developing the marine new energy resources around the remote islands and reefs will help solve these problems.

Nowadays, the development and utilizing of the solar energy and the on shore wind energy has been gradually moving towards industrialization, but the type of energy is restricted by the region difference. Nuclear power can provide enormous energy, but it is easily affected by the calamities and the man-made misfortunes. Such as the nuclear leakage caused by the Tsunami in Japan, March, 2011; the nuclear leakage of the Chernobyl Nuclear Power Plant caused by the faulty operation in April, 1986. All of these have brought about the terrible damage to the human society. Safe, non-pollution, renewable, large reserves, wide distribution and many other advantages make the offshore wind energy and wave energy resources become the focus of the developed countries (Zheng and Li 2011; Zheng et al. 2011, 2015a; Alesbe et al. 2017). During the Chinese Premier Li Keqiang's visit to Britain in January 2011, the master showed the new achievement is the wave power generation.

Wave power generation and wind power generation are the main way to develop and utilize wave energy and wind energy resources, which are also used widely in sea water desalination, navigation, irrigation, heating and other projects. Developing the wave power generation and wind power generation on the important remote islands and reefs of the Maritime Silk Road has a broad prospect. It can not only enhance the ability of the ocean navigation, improve the quality of life of the residents along the route of the Maritime Silk Road, but also help the countries along the Maritime Silk Road to ease the energy crisis and environmental crisis. Resource assessment should be carried out before the resource development. However, as a result of lacking of data and technical difficulty, the researches about the wave energy and wind energy on the Maritime Silk Road are rare, especially, the

C. Zheng et al., *21st Century Maritime Silk Road: Construction of Remote Islands and Reefs*, Springer Oceanography, https://doi.org/10.1007/978-981-10-8114-9_2

resources assessments on the important remote islands and reefs are extremely scarce. In this book, a systematic study on the wave energy and wind energy resources of a series of marine key points on the Maritime Silk Road is presented, which can provide scientific basis for improving the efficiency of resource collection and conversion.

2.1 Advantages of the Wave Energy and Wind Energy Resources

2.1.1 Comparison Among New Energy Resources

As the coal, oil and other conventional energy increasingly scarce, the resources crisis and environment crisis become even more violent, many countries worldwide pay special attention to the energy strategy. China also emphasizes the energy strategy by equal trading exchange with other countries and development and utilization of new energy. Table 2.1 has illustrated the advantages and disadvantages of some typical new resources. Obviously, wave energy and offshore wind energy have the unique advantages in marine construction, especially on the remote islands and reefs.

2.1.2 Prospect of Wave Energy and Wind Energy

Alleviate Energy Crisis and Environmental Crisis Energy crisis and environmental crisis pose a serious threat to human survival and sustainable development, energy crisis has become a bottleneck restricting the sustainable development of many countries worldwide. In today's world, the serious shortage of the convention energy urges human beings to focus on the rich, clean marine energy. In response to the energy crisis, China has adopted the strategy of "transmit the electricity from the western to East", "transmit the natural gas from the western area to East China" and vigorously developing nuclear power, even so, power supply still has a big gap. Fully utilizing the advantages of the renewable energy in coastal and remote islands, and developing the wave energy, offshore wind energy resources will make positive contribution to alleviate the energy crisis, protect the marine eological environment and promote the sustainable development.

Promote the Tourism of Remote Islands and Reefs The complete infrastructure (such as fresh water and electricity) is a prerequisite for economic construction such as island and reef tourism. Application of wave power generation, wind power generation and seawater desalination according to local conditions will solve the power shortage of the islands and reefs. In addition, the wind and wave farms themselves are also beautiful sceneries, which is benefit for the economic development, thus to increase the income of islanders and improve the quality of life of islanders.

Table 2.1 Advantages and disadvantages of the new energy

Wave energy	1. Mechanical energy, with highest power density among marine energy resources, ubiquity in ocean	1. Most unstable energy in ocean, has obvious seasonal variation, energy dispersion and not easy to concentrate, hard to use.
	2. Wave power generation technology tends to mature, the generator tend to miniature.	2. Machinery and equipment are large, complex design and construction, high investment, high material requirements (corrosion resistance, fatigue resistance, stable, relative inexpensive) (You 2006)
	3. Non occupation of the reef land, good concealment, strong ability to resist typhoon strike and ship collision. (The LIMPET power plant in Islay Island stay safe and sound after the striking of the 50 years return period wave) (You and Ma 2003; Ma 2009).	3. Wave power devices are easily affected by the plankton
	4. Energy supply is more stable than solar energy.	4. The current wave power generation is mainly carried out in the near shore, remote island wave power generation is particularly urgent.
	5. Renewable, clean, without destroying the fragile ecological environment (Liao 2007; Liao et al. 2007).	
	6. Theoretical storage of wave energy in China is about 70 million kW (Cheng et al. 2009), South China Sea wave energy reserves of 6.325 million kW, mainly distributed in Xisha Islands area and East Guangdong sea area, which account for 27.5% of the total wave energy reserves.	
	7. Traditional view believe the wave power density in China coast is 2–7 kW/m (Chu 2004; Wang and Lu 2009), by accurate calculation, Zheng and Li (2011) and Zheng et al. (2012a, 2013) find the average annual wave energy density in South China Sea is about 4–20 kW/m (more optimistic than the traditional standpoint), the coefficient of variation of the wave power density in most of the sea area is less than 0.4.	
Offshore wind energy	1. Offshore wind power resources are more abundant than the land wind power generation. Usually the wind speed of offshore 10 km about is 25% larger than the coastal land, available offshore wind resources are 2–3 times of the onshore resources (Wang and Cao 2008; Ling 2008).	1. Away from land, the cost of wind farm construction are high.
	2. Save land resources, non-essential to resettle of the residents, reducing the cost of investment, reduce noise pollution, no interference to human activities.	2. Wind power resources varies with the seasons and regions.

(continued)

Table 2.1 (continued)

	3. Sea surface roughness is low, the sea surface friction is small, the wind speed changes with the height slightly, so, it does not require very high tower and reduce the cost of wind turbines.	3. Electricity grid interconnection is difficult
	4. Low turbulence intensity, low sea surface friction, the fatigue load of the wind effect on the wind turbine is reduced, service life of wind turbine prolonged accordingly, designed life up to 50 years.	4. Tropical cyclones, tornadoes, thunderstorms, cold and ice can cause damage to the offshore wind farm
	5. Unrestricted development space on ocean.	5. It is difficult to obtain ocean observation data, which will affect the evaluation of wind energy resources
	6. Wind power technology has been mature (Ni et al. 2009)	
	7. More and more abundant information on the sea is conductive to evaluate the wind energy in a large area	
Onshore wind energy	1. Pollution-free, renewable, widely distributed	1. Wind power resources varies with the seasons and regions.
	2. Compared with offshore wind power, the installation of the wind turbine is easier, and the cost is much lower	2. Resources are significantly less than offshore wind energy.
	3. Technology is mature, easy to grid interconnect	3. Occupy large area land resource (Zhan et al. 2005)
	4. Observation data is easy to obtain, which is beneficial to the evaluation of wind energy resources. It is also helpful to improve the accuracy of simulation data and optimize the effect of resource evaluation	
Nuclear power	1. High efficiency, long function time, high energy	1. High construction cost
	2. Strong regional adaptability	2. High environment risk, such as the Chernobyl nuclear leakage, Fukushima nuclear leakage, all have a serious impact on human beings
Solar energy	1. Inexhaustible.	1. Intermittent, available in the day and sunny days, varies with the seasons and regions
	2. Pollution-free, inexpensive.	2. The energy is unstable and the conversion efficiency is low, easily affected by the weather, bird droppings, salt fog and other factors
	3. No emissions and noise, the application technology is mature, safe and reliable (Zhao and Wu 2008)	3. Belong to large-scale power generation system, large initial investment, monitoring costs high
		4. Occupying a large area of land or sea

(continued)

Table 2.1 (continued)

Coal, oil and natural gas	1. The technologies of exploitation, transport, storage and use are mature.	1. Low utilization efficiency
	2. Hardly affected by climatic or environmental factors	2. Produce the harmful gases, green house gases, cause the environment pollution
	3. Easy to control, the traditional energy supply can be adjusted as demand	

Zheng (2011a, b)

Protect the Ecosystem of the Reef The ecosystem of the reef is usually fragile. It is hard to be repaired once the ecosystem of the reef is destroyed. The wave energy and offshore wind energy have the advantages of non-pollution, renewable, wide distribution, etc. Developing the wave power and offshore wind power can not only solve the power dilemma of the remote islands and reefs, but also protect the fragile ecosystem of the remote islands and reefs.

Enhance the Ship Oceangoing Voyage and Deep Sea Activities Abilities After solving the problem of electric power, desalination immediately resolved. Application of wave power generation, wind power generation and seawater desalination in the surrounding waters of important remote islands and reefs will enable the islands to replenish fresh water supply for oceangoing ships and deep sea activities, thus to enhance the ability of stepping into the deep and remote sea.

Strong Ability to Resist on the Natural Disaster The wave energy equipments have the strong ability to resist typhoon strike and ship collision. Such as the LIMPET power plant in Islay Island. It stay safe and sound after the striking of the 50 years return period wave.

2.1.3 Introduction of Wave Energy Conversion System

Previous researchers have made great contribution to the wave energy generator design, to improve the collection and conversion capabilities (El-Gohary 2013; Mirab et al. 2015; Amiri et al. 2016; Behzad and Panahi 2017). According to the intermediate link, the wave generator can be classified into pneumatic, mechanical and hydraulic three types. According to the fixed form, the wave generator can be classified into floating, fixed two types, further more; the fixed type can be classified into on-shore and off-shore two types.

The "Python" from UK is a type of classical wave energy generator. The Python's body is made of rubber, soft and flexible, 8 m long, and diameter of 0.32 m. The waves generate pressure waves inside, the pressure wave continue to move forward and eventually drives the generator on the tail. It is tested in the Goose Porter of UK. The "Sea snake" generator from Portugal is brought into operation in 2008, the world's first commercial wave power plant which locates the north coastal of

Portugal. Sea snake generator is a 150 m long steel hinge structure. It generates the electricity by bending and moving to drive the water turbine generator, which can generate about 750 kW. Oceanlinx device from Australia generates electricity from the wave-driven rise and fall of water in a cylindrical shaft. The rising and falling water column drives air into and out of the top of the shaft, powering an air-driven turbine.

Recently, cheaper and cleaner electricity from wave-powered ships is carried out (Phys.org 2011), such as "Power Buoy" Oscillating water column off the Coast of Scotland. This system would be able to return to shore if conditions at sea were to become extreme, unlike fixed devices that must be built to withstand high waves and severe storms. And this system could be constructed on already existing ships to further reduce costs. In addition, this system would be able to generate power for 0.15 $ per kWh (current wave-power systems can generate electricity at a cost of between 0.30 and 0.65 $ per kWh), which is comparable to offshore wind energy and cheaper than solar power (Phys.org 2011). Obviously, the off-grid wave power will have broad prospects.

2.2 Enhance the Viability Ability of Marine Key Points

There are many islands and reefs exist in the South China Sea and the orthern Indian Ocean. They are the important support for human society to step into the deep sea. Endow the remote islands and reefs with a variety of functions, such as integrated supply, ship maintenance, information collection, marine monitoring, humanitarian assistance, medical aid, etc. can enhance the oceangoing capability, improve the ocean engineering capability and enhance the ability of marine rights and interests maintenance. However, these islands and reefs are usually far away from the mainland. The insufficient fresh water and scarce electricity and the fragility of ecosystem seriously restrict the viability and sustainable development of the remote islands and reefs. For a long time, it is a worldwide problem. Zheng and Li (2011) have emphasized that in accordance with local conditions, utilizing and developing the rich, environmentally friendly new energy resources on the marine key points, such as the wave power generation, wind power generation, wind-wave combined power generation, seawater desalination, etc. will effectively improve the survival ability of the remote islands and reefs.

Developing the wave power generation and offshore wind power generation in the surrounding waters of the remote islands and reefs, utilizing the advantages of the new energy, such as strong ability to resist natural disasters, safety, non-pollution, large reserves, wide distribution, renewable, etc., will overcome the energy shortage and protect the ecosystem. Nevertheless, many difficulties, such as instability, difficult to use, difficult to convert and so on, also restrict the development of the marine new energy. As a result, resource assessment should be carried out before the resource development.

Previous scholars have made a great contribution to evaluate the wave energy resources in the coastal area of China under the condition of extreme lack of the data. But so far, the demonstration about the wave energy and offhore wind energy of islands or reefs far away from the mainland is rare. Early in year 2011, the authors paied great attention to the wind climate, wave climate and wave energy resource of the South China Sea and the North Indian Ocean (Zheng et al. 2011, 2012b, c; Zheng 2011a, b), as shown in Table 2.2. In 2015, Zheng and Li (2015a, b) presented a series study of "development of the islands and reefs in the South China Sea", which evaluated the wave energy, offshore energy of the key islands or reefs of the South China Sea, demonstrating the feasibility of the wave power generation, wind power generation on the important islands and reefs, as shown in Table 2.2. Since 2015, the authors take the lead in focus on the analysis on the Maritime Silk Road. And presented a series study of "Series research of the 21st Century Maritime Silk Road", which exhibited the overall characteristics of marine resources and marine environment on the Maritime Silk Road, the overall characteristics of the important harbors, overall development status of marine new energy the involving countries, construction of integrated application platform and big data construction of new marine resources of the 21st Century Maritime Silk Road are presented, which lay the theoretical foundation for the Maritime Silk Road initiative (Zheng et al. 2015b, c, d, e, 2016a, b, c, d, 2017), as shown in Table 2.3. Since 2017, the authors presented a series study on the "Wave energy and offshore wind energy resources of the 21st Century Maritime Silk Road", which presented the temporal-spatial distribution characteristics, long term trends of the key factors of offshore wind energy and wave energy resource, energy classification of wave/offshore wind enrgy of the Maritime Silk Road, especially exhibited a fucos on the key point, as shown in Table 2.3 (Table 2.4).

Table 2.2 Early studies on the wind climate, wave climate and wave energy of the South China Sea and the North Indian Ocean presented by the authors

No	Manuscript title	Publication
1	Seasonal variation of wave and wave energy in xisha and nansha sea area.	Advances in Marine Science, 2011, 29(4): 419–426.
2	Wave energy and other renewable energy resources in South China Sea: Advantages and disadvantages.	Journal of Subtropical Resources and Environment, 2011, 6(3): 76–81.
3	Research on wave energy resources in the northern South China Sea during recent 10 years using SWAN wave model.	Journal of Subtropical Resources and Environment, 2011, 6(3): 76–81.
4	Simulation of wave energy resources in the South China Sea during the past 22 years.	Journal of Tropical Oceanography, 2012, 31(6): 13–19.
5	Wave energy analysis of the South China Sea and the North Indian Ocean in recent 45 years.	Marine Sciences, 2012, 36(6): 101–104.
6	Development of the islands and reefs in the South China Sea: Wind climate and wave climate analysis	Periodical of Ocean University of China, 2015, 45(9): 1–6.
7	Development of the islands and reefs in the South China Sea: Wind power and wave power generation.	Periodical of Ocean University of China, 2015, 45(9): 7–14.

Table 2.3 Series research of the 21st Century Maritime Silk Road

No	Manuscript title	Publication
1	Ocean environment of the 21st Century Maritime Silk Road.	Ocean Development and Management, 2015, 32(7): 4–9.
2	21st Century Maritime Silk Road: Wind climate analysis.	Ocean Development and Management, 2015, 32(8): 4–11.
3	The importance of ocean in the development of modern society.	Ocean Development and Management, 2015, 32(9): 4–12.
4	21st Century Maritime Silk Road: Wave climate analysis.	Ocean Development and Management, 2015, 32(10): 1–7.
5	21st Century Maritime Silk Road: Extreme wind speed and extreme wave height.	Ocean Development and Management, 2015, 32(11): 4–8.
6	21st Century Maritime Silk Road: Legal escort.	Ocean Development and Management, 2015, 32(12): 4–9.
7	21st Century Maritime Silk Road: important route, crucial node and port feature.	Ocean Development and Management, 2016, 33(1): 4–13.
8	21st Century Maritime Silk Road: Geography and climate characteristic.	Ocean Development and Management, 2016, 33(2): 3–10.
9	21st Century Maritime Silk Road: Marine resources and development status.	Ocean Development and Management, 2016, 33(3): 3–8.
10	Strategic of the 21st Century Maritime Silk Road: Ocean current.	Ocean Development and Management, 2016, 33(4): 3–7.
11	21st Century Maritime Silk Road: Construction of Integrated Application Platform.	Ocean Development and Management, 2017, 34(2): 52–57.
12	21st Century Maritime Silk Road: Big Data Construction of New Marine Resources: Wave Energy as a Case Study.	Ocean Development and Management, 2017, 34(12): 61–65.

Table 2.4 Series study of wave energy and offshore wind energy resources of the 21st Century Maritime Silk Road

No	Manuscript title	Publication
1	Wind energy evaluation of the 21st Century Maritime Silk Road.	Journal of Harbin engineering university, 2018, 39(1): 16–22.
2	An overview and suggestions on the difficulty of site selection for marine new energy power plant—wave energy as a case study.	Journal of Harbin engineering university, 2018, 39(2): 200–206.
3	Wind energy trend in the 21st Century Maritime Silk Road.	Journal of Harbin engineering university, 2018, 39(3): 399–405.
4	21st Century Maritime Silk Road: wave energy evaluation and decision and proposal of the Sri Lankan waters.	Journal of Harbin engineering university, 2018, 39(4): 614–621.
5	Climatic long term trend and prediction of the wind energy resource in the Gwadar Port.	Acta Scientiarum Naturalium Universitatis Pekinensis, 2017, 53 (4): 617–626.
6	Analysis of wind energy resource in the Pakistan's Gwadar Port.	Journal of Xiamen University (Natural Science Edition), 2016, 55(2): 210–215.

2.3 Prospect

A series of marine key points with high efficiency and high quality are the powerful support for the construction of the Maritime Silk Road. The wave power generation and offshore wind power generation around the important remote islands and reefs are the best choice to overcome the insufficiency of the electricity and fresh water.

The full assessment of energy should be carried out before the resource development. In the future, it is necessary to analyze the climate characteristics of wave energy and wind energy resources, as well as the medium- to long-term prediction and the short term forecasting, to service for the location choice, daily operation and long term plan of energy development. The analysis of the climate characteristics of the resources mainly includes the value size of the wind and wave power density, the stability (coefficient of variation, monthly variation index, seasonal variation index), energy level occurrence (available level occurrence (ALO), rich level occurrence (RLO)), long term trends of the resources, storage of the resources (total storage, effective storage, exploitable storage), wind/wave energy rose diagram (co-occurrence of energy direction and wind/wave power density), available rate of energy (effective wind speed occurrence, effective wave height occurrence), etc. These works can provide a scientific basis for site selection of the wave power generation and offshore wind power generation. The medium and long term prediction of the resources mainly include the factors of wind power density and wave power density, effective wind speed occurrence, effective wave height occurrence, stability, etc. These can provide scientific basis for medium and long term planning of resources development. The short term forecasting of the resources can provide the support for the operation of the wave energy and wind energy. In addition, the marine environment researches should be completed, including water depth, seabed geology, seasonal characteristics of wind speed and wind direction, gale occurrence, rough sea occurrence, wind direction occurrence and wave direction occurrence, extreme wind speed and extreme wave height, etc., so as to improve the collection and conversion efficiency of resources, prolong the life of equipment, provide scientific basis for disaster prevention and reduction.

References

Alesbe I, Abdel-Maksound M, Aljabair S (2017) Analysis of unsteady flow over offshore wind turbines in combination with different types of foundations. J Mar Sci Appl 16(2):190–198

Amiri A, Panahi R, Radfar S (2016) Parametric study of two-body floating-point wave absorber. J Mar Sci Appl 15(1):41–49

Behzad H, Panahi R (2017) Optimization of bottom-hinged flap-type wave energy converter for a specific wave rose. J Mar Sci Appl 16(2):159–165

Cheng Y-l, Dang Y, Wu Y-j (2009) Status and trends of the power generation from wave. Appl Energy Technol 12:26–30

Chu T-j (2004) Exploitation and utilization of ocean energy. Chemical Industry Press, Beijing

El-Gohary MM (2013) Overview of past, present and future marine power plants. J Mar Sci Appl 12 (2):219–227
Huang Yi-cheng Reanalysis on the wind power genaration. Available at http://www.efchina.org/csepupfiles/report/2006102695218370.46950329 443723.pdf/Wind_Generation.pdf
Liao L-z (2007) Ecological restoration of non-resident Houyu marine island in Xiamen. J Subtrop Resour Environ 2(2):57–61
Liao L-z, Fang J-y, Lei G (2007) Non-resident islands resources and projective utilization in Eastern Fujian. J Subtrop Resour Environ 2(4):49–53
Ling S (2008) Thinking of wind power development and use in China Coastland. Resour Dev Mark 24(7):634–635
Ma Y-y (2009) Wave energy resources application. Express Water Resour Hydropower Inf 30 (3):31–32
Mirab H, Fathi R, Jahangiri V, Ettefagh M, Hassannejad R (2015) Energy harvesting from sea waves with consideration of airy and JONSWAP theory and optimization of energy harvester parameters. J Mar Sci Appl 14(4):440–449
Ni Y-l, Xin H-l, Liu Y (2009) Analysis on the development and present technology status of offshore wind power in China. Energy Eng 4:21–25
Phys.org (2011) Cheaper and cleaner electricity from wave-powered ships (w/video). Available at https://phys.org/news/2011-07-cheaper-cleaner-electricity-wave-powered-ships.html
Wang X-d, Cao Y-y (2008) The wind energy source application in the sea environment. Sci Technol Consult Herald 5:92
Wang C-k, Lu W (2009) Analysis methods and reserves evaluation of ocean energy resources. Ocean Press, Beijing
You Y-g (2006) Wave energy resources development in China. China Sci Technol Achiev 2:17–19
You Y-g, Ma Y-j (2003) The sea energy source application in the sea environment. Meterol Hydrol Mar Instrum 3:32–35
Zhan P-g, Yu H, Hou B (2005) Technical summary of wind power generation on the sea. Electr Equip 6(12):42–44
Zhao H-t, Wu T-q (2008) Some ideas about further development of the Xisha, Nansha and Zhongsha Islands. Trop Geograph 28(4):369–375
Zheng CW (2011a) Wave energy and other renewable energy resources in South China Sea: advantages and disadvantages. J Subtrop Resour Environ 6(3):76–81
Zheng CW (2011b) Research on wave energy resources in the northern South China Sea during recent 10 years using SWAN wave model. J Subtrop Resour Environ 6(3):76–81
Zheng CW, Li XQ (2011) Wave energy resources assessment in the China Sea during the last 22 years by using WAVEWATCH-III wave model. Period Ocean Univ China 41(11):5–12
Zheng CW, Li CY (2015a) Development of the islands and reefs in the South China Sea: wind climate and wave climate analysis. Period Ocean Univ China 45(9):1–6
Zheng CW, Li CY (2015b) Development of the islands and reefs in the South China Sea: wind power and wave power generation. Period Ocean Univ China 45(9):7–14
Zheng CW, Zhou L, Zhou LJ (2011) Seasonal variation of wave and wave energy in xisha and nansha sea area. Adv Mar Sci 29(4):419–426
Zheng CW, Zhuang H, Li X, Li XQ (2012a) Wind energy and wave energy resources assessment in the East China Sea and South China Sea. Sci China Technol Sci 55(1):163–173
Zheng CW, Li XQ, Pan J (2012b) Wave energy analysis of the South China Sea and the North Indian Ocean in recent 45 years. Mar Sci 36(6):101–104
Zheng CW, Lin G, Sun Y (2012c) Simulation of wave energy resources in the South China Sea during the past 22 years. J Trop Oceanogr 31(6):13–19
Zheng CW, Pan J, Li JX (2013) Assessing the China Sea wind energy and wave energy resources from 1988 to 2009. Ocean Eng 65:39–48
Zheng CW, You XB, Zhou GQ, Chen XB (2015a) Ocean environment characteristic and wave energy resource in the China Sea and adjacent waters. China Ocean Press, Beijing

Zheng CW, Pan J, Sun W et al (2015b) Strategic of the ocean environment of the 21st century Maritime Silk Road. Ocean Dev Manag 32(7):4–9
Zheng CW, Li XQ, Gao ZS et al (2015c) Strategic of the 21st century Maritime Silk Road: wind climate analysis. Ocean Dev Manag 32(8):4–11
Zheng CW, Fu M, Rui ZF et al (2015d) Strategic of the 21st century Maritime Silk Road: wave climate analysis. Ocean Dev Manag 32(10):1–7
Zheng CW, Gao ZS, Zhang Y et al (2015e) Strategic of the 21st century Maritime Silk Road: extreme wind speed and extreme wave height. Ocean Dev Manag 32(11):4–8
Zheng CW, Sun W, Li X et al (2016a) Strategic of the 21st century Maritime Silk Road: important route, crucial node and port feature. Ocean Dev Manag 33(1):4–13
Zheng CW, Li X, Chen X et al (2016b) Strategic of the 21st century Maritime Silk Road: geography and climate characteristic. Ocean Dev Manag 33(2):3–10
Zheng CW, Li X, Chen X et al (2016c) Strategic of the 21st century Maritime Silk Road: marine resources and development status. Ocean Dev Manag 33(3):3–8
Zheng CW, Li CY, Yang Y, Chen X (2016d) Analysis of wind energy resource in the Pakistan's Gwadar Port. J Xiamen Univ (Natural Science Edition) 55(2):210–215
Zheng CW, Sun W, Chen X et al (2017) Strategic of the 21st century Maritime Silk Road: construction of integrated application platform. Ocean Dev Manag 34(2):52–57

Chapter 3
Wind Energy Resource Assessment in the Gwadar Port

The Gwadar Port that located in southwestern Baluchistan province, Pakistan, grip the throat of the Persian Gulf, is a deepwater port. It is the key node of both the "21st century Maritime Silk Road" and the "Silk Road Economic Belt". The construction of the Gwadar Port can benefit the countries and regions along the Maritime Silk Road (Zheng et al. 2016), such as energy supply, cargo transport, and so on. The infrastructure construction of the Gwadar Port is important, especially the electricity supply. The development of clean and renewable energy (such as wind energy and wave energy) will effectively improve the ability of sustainable development of the important ports.

Resource assessment should be carried out before the resource development (Zheng 2018a, b, c; Zheng and Li 2018). Chang et al. (2003) analyzed the characteristics of the Taiwan's wind speed and wind energy resources. It is found that Taiwan is rich in wind energy resources. Chen et al. (2008) utilized more than 30 yeas' meteorology data to analyze the wind energy resources of the Lianyungang area and its offshore waters. It is found the wind speed of this area is stable and wind energy is rich. Mao et al. (2005) used more than 100 observation stations' data to analyze the wind energy of the Guangdong Province of China. The results show the potential development zones of wind energy in Guangdong are distributed along the coast and estuary, and the theoretical wind energy storage is 7.99×10^3 MW. Zhou et al. (2010) pointed out China's coastal wind energy resources are very rich, the annual average wind power density is about 300–800 W/m^2. Zheng and Li (2015a, b) have discussed on the feasibility of wave power generation and offshore wind power generation of the remote island and reef in the South China Sea, the results can provide scientific basis for the construction of the islands and reefs, thus to improve their survival ability.

Previous scholars have made great contributions to the evaluation of offshore wind energy resources in the China seas. However, about the evaluation of wind energy resource in the Gwadar Port is still in blank. This chapter utilize the

C. Zheng et al., *21st Century Maritime Silk Road: Construction of Remote Islands and Reefs*, Springer Oceanography, https://doi.org/10.1007/978-981-10-8114-9_3

ERA-interim wind production from the European Centre for Medium-Range Weather Forecast's (WCMWF) for the period 1979–2014 to evaluate the wind energy resources of the Gwadar Port, in hope of making contribution to promote the sustainable development of Gwadar Port (Zheng et al. 2016, 2017).

3.1 Data and Methodology

The ERA-interim wind data including the wind direction and wind speed of 10 m above the sea surface comes from the ECMWF. The spatial scope are 90°S~90°N, 180°W~180°E, and the spatial resolution contains 0.125 × 0.125, 0.25 × 0.25, 0.5 × 0.5, 0.75 × 0.75, 1.0 × 1.0 and 2.5 × 2.5, and this chapter chooses the spatial resolution of 0.125 × 0.125 as the analysis basis. The time series of the ERA-interim wind data is from Jan. 1 1979 00:00 up to now, and this chapter chooses the scope from 1979 to 2014, which has a time resolution of 6 h. (Data URL: http://data-portal.ecmwf.int/data/d/interim_daily/).

The ERA-Interim reanalysis data is the new product after its early product ERA-40. The data use a higher resolution meteorological model, the application of observation data and assimilation methods have also been greatly improved. It uses the latest four-dimensional variation assimilation technique of 12 h window to assimilate the satellite data (ERS-1, ERS-2 and QuikSCAT), conventional observation data, and numerical model data, so as to provide a link between the early ECMWF products and a new generation of products, and to improve and perfect the ERA-40 or earlier data. Theoretically, ERA-Interim as newly developed ECMWF assimilation data set should be more accurate than the previous ERA-15 and ERA-14. Dee et al. (2011) demonstrated the superiority of ERA-interim and believed the ERA-interim has made good progress compare to the early data. Song et al. (2015) compared the ERA-interim wind data with the observation data of 8 buoys in China. It is found that the ERA-interim has a good correlation with the buoy data, and the regression coefficient of the wind speed is about 0.7, and the regression coefficient of wind direction is about 0.79; the ERA-interim wind speed is slight higher than the wind speed observed from buoy. Bao and Zhang (2013) have compared the NCEP-CFSR, NCEP-NCAR, ERA-Interim, and ERA-40 reanalysis data with the observation data from 11 stations in the Tibet Plateau. It is found that the NCEP-CFSR and ERA-Interim are better than NCEP-NCAR and ERA-40 data in terms of root mean square error and bias.

This chapter uses the ERA-Interim wind data to analyze the characterristics of wind energy resource of the Gwadar Port, including the value size of the wind power density, effective wind speed occurrence (EWSO), richness of wind energy (energy level occurrence), wind energy rose diagram (co-occurrence of wind energy direction and wind power density value size), long term trends of wind energy resources, wind class occurrence, etc.

3.2 Monthly Variation of Wind Power Density

The wind power density is wind power on the per unit section that perpendicular to airflow, can be calculated as follows:

$$W = \frac{1}{2}\rho V^3 \tag{3.1}$$

where, W/m^2 is the wind power density, unit is W/m^2, W/m^2 is the wind speed, unit is W/m^2, ρ is the standard sea-level air density (1.225 kg/m^3). Utilizing the ERA-interim wind data from 1979 to 2014, combined with the calculation method of wind power density, the 6-hourly wind power density of the Gwadar Port for the past 36 years (1979–2014) is obtained.

Averaging the wind power density from 0000 UTC on January 1st, 1979 to 1800 UTC on January 31st 1979, a month average value of wind power density of the Gwadar Port is obtained. Similarly, the month average value of wind power density in each January for the past 36 years is obtained. Then the multi-year average value of wind power density in January of the Gwadar Port is obtained. Using the same method, the multi-year average value of wind power density from January to December is obtained to exhibit the monthly variation of wind energy of the Gwadar Port, as shown in Fig. 3.1.

Obviously, the wind power density in the Gwadar Port appears a single peak in monthly variation. The peak value appears from April to May, of about 190 W/m^2; while the trough appears from November to December, of about 70 W/m^2. It is worth noting that more than half of the year the value is greater than 100 W/m^2, and the annual average wind power density is 121 W/m^2. It is believed the wind power density that greater than 50 W/m^2 is available, and the value greater than 200 W/m^2 is regarded as rich (Zheng et al. 2013). Obviously, the wind energy in the Gwadar Port is in an available condition. From April or May, the wind energy can be even up to rich.

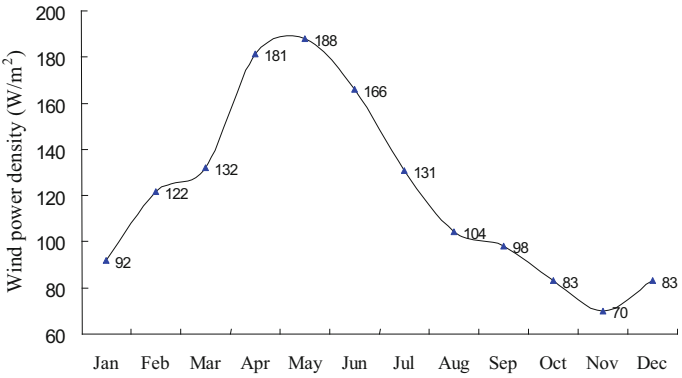

Fig. 3.1 Monthly variation of the wind power density of the Gwadar Port. (After Zheng et al. 2016)

3.3 Effective Wind Speed Occurrence

Generally, it is believed that the wind speed between 5 and 25 m/s is conducive to the collection and conversion of the wind energy resources. And the wind speed in this interval is defined as the effective wind speed (Zheng and Pan 2012). This chapter statistics analyzes the effective wind speed occurrence (EWSO) in each month to exhibit the monthly variation of available rate of wind energy in the Gwadar Port. Using the 6-hourly wind speed data in January 1979, the EWSO in this month is counted. Similarly, the EWSO in each January for the past 36 years is obtained. Then the multi-year average EWSO in January is obtained. The same method is employed to calculate the multi-year average value of EWSO from January to December, as shown in Fig. 3.2.

Similar to the monthly variation of wind power density, the EWSO of the Gwadar Port shows a single peak in monthly variation. The peak value appears from April to May, the occurrence is greater than 60%; the tough value appears from November to December, the occurrence is about 25%. Affected by day and night, the available rate of solar energy is usually below 50% (Zheng 2011). The annual available rate of wind energy in the Gwadar Port is 43%, much more optimistic than the solar energy.

3.4 Energy Level Occurrences

Generally, it is believed the wind power density higher than 50 W/m^2 (some of the standard is 100 W/m^2) is available, and the value higher than 200 W/m^2 is rich. This chapter statisticed and analyzed the occurrences of the wind power density greater than 50 W/m^2 (available level occurrence, ALO), greater than 100 W/m^2, greater than 200 W/m^2 (rich level occurrence, RLO) separately. Based on the 6-hourly wind power density data in January 1979, the method in Fig. 3.2 is employed to calculate the multi-year average value of occurrences of the wind power density greater than 50 W/m^2, greater than 100 W/m^2, greater than 200 W/m^2 from January to December, as shown in Fig. 3.3. Similar to the monthly variation of the wind power density, the occurrence of the wind power density on different energy levels have a single peak in monthly variation. The peak value of ALO appears from April to May, of above 70%, while the occurrences in the other months are higher than 40%. And the annual mean ALO is 55%. It indicates the availability of the wind energy of the Gwadar Port is considerable. The occurrence characteristics of the energy level greater than 100 W/m^2 or greater than 200 W/m^2 are similar to the energy level greater than 50 W/m^2, just with smaller values.

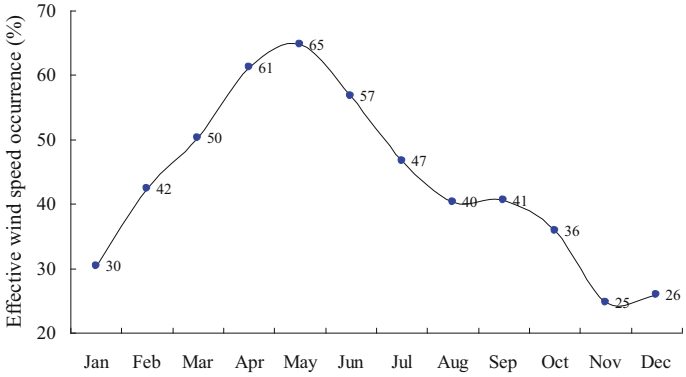

Fig. 3.2 Monthly variation of the effective wind speed occurrence in the Gwadar Port. (After Zheng et al. 2016)

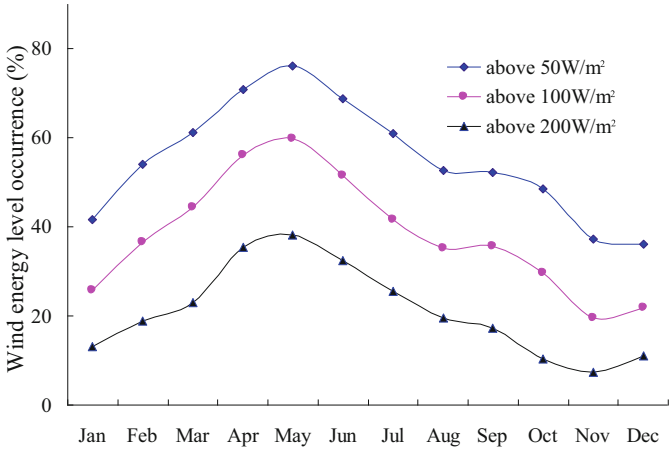

Fig. 3.3 Monthly variation of the energy level occurrences of the Gwadar Port. (After Zheng et al. 2016)

3.5 Wind Energy Rose

In the process of wind energy development, the co-occurrence of wind energy direction and wind power density value size is one of the most important factors. If the wind energy direction is stable (dominated by one or two wind direction), it is very beneficial to the wind energy capture, improve the efficiency of collection and conversion and prolong the life of the wind turbine. The traditional radar chart can only exhibit the wind energy direction; can not show the wind power density value size at the same time. In this chapter, we designed a wind energy rose diagram that can exhibit the combination occurrence of wind energy direction and wind energy

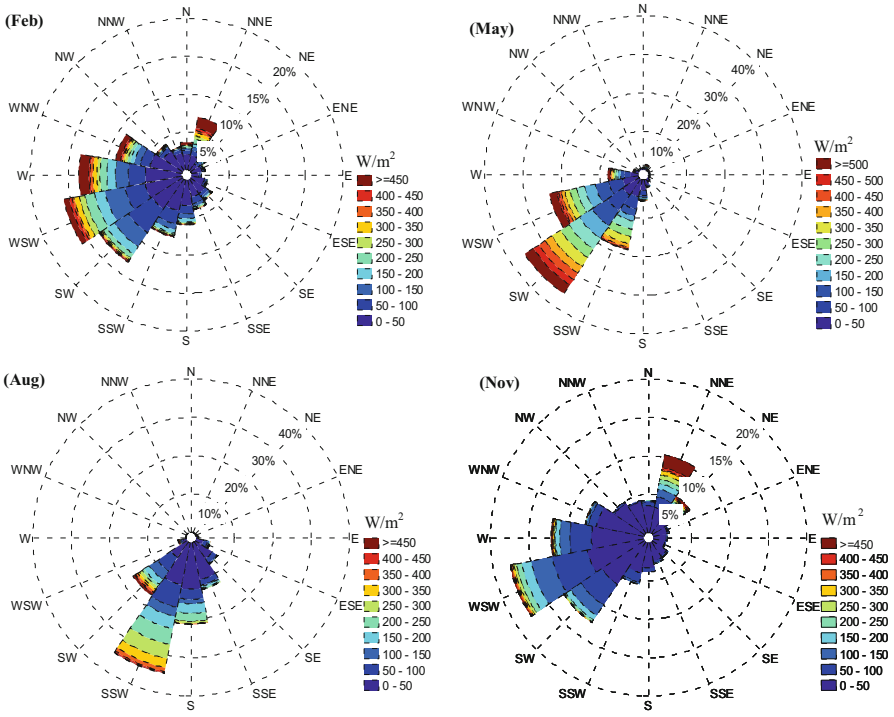

Fig. 3.4 Wind energy rose in February, May, August and November of the Gwadar Port. (After Zheng et al. 2016)

value size at the same time. Figure 3.4 presents the wind energy rose of the Gwadar Port. The wind energy direction is classified into 16 orientations, on every orientation, the occurrence of the wind power density value size of different level are statistic analyzed. Approximately, the February, May, August, November on behalf of the four seasons.

Generally, the wind energy in the Gwadar Port steadily comes from southwest (SW) direction all year round, which is an optimistic phenomenon for wind energy development.

In February, the highest frequency of the wind energy direction is west-southwest (WSW), accounted for 15.9%. Among them, the levels of 0–50 W/m^2 and 100–200 W/m^2 are the largest contribution, of 5.5% and 4.6% respectively. The occurrences of west (W) and SW direction are the next to WSW. The high energy level greater than 500 W/m^2 is contributed by the north-northeast (NNE) direction, about 1.5%, the next is W, WSW and west-northwest (WNW).

In May, the wind energy direction of the Gwadar Port is mainly contributed by the SW, accounted for 35.8%, among them, the levels 100–200 W/m^2, 200–300 W/m^2 and 300–400 W/m^2 are the highest contributions, of 10.0%, 6.0% and 4.0% respectively. The occurrence of WSW is the next to SW, accounted for 8.0%. It is

worth noting that the wind energy greater than 500 W/m^2 is mainly contributed by the SW direction, about 2.6%, followed by WSW dirrection.

In August, the wind energy direction of the Gwadar Port is mainly contributed by the south-southwest (SSW), accounted for 34.8%, followed by the SW and south (S) direction.

In November, the wind energy direction is mainly contributed by WSW, accounted for 17.8%, followed by the SW and W direction. However, the wind energy greater than 400 W/m^2 mainly comes from the NNE direction.

3.6 Long Term Trend of Wind Energy

Averaging the wind power density from 0000 UTC on January 1st, 1979 to 1800 UTC on December 31st 1979, a yearly average value of wind power density of the Gwadar Port is obtained. Using the same method, we obtain 36 yearly average values of wind power density for the period 1979–2014. Then the annual trend of the wind power density of the Gwadar Port is analyzed using linear regression method, as shown in Fig. 3.5a. Similarly, the annual trend of the EWSO of the Gwadar Port is also analyzed, as shown in Fig. 3.5b.

As shown in Fig. 3.5a, correlation coefficient (R) of the wind power density is 0.57, significant at the 95% reliability level t-test. The regression coefficient is −0.59. It means that the wind power density exhibits a significant decreasing trend of −0.59 (W/m^2)/year in the Gwadar Port as a whole for the past 36 years. As shown in Fig. 3.5b, correlation coefficient (R) of the effective wind speed occurrence is 0.60, significant at the 95% reliability level t-test. The regression coefficient is −0.17. It indicates that the effective wind speed occurrence exhibits a significant decreasing trend of −0.17%/year (here the % is the effective wind speed occurrence, not the variation of effective wind speed occurrence) in the Gwadar Port as a whole for the past 36 years.

It is found that the variation of the wind energy of the Gwadar Port can be classified into two major stages. From 1979 to 2000, the variation trend is relatively violent, and the wind power density fluctuate around 120 W/m^2, the EWSO fluctuate around 45%. From 2001 to 2014, the variation trend is flat, the wind power density fluctuate around 110 W/m^2, the EWSO fluctuate around 40%.

3.7 Wind Class Occurrence

Both the wind energy resources development and the disaster prevention and reduction are paid great attention to the wind class occurrence especially the gale occurrence (Zheng et al. 2014). According to the Beaufort wind scale table, the wind class occurrence of the Gwadar Port in the representative months are statistic analyzed, as shown in Table 3.1.

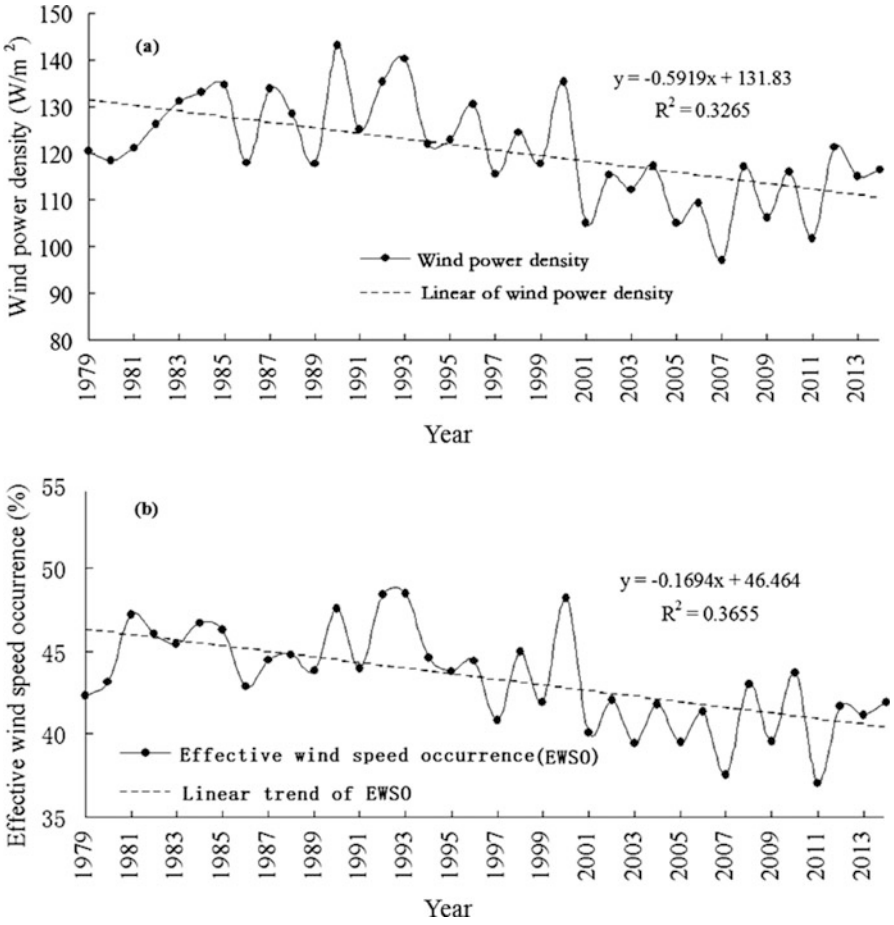

Fig. 3.5 Annual trends of wind power density (**a**) and effective wind speed occurrence (**b**) of the Gwadar Port. (After Zheng et al. 2016)

Table 3.1 Wind class occurrence in the Gwadar Port (%)

Wind class	Wind speed scale (m/s)	February	May	August	November	Annual ocurrence
0	0.0~0.2	0.25	0.07	0.00	0.19	0.08
1	0.3~1.5	6.22	1.48	1.59	9.07	4.77
2	1.6~3.3	23.56	10.22	25.09	35.00	23.11
3	3.4~5.4	33.86	28.92	38.49	36.37	34.29
4	5.5~7.9	26.72	39.70	29.68	15.79	28.32
5	8.0~10.7	8.07	18.77	4.93	2.94	8.71
≥6	≥10.8	1.32	0.85	0.22	0.65	0.71

In February, the highest occurrence wind speed scale is class 3, followed by class 4 and class 2. The occurrence of wind speed greater than class 6 is relatively low, about 1.32%. In May, the highest occurrence wind speed scale is class 4, followed by class 3 and class 5. The occurrence of greater than class 6 is low. In August, the highest occurrence wind speed scale is class 3, followed by class 4 and class 2. The occurrence of greater than class 6 is low. In November, the highest occurrence wind speed scale is class 3 and class 2, followed by class 4. The occurrence of greater than class 6 is low. For the whole year, the highest occurrence wind speed scale is class 3, accounted for 34.29%, followed by class 4 (28.32%) and class 2 (23.11%). The occurrence of greater than class 6 is below 1.5%.

3.8 Summary and Prospect

This chapter utilizing the ERA-interim wind production to evaluate the characteristics of wind energy in the Gwadar Port, systematically including the value size of the wind power density, effective wind speed occurrence (EWSO), energy level occurrence, wind energy rose diagram (co-occurrence of wind energy direction and wind energy value size, exhibits the coming direction of wind energy), long term trends of wind energy resources, wind class occurrence, etc. It is not hard to find that the Gwadar Port obtains relative optimistic wind energy: high available rate and low gale occurrence. The important conclusions are as follows.

The wind energy resource of the Gwadar Port is available throughout in the year. The wind power density, effective wind speed occurrence, wind energy level occurrence have a prominent single peak in monthly variation. The peak value appears from April to May and the trough value appears from November to December. The annual average value of the wind power density, effective wind speed occurrence, and the occurrences of the energy level greater than 50 W/m^2 are 121 W/m^2, 43% and 55% respectively.

The wind energy in the Gwadar Port steadily comes from southwest (SW) direction all year round, which is an optimistic phenomenon for wind energy development. In February and November, the occurrences of wind power density greater than 400 and 500 W/m^2 are mainly the north-northeast direction. In May and August, the occurrence of wind power density is mainly the southwest direction.

During the past 36 years, the wind power density of the Gwadar Port decreased sinificantly with a speed of -0.59 (W/m^2)/year, and the effective wind speed occurrence decreased sinificantly with a speed of -0.17%/year. From 1979 to 2000, the variation trend is relatively violent, and the wind power density fluctuates around 120 W/m^2, the effective wind speed occurrence fluctuates around 45%. From 2001 to 2014, the variation trend is flat, the wind power density fluctuates around 110 W/m^2, the effective wind speed occurrence frequency fluctuates around 40%.

The wind speed greater than class 6 is lower than 1.5% all year round. The highest occurrence wind speed scale is class 3 (34.29%), followed by class 4 (28.32%) and class 2 (23.11%), which is beneficial for the wind energy development.

In this chapter, we mainly analyzed the wind energy at 10 m above sea surface. It is also necessary to analyze the characteristics of wind energy at hub height. In the future work, we can use the values of wind energy at 10 m above surface and vertical velocity profile (Generally to be a logarithmic law or exponential law. For example, the exponential law is $V = V_1\left(\frac{Z}{Z_1}\right)^{\alpha}$) to calculate the wind energy at 30 m, 50 m, 70 m and 90 m above surface to provide reference for the wind turbines at different heights.

In this chapter, the characteristics of wind energy resources of the Gwadar Port is analyzed, systematically including the value size of wind power density, effective wind speed occurrence, energy level occurrence, wind energy rose (the coming direction of wind energy) and wind class occurrence. The results can provide scientific reference for the wind energy development. In the future work, the scheme formed in this chapter can be popularized in other marine key points of the global oceans, especially the Maritime Silk Road, to provide guidance for the wind energy development.

References

Bao XH, Zhang FQ (2013) Evaluation of NCEP–CFSR, NCEP–NCAR, ERA-Interim, and ERA-40 reanalysis datasets against independent sounding observations over the Tibetan Plateau. J Clim 26:206–214

Chang TJ, Wu YT, Hsu HY et al (2003) Assessment of wind characteristics and wind turbine characteristics in Taiwan. Renew Energy 28:851–871

Chen F, Ban X, Qi X (2008) Evaluation of wind energy resource on the coastland and adjacent sea of Lianyungang. Sci Meteorol Sin 28(Suppl):101–106

Dee DP, Uppala SM, Simmons AJ et al (2011) The ERA-Interim reanalysis: configuration and performance of the data assimilation system. Q J R Meteorol Soc 137(656):553–597

Mao HQ, Song LL, Huang HH (2005) Study on the wind energy resource division in Guangdong Province. J Nat Resour 20(5):679–683

Song LN, Liu ZL, Wang F (2015) Comparison of wind data from ERA-Interim and buoys in the Yellow and East China Seas. Chin J Oceanol Limnol 33(1):282–288

Zheng CW (2011) Wave energy and other renewable energy resources in South China Sea: advantages and disadvantages. J Subtrop Resour Environ 6(3):76–81

Zheng CW (2018a) Wind energy evaluation of the 21st Century Maritime Silk Road. J Harbin Eng Univ 39(1):16–22

Zheng CW (2018b) Wind energy trend in the 21st Century Maritime Silk Road. J Harbin Eng Univ 39(3):1–8

Zheng CW (2018c) 21st Century Maritime Silk Road: wave energy evaluation and decision and proposal of the Sri Lankan waters. J Harbin Eng Univ 39(4):1–8

Zheng CW, Li CY (2015a) Development of the islands and reefs in the South China Sea: wind climate and wave climate analysis. Period Ocean Univ China 45(9):1–6

Zheng CW, Li CY (2015b) Development of the islands and reefs in the South China Sea: wind power and wave power generation. Period Ocean Univ China 45(9):7–14

Zheng CW, LI C Y. (2018) An overview and suggestions on the difficulty of site selection for marine new energy power plant—wave energy as a case study. J Harbin Eng Univ 39 (2):200–206

Zheng CW, Pan J (2012) Wind energy resources assessment in Global Ocean. J Nat Resour 27 (3):364–371
Zheng CW, Pan J, Li JX (2013) Assessing the China Sea wind energy and wave energy resources from 1988 to 2009. Ocean Eng 65:39–48
Zheng CW, Zhou L, Song S et al (2014) Simulation of the wave field caused by 1307 Typhoon "Soulik". J Xiamen Univ (Natural Science) 53(2):257–262
Zheng CW, Li CY, Yang Y, Chen X (2016) Analysis of wind energy resource in the Pakistan's Gwadar Port. J Xiamen Univ (Nat Sci Ed) 55(2):210–215
Zheng CW, Gao Y, Chen X (2017) Climatic long term trend and prediction of the wind energy resource in the Gwadar Port. Acta Sci Nat Univ Pekin 53(4):617–626
Zhou RW, He XF, Zhu R (2010) Numerical simulation of the development potential of wind energy resources over China's offshore areas. Resour Sci 32(8):1434–1443

Chapter 4
Climatic Trend and Prediction of the Wind Energy in the Gwadar Port

The development of wind energy resource could make a positive contribution to the construction of the Gwadar Port, thus to contribute to the construction of the Belt and Road. The evaluation of the potential to exploit wind energy must precede resource exploitation. In the actual development of the wind energy, it is necessary to pay attention to the climatic trend and future prediction of wind energy so as to provide scientific basis for mid-long term planning. Until now, the research on the climatic trend of oceanic and meteorology parameters are abundant. Previous researchers have also made great contribution to the analysis of temporal-spatial distribution of wind energy (Zheng et al. 2013, 2015a, b, 2016a, 2017a). However, the research on the climatic trend of the wind energy is scarce (Zheng et al. 2016b, 2017b). The traditional long term trend analysis of wind energy usually considered only the trend of wind power density (WPD). In the development of wind energy, the value size of WPD is the direct exhibition of wind energy. The effective wind speed occurrence (EWSO) is directly related to the utilization rate of wind energy. The occurrence of energy levels greater than 100 W/m^2 (Available level occurrence, ALO) directly exhibits the richness of wind energy. As a result, the long term trend analysis of wind energy is concerned not only with the trend of WPD, but also the trends of EWSO and ALO. In addition, the research on prediction of oceanic and meteorology parameters are abundant. However, the research on prediction of wind energy is scarce until now, which is not benefit for the mid-long term planning of wind energy development.

In this chapter, we use the ERA-interim wind field data of 10 m above the sea surface for the past 36 years (1979–2014), to calculate the climatic trend of wind energy parameters in the Gwadar Port, and utilize two methods to make long term prediction (forecast less than 30 min is ultra short term prediction; less than 72 h is short term forecast; more than 10 days is long term forecast (Gu et al. 2007)) of wind energy parameters in the Gwadar Port, which can provide the scientific basis for the long term planning of wind energy development, and provide scientific support for the construction of the Maritime Silk Road.

C. Zheng et al., *21st Century Maritime Silk Road: Construction of Remote Islands and Reefs*, Springer Oceanography, https://doi.org/10.1007/978-981-10-8114-9_4

4.1 Data and Methodology

Based on the 6-hourly wind power density for the past 36 years (1979–2014) of the Gwadar Port obtained in section 3.1, the climatic trends of wind energy factors (including the wind power density, effective wind speed occurrence, energy level occurrence, gale occurrence, stability of wind energy, etc.) for the past 36 years (1979–2014) were calculated using the one linear regression method. In addition to the annual trend, we also calculate the climatic trends of wind energy in January and July. Then, using the BP neural network and linear prediction method, the wind energy resources of the Gwadar Port is predicted. And this work mainly includes the prediction of wind power density, effective wind speed occurrence, energy level occurrence and the stability.

Currently, linear prediction and BP neural network prediction method are relatively mature, which are widely use in climate analysis and prediction, urban sustainable development, sea level prediction, ecosystem risk research and financial forecast and many other fields (Chen et al. 2008; Duan et al. 2014; Mao et al. 2005).

Linear regression model: Assuming that the predictand is y, the predictive factor vector is x, then the equation can be written as $\widehat{y} = \mathbf{a}\mathbf{x}' + b$, where, $\widehat{y}$ is the forecast form of y; $\mathbf{x}'$ is the transpose form the x, $\mathbf{a}$ and b are the fitting coefficients of the equation. Generally, the equation is overdetermined, so, the least squares method is used to solve the coefficients, that is: obtain the fitting coefficients when the value of the error equation $\sum_{i=1}^{n} \left(y_j - \mathbf{a}\mathbf{x}_i' - b\right)^2$ is the minimum, where, n is the sample size, y_i and $\mathbf{x}_i'$ are the correspondingly samples.

4.2 Climatic Trend of Wind Power Density

Averaging the wind power density (WPD) from 0000 UTC on January 1st, 1979 to 1800 UTC on January 31st 1979, a month average value of WPD in the Gwadar Port is obtained. Similarly, the WPD in each month for the period 1979.01–2014.12 is obtained. Then the climatic trend of wind power density in January for the past 36 years (1979–2014) is calculated, as shown in Fig. 4.1a. In addition, in order to reflect the climatic trend of wind energy more realistically, the time series of WPD is coped with the moving average method. The climatic trends after 5-point moving average of time series of WPD is calculated, as shown in Fig. 4.1b. Similarly, the climatic trend of the WPD in July and annual trend of the Gwadar Port is calculated separately (also including the long term trend of the WPD after 5-point moving average), as shown in Fig. 4.1c, f.

In January, the WPD of the Gwadar Port severely varies around the scale of 50–170 W/m^2. About the trend of the original data of WPD, the correlation coefficient (R) is 0.01, does not pass the reliability level test. About the trend of 5-point moving average of WPD, R = 0.03, does not pass the reliability level test. It

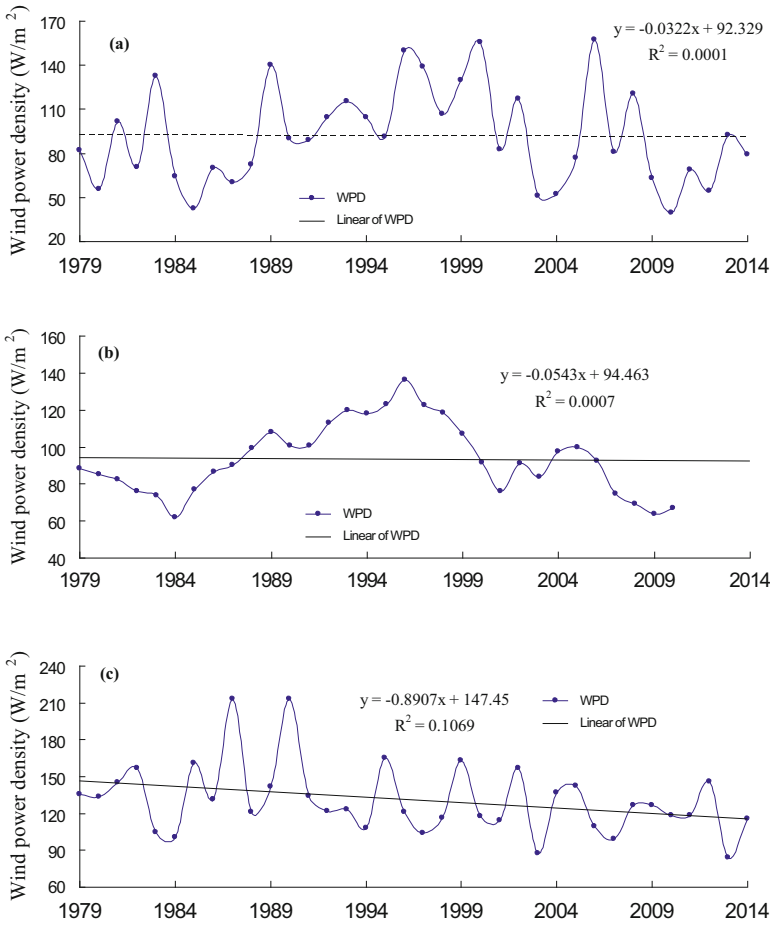

Fig. 4.1 Original data of wind power density (WPD) and its climatic trends of the Gwadar Port in January (**a**), July (**c**) and annual trend (**e**), and WPD after 5-point moving average and its trend in January (**b**), July (**d**) and annual trend (**f**) for the past 36 years. (After Zheng et al. 2017c)

indicates that the WPD of the Gwadar Port does not have a significant climatic trend in January for the past 36 years.

In July, under the obviously impact of strong southwest monsoon, the wind power density of the Gwadar Port fluctuates around the scale of 90–210 W/m^2. And the value is apparently greater than that in January. It can be attributed to the effect of the southwest monsoon in summer stronger than the cold air in winter. It is noticed that the situation of the Gwadar Port opposite to the South China Sea. In the South China Sea, the cold air in winter apparently stronger than the southeast monsoon in summer. About the trend of the original data of WPD, the correlation coefficient (R) is 0.33, significant at the 95% reliability level. The regression coefficient is −0.89. About the trend of 5-point moving average of WPD, R = 0.67, significant at

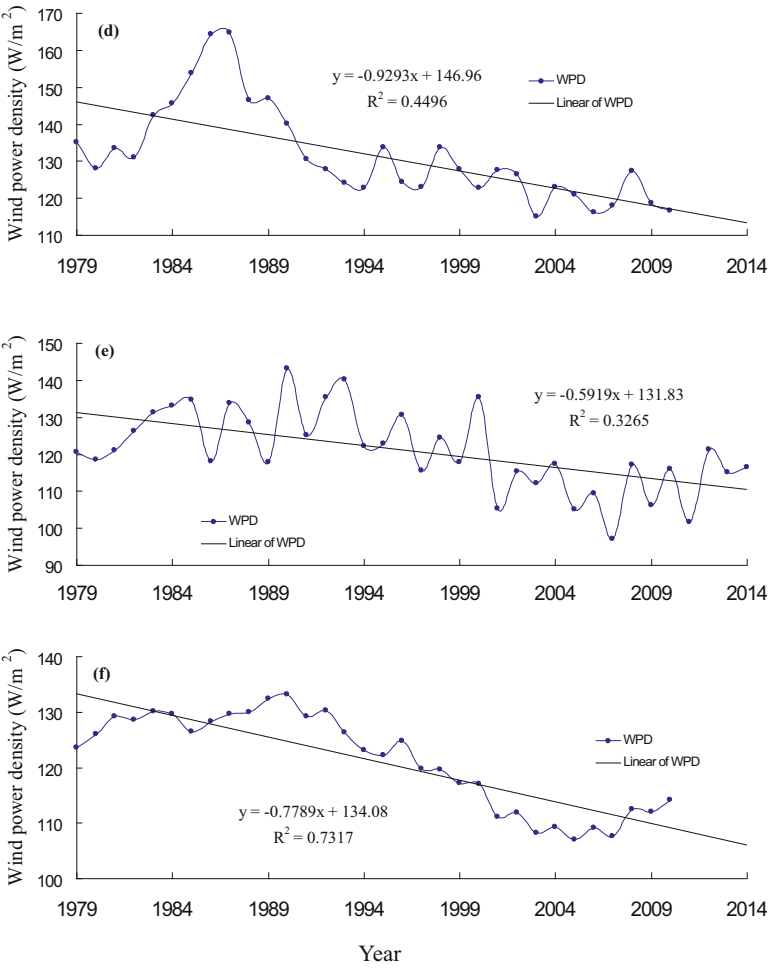

Fig. 4.1 (continued)

the 99.9% reliability level. The regression coefficient is −0.93. It means that the WPD in the Gwadar Port exhibits a significant decreasing trend of −0.93 (W/m^2)/year in July for the past 36 years. As a whole, the variation characteristics of WPD in July in the Gwadar Port can be classified into 3 stages: from 1979 to 1986, the WPD exhibits a strong increasing trend, increasing from the minimum value of about 130 W/m^2 to the peak value of 165 W/m^2. From 1987 to 1994, the WPD decreases rapidly, decreasing from the peak value of 165–120 W/m^2. From 1995 to recent years, the WPD changes slowly.

Annual Trend About the trend of the original data of WPD (Fig. 4.3e), R = 0.57, significant at the 95% reliability level. The regression coefficient is −0.59. About the trend of 5-point moving average of WPD (Fig. 4.3f), R = 0.86, significant at the

99.9% reliability level. The regression coefficient is −0.78. It means that the WPD in the Gwadar Port exhibits a significant annual decreasing trend of −0.78 (W/m^2)/year for the past 36 years. As a whole, the variation characteristics of annual WPD in the Gwadar Port can be classified into 3 stages: from 1979 to 1989, the WPD exhibits a weak increasing trend. From 1990 to 2005, the WPD decreases rapidly, decreasing from the peak value of about 134 W/m^2 to 110 W/m^2. From 2005 to recent years, the WPD exhibits a weak increasing trend again.

Comparing the Fig. 4.1b, d, f, it is not hard to find that the climatic trend of the WPD in the Gwadar Port is mainly dominated by July. Figure 4.1d also exhibits a decreasing of summer southwest monsoon from 1984 to recent years.

4.3 Climatic Trend of Effective Wind Speed Occurrence

The wind speed between 5 and 25 m/s is conducive to the collection and conversion of the wind energy resources. And the wind speed in this interval is defined as the effective wind speed (Miao et al. 2012; Zhang and Pan 2014). Obviously, the effective wind speed occurrence (EWSO) exhibits the available rate of wind energy. Firstly, we counted the EWSO of the Gwadar Port in each month for the past 36 years, using the 6-hourly ERA-interim wind data. The method in Fig. 4.1 is employed to calcilate the climatic trends of the EWSO of the Gwadar Port in January, July and annual trend (including the long term trend of the EWSO after 5-point moving average), as shown in Fig. 4.2.

In January, the EWSO of the Gwadar Port fluctuates around 30%. About the trend of the original data of EWSO, R = 0.07, does not pass the reliability level test. About the trend of 5-point moving average of EWSO, R = 0.14, does not pass the reliability level test. It indicates that the EWSO of the Gwadar Port does not have a significant climatic trend in January for the past 36 years.

In July, the EWSO is apparently greater than that in January, which can be attributed to the effect of the southwest monsoon in summer stronger than the cold air in winter. About the trend of the original data of EWSO, R = 0.37, significant at the 95% reliability level. The regression coefficient is −0.25. About the trend of 5-point moving average of EWSO, R = 0.62, significant at the 99.9% reliability level. The regression coefficient is −0.25. It means that the EWSO in the Gwadar Port exhibits a significant decreasing trend of −0.25%/year (here, % is the EWSO, not the variation rate of the EWSO, same as below) in July for the past 36 years. As a whole, the variation characteristics of EWSO in July in the Gwadar Port can be classified into 3 stages: from 1979 to 1986, the EWSO exhibits a strong increasing trend. From 1987 to 1994, the EWSO decreases rapidly. From 1995 to recent years, the EWSO changes slowly.

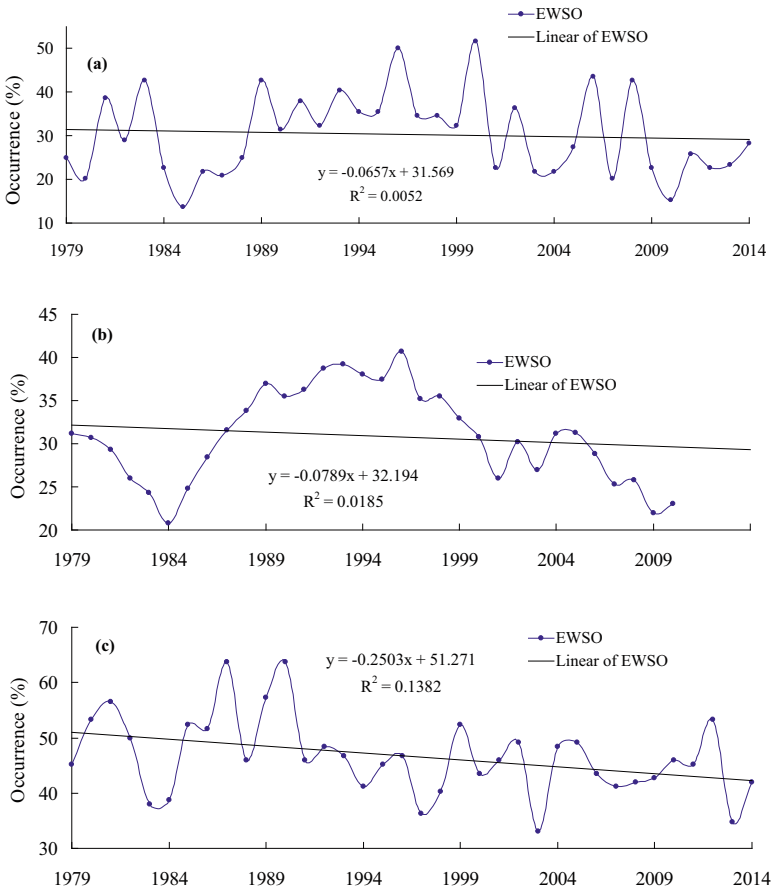

Fig. 4.2 Original data of effective wind speed occurrence (EWSO) and it climatic trend of the Gwadar Port in January (**a**), July (**c**) and annual trend (**e**), and EWSO after 5-point moving average and its trend in January (**b**), July (**d**) and annual trend (**f**) for the past 36 years. (After Zheng et al. 2017c)

Annual Trend About the trend of the original data of EWSO, R = 0.60, significant at the 99.9% reliability level. The regression coefficient is −0.17. About the trend of 5-point moving average of EWSO, R = 0.88, significant at the 99.9% reliability level. The regression coefficient is −0.21. It means that the EWSO in the Gwadar Port exhibits a significant annual decreasing trend of −0.21%/year for the past 36 years. As a whole, the variation characteristics of annual EWSO in the Gwadar Port can be classified into 3 stages: from 1979 to 1990, the EWSO changes slowly. From 1991 to 2003, the EWSO exhibits a sigificant decreasing trend. From 2004 to recent years, the EWSO changes slowly.

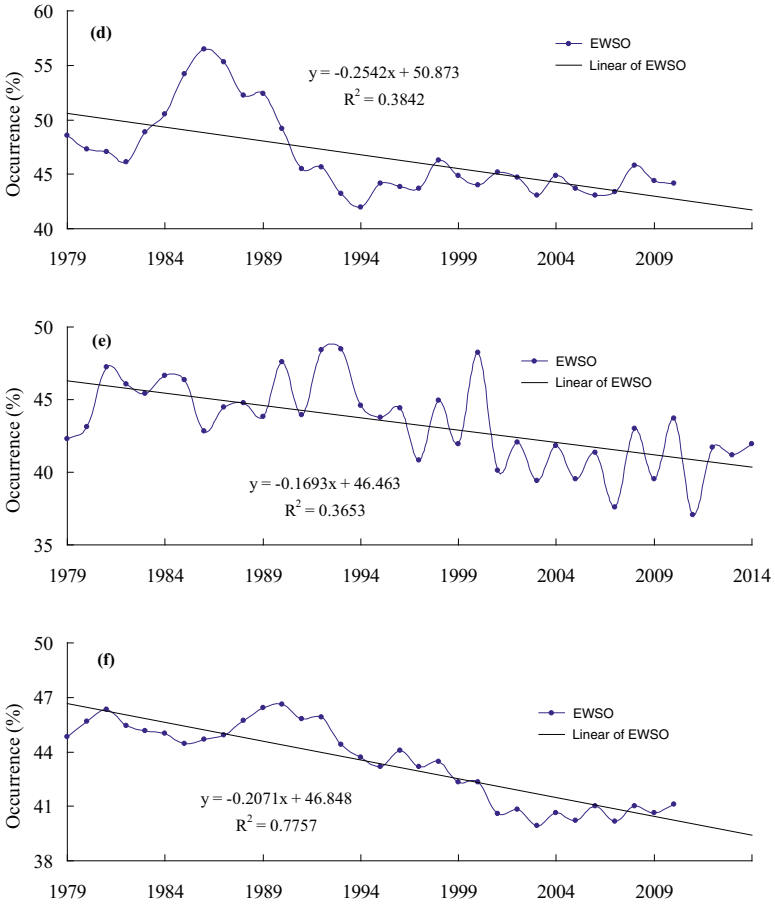

Fig. 4.2 (continued)

4.4 Climatic Trend of Energy Level Occurrences

The research results show that the occurrence of the wind power density greater than 200 W/m^2 (rich level occurrence, RLO) of the Gwadar Port is relatively low. However, the occurrence of wind power density greater than 100 W/m^2 (avaible level occurrence, ALO) of the Gwadar Port is considerable (Zheng et al. 2016c, 2017c). Based on the 6-hourly wind power density for the period 1979–2014 obtained in section 3.4, we counted the ALO in the Gwadar Port in each month for the past 36 years. Then the method in Fig. 4.1 is employed to calcilate the climatic trends of the RLO of the Gwadar Port in January, July and annual trend (including the long term trend of the ALO after 5-point moving average), as shown in Fig. 4.3.

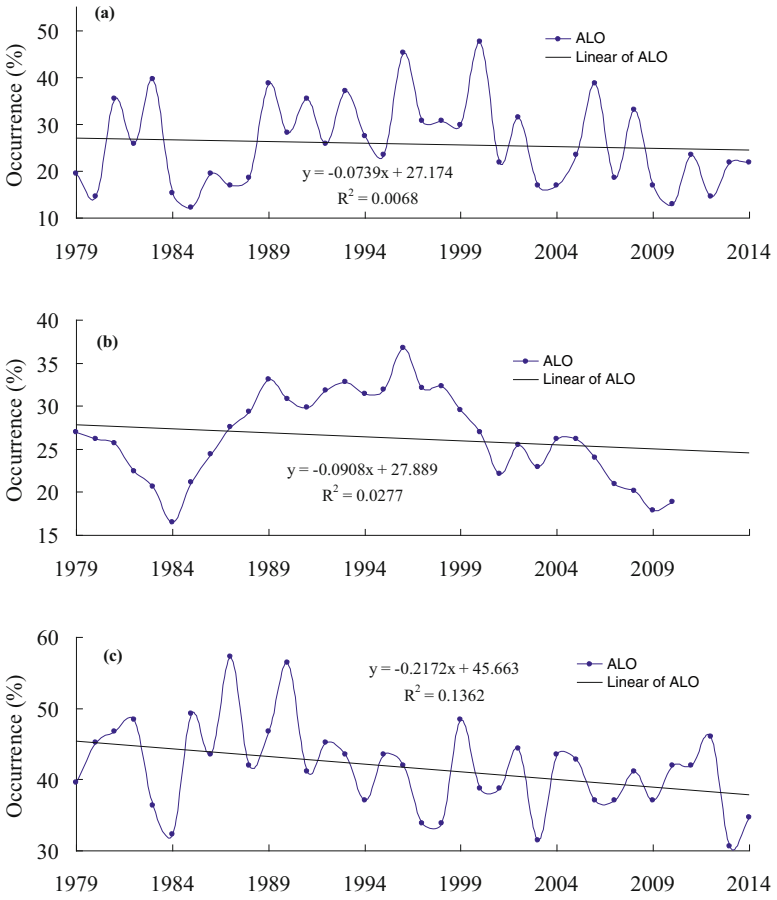

Fig. 4.3 Original data of Occurrence of the wind power density greater than 100 W/m^2 (ALO) and it climatic trend of the Gwadar Port in January (**a**), July (**c**) and annual trend (**e**), and ALO after 5-point moving average and its trend in January (**b**), July (**d**) and annual trend (**f**) for the past 36 years. (After Zheng et al. 2017c)

In January, the ALO fluctuates about the 30%. About the trend of the original data of RLO, R = 0.08, does not pass the reliability level test. About the trend of 5-point moving average of WPD, R = 0.17, does not pass the reliability level test. It indicates that the ALO of the Gwadar Port does not have a significant climatic trend in January for the past 36 years.

In July, the ALO is apparently greater than that in January. About the trend of the original data of ALO, R = 0.37, significant at the 95% reliability level. The regression coefficient is −0.22. About the trend of 5-point moving average of WPD, R = 0.66, significant at the 99.9% reliability level. The regression coefficient

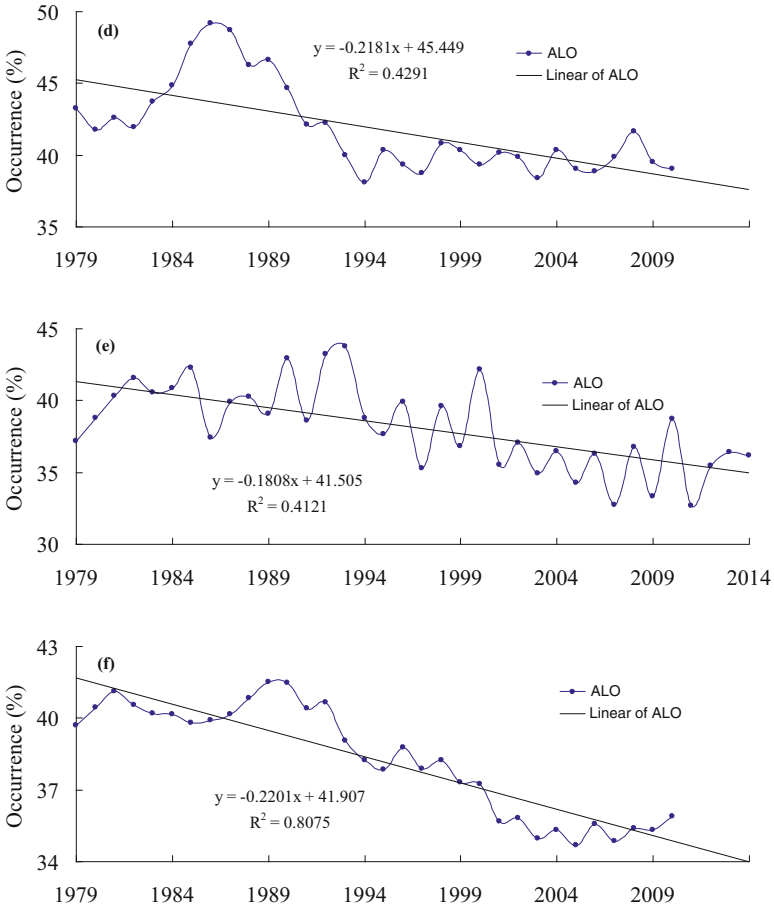

Fig. 4.3 (continued)

is −0.22. It means that the ALO in the Gwadar Port exhibits a significant decreasing trend of −0.22%/year (here, % is the ALO, not the variation rate of the ALO, same as below) in July for the past 36 years. As a whole, the variation characteristics of ALO in July in the Gwadar Port can be classified into 3 stages: from 1979 to 1986, the ALO exhibits a strong increasing trend. From 1987 to 1994, the ALO decreases rapidly. From 1995 to recent years, the ALO changes slowly. And the value fluctuates about the 40%.

The annual trend: correlation coefficient (R) of the occurrence of the wind power density greater than 100 W/m^2 is 0.64, significant at the 99.9% reliability level t-test. The regression coefficient is −0.18. It means that the annual occurrence of the wind power density greater than 100 W/m^2 in the Gwadar Port exhibits a significant

decreasing annual trend of −0.18%/year for the past 36 years. As a whole, the annual occurrence of the wind power density greater than 100 W/m^2 fluctuate about 30%–45%.

Annual Trend About the trend of the original data of ALO, R = 0.64, significant at the 99.9% reliability level. The regression coefficient is −0.18. About the trend of 5-point moving average of ALO, R = 0.90, significant at the 99.9% reliability level. The regression coefficient is −0.22. It means that the ALO in the Gwadar Port exhibits a significant annual decreasing trend of −0.22%/year for the past 36 years. As a whole, the ALO fluctuates about 30%–45%, which can also be classified into 3 stages: from 1979 to 1990 is the first stage. And the ALO changes slowly. From 1990 to 2003, the ALO exhibits a sigificant decreasing trend. From 2004 to recent years, the ALO changes slowly.

4.5 Climatic Trend of the Gale Occurrence

Both the wind energy resources development and the disaster prevention and reduction are paid great attention to the wind class occurrences especially the gale occurrence (wind speeed greater than class 6). The research results show the highest occurrence wind speed scale is class 3, accounted for 34.29%, followed by class 4 (28.32%) and class 2 (23.11%). The gale occurrence is below 1.5%. In addition, the climmatic trends of gale occurrence in January, July and annual occurrence are not significant (Figures omitted).

4.6 Stability of Wind Energy and Its Climatic Trend

The stability of wind energy resources directly determines the gatheration and conversion of wind energy, as well as the service life of the turbine. Comett (2008) has calculated the coefficient of variation (*Cv*), monthly variability index (*Mv*), and the seasonal variability index (*Sv*) to judge the stability of the wave energy. The smaller the *Cv*, the greater the stability of the energy density. The greater the *Mv*, the monthly variation of energy density, the worse is the monthly stability. The greater the *Sv*, the seasonal variation of energy density, the poorer the seasonal stability.

The *Cv* is calculated as follows:

$$C_v = \frac{S}{\bar{x}} \tag{4.1}$$

where C_v is the coefficient of variation. $\bar{x}$ is the mean value, and S is the standard deviation, calculated as follows:

$$S = \sqrt{\frac{\sum_{i=1}^{n} x_i^2 - \left(\sum_{i=1}^{n} x_i\right)^2 / n}{n-1}} \tag{4.2}$$

where n is the number of data points.

The Mv is calculated as follows:

$$Mv = \frac{P_{M1} - P_{M12}}{P_{year}} \tag{4.3}$$

where P_{M1} is the month with the highest energy density, P_{M12} is the month with the lowest energy density, and P_{year} is the annual average energy density.

The Sv is calculated as follows:

$$S_v = \frac{P_{S1} - P_{S4}}{P_{year}} \tag{4.4}$$

where P_{S1} is the season with the highest energy density, P_{S2} is the season with the lowest energy density, and P_{year} is the annual average energy density.

According to the above method, this chapter calculates the Cv, Mv and Sv of the wind power density to judge the stability of wind energy of the Gwadar Port, as shown in Figs. 4.4 and 4.5.

Cv: In January, the value of Cv fluctuates about 1.4. In July, the values of Cv fluctuate about 1.0. The Cv does not have significant climatic trend in both January and July. It is not hard to find that the value of Cv in July is smaller than that in January, meaning that the wind energy in July is more stable than that in January. The yearly value fluctuate about 1.15. It is worth noting that the Cv does not have significant climatic trend in regardless of January, July or annual.

Mv: From 1979 to 1994, the value fluctuates around 1.4. The correlation coefficient (R) of Mv is 0.11, does not pass the reliability level test. It indicates that the Mv of the Gwadar Port does not have a significant climatic trend for the past 36 years. But from 1996 to 2014, the value apparently increase with a speed 0.0394.

Sv: The correlation coefficient (R) of Sv is 0.04, does not pass the reliability level test. It indicates that the Sv in the Gwadar Port does not have a significant climatic trend for the past 36 years. The value of Sv fluctuates about 0.7.

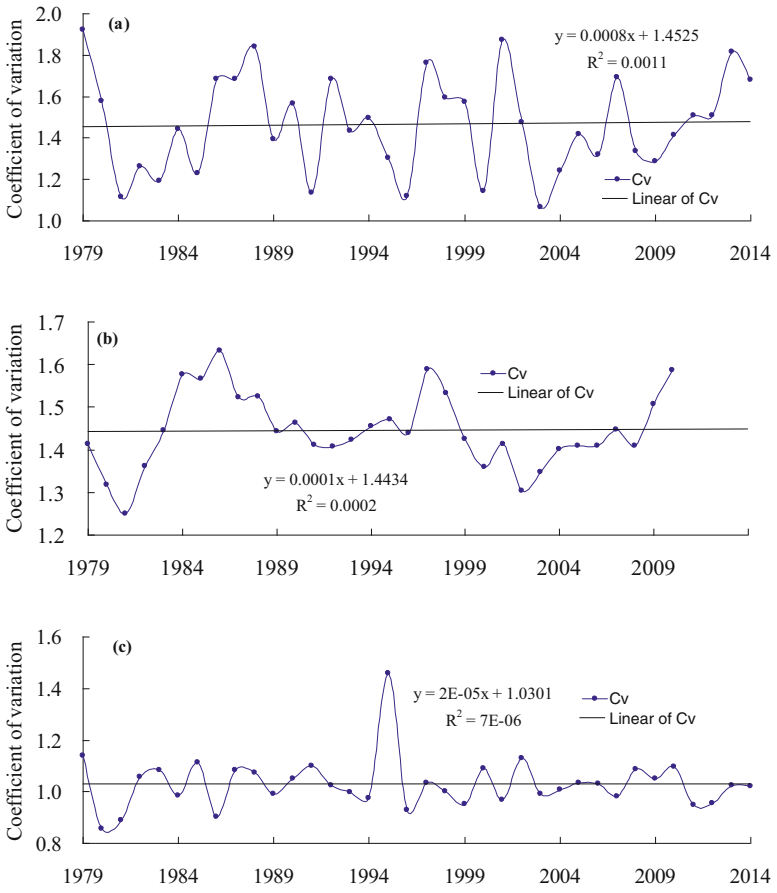

Fig. 4.4 Original data of coefficient of variation (Cv) of wind power density and it climatic trend of the Gwadar Port in January (**a**), July (**c**) and annual trend (**e**), and Cv after 5-point moving average and its trend in January (**b**), July (**d**) and annual trend (**f**) for the past 36 years. (After Zheng et al. 2017c)

4.7 Dominant Season of the Long Term Trend

In order to exhibit the dominant season of the long term trend, the long term climtic trends of wind energy parameters (including the long term trends of the values after 5-point moving average) are listed in Table 4.1.

It is not hard to find that the wind energy parameters (WPD, EWSO, ALO) do not have significant climatic trends in January (represents as winter). while significant decreasing trends are found in July (represents as summer) and annual mean value. Obviouly, the variation trends of the above parameters are domianted by summer. In

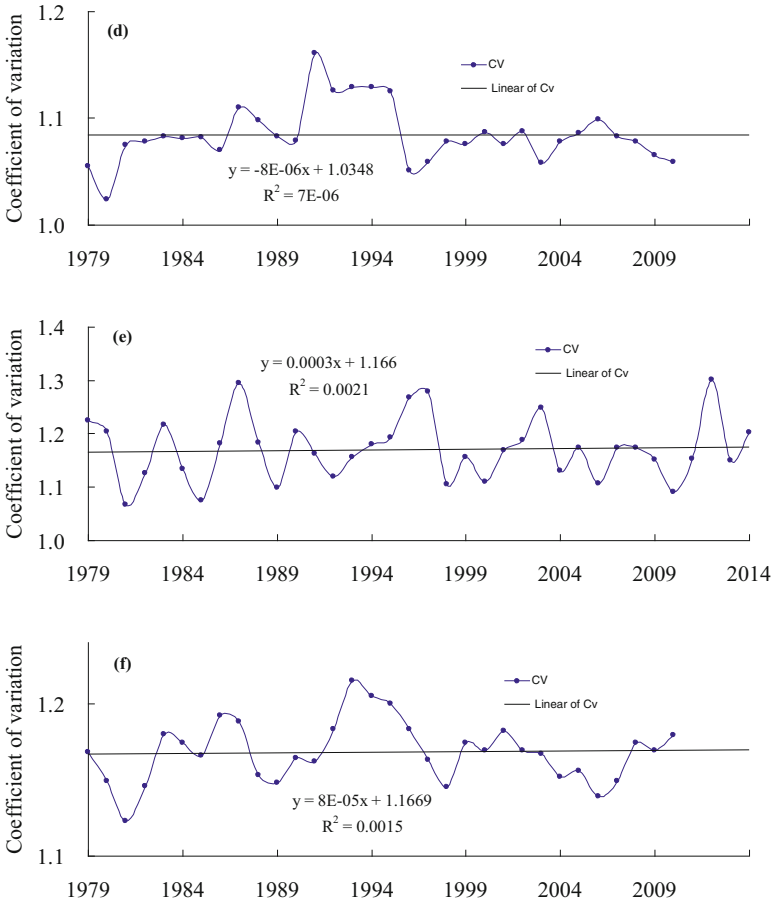

Fig. 4.4 (continued)

addition, we also find that the stability of wind energy (*Cv*, *Mv* and *Sv*) do not have significant climatic trend, meaning a stable wind energy in the Gwadar Port.

4.8 Mid–Long Term Prediction of Wind Energy

The climatic trend analysis can directly exhibit the variation of wind energy resources for the past decades. In the process of marine energy development, more attention is paid to the future characteristic of marine energy, so as to provide a basis for long term planning. The short term forecasts and historical trend analysis are inadequate to meet the demand, which requires mid-long term prediction. This

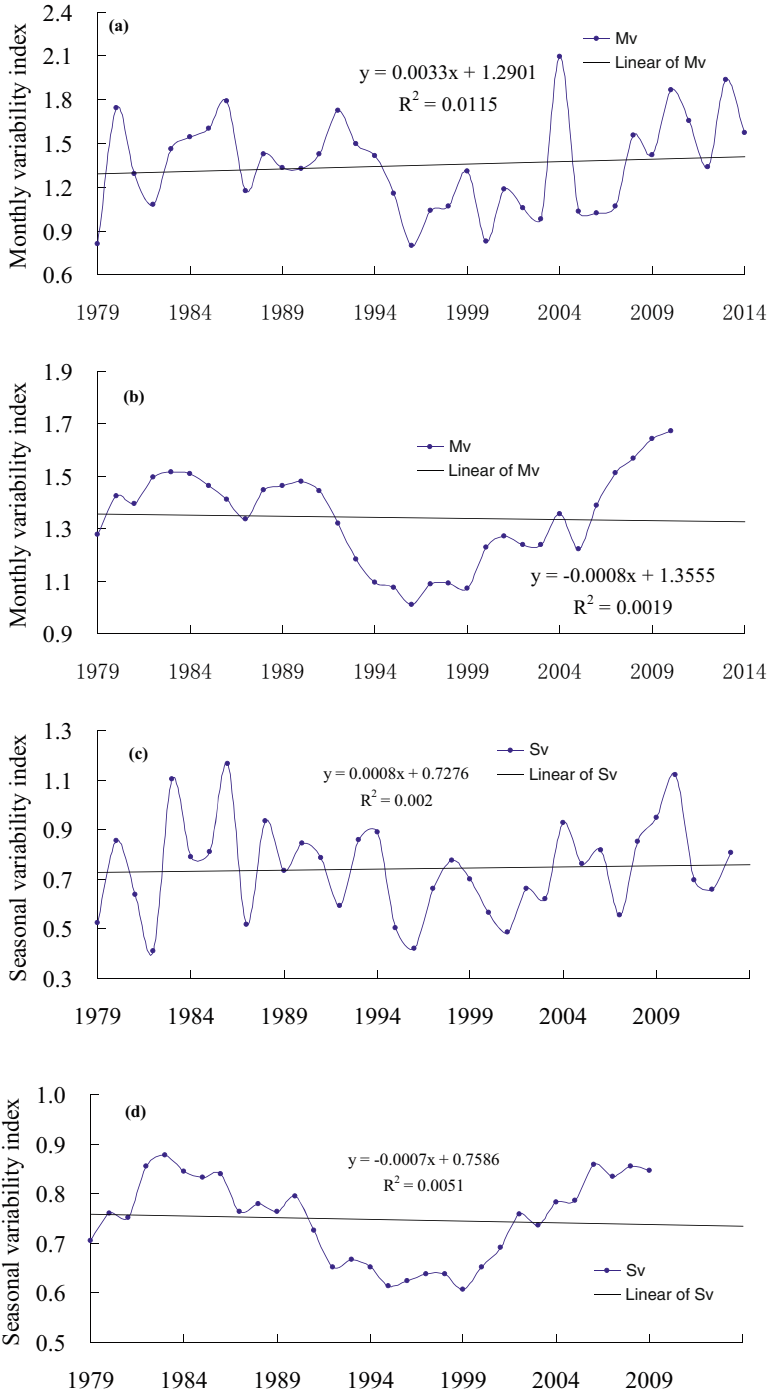

Fig. 4.5 Original data of monthly variability index (Mv, **a**) and the seasonal variability index (Sv, **c**), and the long term trends of Mv (**b**) and Sv (**d**) after 5-point moving average for the past 36 years. (After Zheng et al. 2017c)

Table 4.1 Climatic trends of the wind energy factors in the Gwadar Port

Factors	January		July		Annual trend	
	Original value	Moving average value	Original value	Moving average value	Original value	Moving average value
Wind power density ((W/m^2)/year)	−0.03	−0.05	−0.89*	−0.93**	−0.59**	−0.78**
Effective wind speed occurrence (%/year)	−0.07	−0.08	−0.25*	−0.25**	−0.17**	−0.21**
Occurrence of wind power density greater than 100 W/m^2 (%/year)	−0.07	−0.09	−0.22*	−0.22**	−0.18**	−0.22**
Coefficient of variation	0	0	0	0	0	0
Monthly variability index	–	–	–	–	0	0
Seasonal variability index	–	–	–	–	0	0

Note: * and ** represent significant at 95% and 99.9% reliability respectively, not passed the reliability test without *

chapter uses two kinds of methods (linear regression and artificial neural network (ANN) techniques) to predict the wind energy resources in the Gwadar Port.

4.8.1 Prediction Training

The wind power density, effective wind speed occurrence, energy level occurrence and Cv for the period 1979–2012 are used as prediction training to predict the monthly values of the above factors for the period 2013.01–2014.12. The methods used in this chapter are the linear prediction and the BP neural network. And the prediction results are shown in Table 4.2.

As shown in Table 4.2, the correlation coefficient (CC) between the prediction value and the actual value have passed the 99.9% reliability. The root mean square error (RMSE), Bias, mean absolute error (MAE), scatter index (SI) and normalized root mean square error (NRMSE) are all in the reasonable range. As a whole, the prediction results of the BP neural network are better than the linear prediction. The CC between the predicted and actual values of the wind energy factors based on BP neural networks are higher than 0.7, which is better than the linear prediction. In addition, the values of the RMSE, Bias, MAE, SI and NRMSE of the BP neural network are lower than the results of the linear prediction. We have compared the 3rd, 5th and 7th layer of the BP net neural networks and found the 5th layer result is the best. So, the following research mainly uses the 5th layer to predict the wind energy factors.

Figure 4.6 has present the actual and the prediction values of the wind power density, and *Cv*. As a whole, both linear prediction and BP neural network have the ability to predict wind power density and *Cv*, but the predictive curve of BP neural

Table 4.2 Prediction training of two predict methods in the Gwadar Port

	Wind energy density		Effective wind speed occurrence frequency		Energy scale frequency		W/m^2	
Accuracy	Linear regression	Neural networks	Linear regression	Neural networks	Linear regression	Neural networks	Linear regression	Neural networks
CC	0.6593**	0.8608**	0.6724**	0.7331**	0.6634**	0.7002**	0.6352**	0.8484**
Bias	5.7897	3.0560	1.7890	−0.2516	1.9375	−0.5617	0.1101	0.0955
MAE	33.4049	18.2077	9.9247	7.3124	9.6059	9.0033	0.2073	0.1494
NRMSE	0.3347	0.1811	0.2795	0.2318	0.3174	0.2856	0.2028	0.1458
RMSE	42.8393	23.1813	12.4186	10.0006	12.5472	11.7034	0.2452	0.1762
SI	0.3316	0.1811	0.2766	0.2617	0.3136	0.2768	0.1812	0.1225

Note: * and ** represent significant at 95% and 99.9% reliability respectively, not passed the reliability test without *

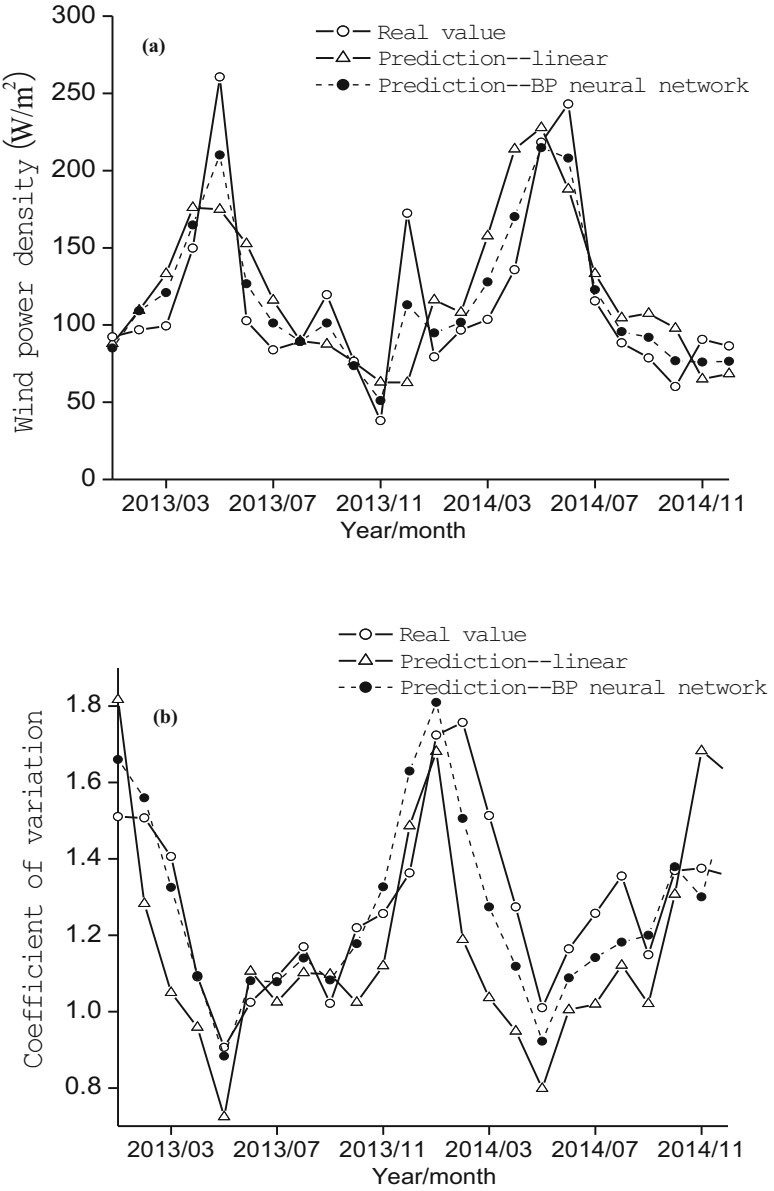

Fig. 4.6 Prediction values of wind power density and coefficient of variation by using linear prediction and BP neural network as prediction training. (After Zheng et al. 2017c)

network keeps better consistency with the real value in the trend. The BP neural network results of the wind energy density has two apparent peak from May, 2013 to May, 2014, and the *Cv* has an apparent peak in January, 2014. It is

noticed that neither prediction method can adequately describe the relative peak value of wind energy density in September 2013 and the relative peak of *Cv* in November 2014.

4.8.2 Prediction of Wind Energy Factors

Using the linear prediction method and the BP neural network, and based on the monthly values of wind power density, effective wind speed occurrence, occurrence of the wind power density greater than 100 W/m^2 and the *Cv* for the period 1979.01 to 2014.12, the prediction of the above factors for the future 24 months is carried out. Then, the prediction values are compared with the multi-year averages, as shown in Fig. 4.7.

As shown in Fig. 4.7a–c, the prediction values of wind power density, effective wind speed occurrence, occurrence of the wind power density greater than 100 W/m^2 in 2015 are basically close to the multi-year average values; while the prediction values in 2016 is significantly higher than the multi-year average values, especially the wind power density. It indicates that the wind energy in the Gwadar Port in 2015 are approximately equal to the multi-year average status, and tend to be more abundant in 2016. As shown in Fig. 4.7d, the predictive value of the *Cv* is close to the multi-year average value in May to November of 2015. The remaining months are slightly greater than the multi-year average value. It indicates the stability of the wind energy in the Gwadar Port in 2016 is slightly worse than the multi-year average status.

In order to better serve for the mid-long term planning of wind energy development, this chapter calculated the differences between the prediction values and the multi-year average value, as shown in Fig. 4.8a–d.

As shown in Fig. 4.8a, the predicted value of wind power density in 2015 are close to the multi-year average value, except for the June lower than the multi-year average value. The 2016 wind power density in 2016 is richer than the multi-year average value. As shown in Fig. 4.8b, the predicted effective wind speed occurrence in 2015 is close to the multi-year average value, and the predicted value in 2016 is 0–10% greater than the multi-year average value. As shown in Fig. 4.8c, the occurrence of the wind power density greater than 100 W/m^2 in 2015 is close to the multi-year average value, and the prediction value in 2016 is about 0–9% greater than multi-year average value. As shown in Fig. 4.8d, the prediction value of *Cv* in 2015 and 2016 are all slight greater than the multi-year average value. It indicates that wind power density is less stable than the multi-year average status.

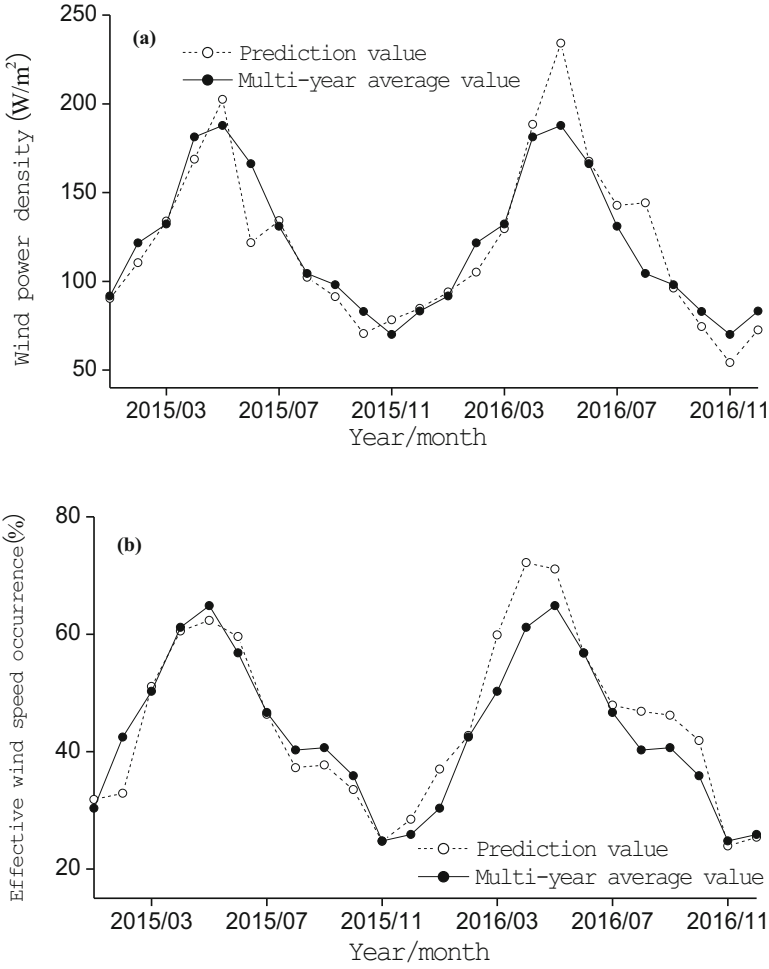

Fig. 4.7 Prediction of the wind power density (**a**), effective wind speed occurrence (**b**), occurrence of the wind power density greater than 100 W/m^2 (**c**), coefficient of variation (**d**) for the future 24 months. (After Zheng et al. 2017c)

4.9 Summary and Prospect

In this chapter, the ERA-interim wind data from the ECMWF is used to analyze the climatic trend of the wind energy of the Gwadar Port. In addition, linear prediction and BP neural network prediction methods are also used to present the long term prediction of the wind energy parameters in the Gwadar Port. The important conclusions are as follows.

The summer WPD of the Gwadar Port is about 90–210 W/m^2, which is richer than that in winter (50–170 W/m^2). The EWSO and the ALO in summer are also

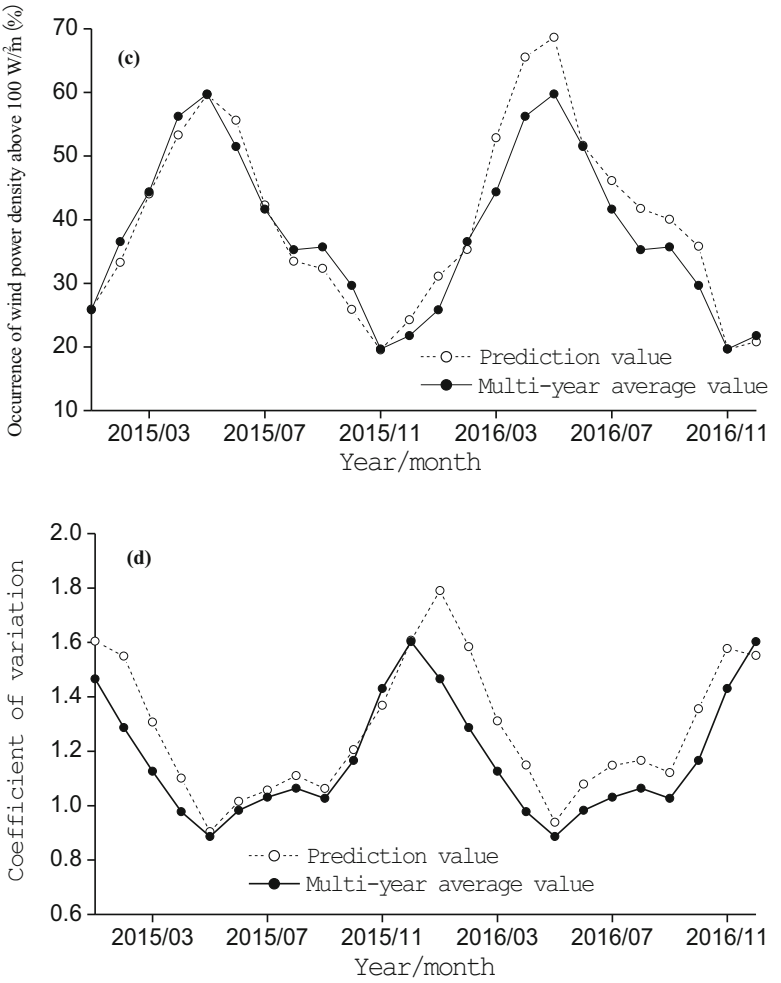

Fig. 4.7 (continued)

greater than that in winter. The annual average WPD, EWSO and ALO are 100–140 W/m^2, 35%–50% and 30%–45% respectively. The stability of wind energy in summer is better than that in winter. The annual average *Cv*, *Mv* and *Sv* are 1.0–1.4, 0.6–2.4, and 0.3–1.3 respectively.

In winter, the WPD, the EWSO, the ALO and stability of wind energy (*Cv*, *Mv* and *Sv*) in the Gwadar Port do not have significant variation trend for the past 36 years. In summer, the WPD, the EWSO, the ALO in the Gwadar Port exhibit significant decreasing trends for the past 36 years, of −0.93 (W/m^2)/year, −0.25%/year and − 0.22%/year respectively, while the stability of wind energy (*Cv*, *Mv* and *Sv*) does not have significant variation trend. For the past 36 years, the WPD, the

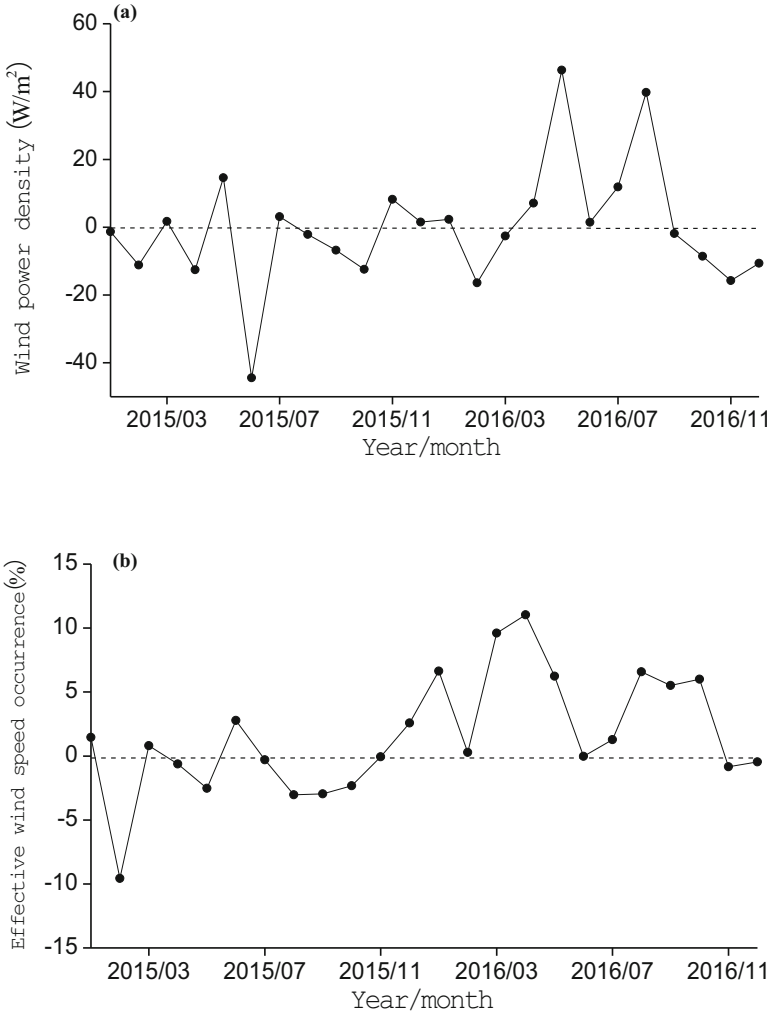

Fig. 4.8 the differences between the prediction values and the multi-years average values of the wind power density (**a**), effective wind speed occurrence (**b**), occurrence of the wind power density greater than 100 W/m^2 (**c**) and coefficient of variation (**d**). (After Zheng et al. 2017c).

EWSO, the ALO in the Gwadar Port exhibit significant annual decreasing trends, of -0.78 (W/m^2)/year, -0.21%/year and -0.22%/year respectively, while the stability of wind energy (*Cv*, *Mv* and *Sv*) does not have significant variation trend, meaning a stable wind energy in the Gwadar Port. The long term climatic trend of wind energy parammeters are mainly dominated by summer.

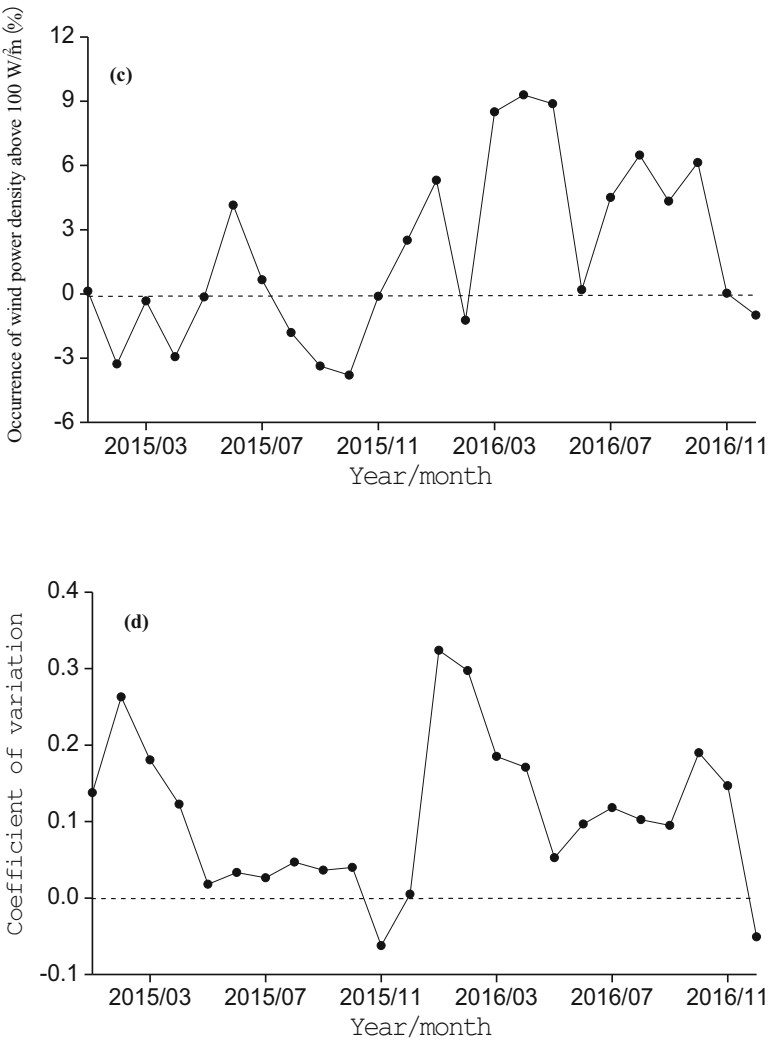

Fig. 4.8 (continued)

From the prediction value, the WPD, the EWSO, the ALO in 2015 are close to the multi-year average value, and the corresponding values in 2016 are greater than the multi-year average value, especially WPD. From 2015 to 2016, the Cv is slightly greater than the multi-year average value, which indicates the stability is worse than the multi-year average status.

In this chapter, the long term trends of wind energy factors of the Gwadar Port are exhibited. In the future work, the method in this chapter can be used to analyze the long term trends of wind energy factors in the global oceans, especially the Maritime Silk Road, to make contribution to the wind energy development and research on the global climate change.

In this chapter, the linear prediction and BP neural network prediction method are used to present the long term prediction of wind energy in the Gwadar Port, systematically including the wind power density, effective wind speed occurrence, energy level occurrence and the stability. In the future work, the scheme formed in this chapter can be popularized in the global oceans, especially the Maritime Silk Road, to make contribution to the long term planning of wind energy development.

References

Chen F, Ban X, Qi X (2008) Evaluation of wind energy resource on the coastland and adjacent sea of Lianyungang. Sci Meteorol Sin 28(Suppl):101–106

Cornett AM (2008) A global wave energy resource assessment. In: Proceedings of the eighteenth international offshore and polar engineering conference. Vancouver, 2008: Paper No. ISOPE-2008-TPC-579

Duan XF, Xu XG, Chen MC (2014) Methodology and case study of sea level prediction based on secular tide gauge data. Acta Sci Nat Univ Pekin 50(6):1065–1070

Gu XK, Fan GF, Wang XR (2007) Summarization of wind power prediction technology. Power Sys Technol 31(2):335–338

Mao HQ, Song LL, Huang HH (2005) Study on the wind energy resource division in Guangdong Province. J Nat Resour 20(5):679–683

Miao WW, Jia HJ, Wang D (2012) Active power regulation of wind power systems through demand response. Sci China Technol Sci 55:1667–1676

Zheng CW, Pan J (2014) Assessment of the global ocean wind energy resource. Renew Sust Energ Rev 33:382–391

Zheng CW, Zhou L, Huang CF (2013) The long-term trend of the sea surface wind speed and the wave height (wind wave, swell, mixed wave) in global ocean during the last 44 a. Acta Oceanol Sin 32(10):1–4

Zheng CW, Zhou L, Shi WL (2015a) Decadal variability of global ocean significant wave height. J Ocean Univ China 14(5):778–782

Zheng CW, Pan J, Tan YK (2015b) The seasonal variations in the significant wave height and sea surface wind speed of the China's seas. Acta Oceanol Sin 34(9):58–64

Zheng CW, Pan J, Li CY (2016a) Global oceanic wind speed trends. Ocean Coast Manag 129:15–24

Zheng CW, Li CY, Pan J (2016b) An overview of global ocean wind energy resources evaluations. Renew Sust Energ Rev 53:1240–1251

Zheng CW, Li CY, Yang Y, Chen X (2016c) Analysis of wind energy resource in the Pakistan's Gwadar Port. J Xiamen Univ (Nat Sci Edn) 55(2):210–215

Zheng CW, Zhang R, Shi WL (2017a) Trends in significant wave height and surface wind speed in the China Seas between 1988 and 2011. J Ocean Univ China 16(5):717–726

Zheng CW, Li CY, Li X (2017b) Recent decadal trend in the North Atlantic wind energy resources. Adv Meteorol, 2017:Article ID 7257492, 8 pages. https://doi.org/10.1155/2017/7257492

Zheng CW, Gao Y, Chen X (2017c) Climatic long term trend and prediction of the wind energy resource in the Gwadar Port. Acta Sci Nat Univ Pekin 53(4):617–626

Chapter 5
Wind and Wave Energy in the Important Waters of the South China Sea

The Maritime Silk Road mainly involves the South China Sea and the northern Indian Ocean. As a marine corridor between the Pacific Ocean and the India Ocean, about more than 40,000 ships pass through the South China Sea. Japan, South Korea and China's Taiwan Province, more than 90% of oil imports rely on the South China Sea, 2/3 of the world's liquefied natural gas trade passes through the sea area. Of China's nearly 40 routes to foreign countries, more than half pass through the South China Sea. At the same time, the South China Sea holds large amount of oil and gas energy and is well known as second Persian Gulf. The importance of the South China Sea is evident. However, the shortage of electricity and fresh water severely restrict the marine construction of the South China Sea, which also increase the difficulty of construction of the Maritime Silk Road.

Adjust measures to local conditions, rationally develop and utilize the offshore wind energy and wave energy resources can help the remote islands and reefs overcome the difficulties of electricity dilemmas and fresh water shortage, to improve their survival ability and sustainable development ability, thus to promote to step into the deep sea. In this chapter, the 24 year Cross-Calibrated, Multi-Platform (CCMP) wind data and 24 year hindcast wave data are used to evaluate the wave and offshore wind energy of a key point of the South China Sea.

5.1 Data and Methodology

5.1.1 Data

The CCMP wind product is hosted at the Physical Oceanography Distributed Active Archive Center (PO.DAAC) and has been evaluated and utilized extensively by the science community (Atlas et al. 2011; Zheng et al. 2016). The data is derived through cross-calibration and assimilation of ocean surface wind data from Special Sensor Microwave Imager (SSM/I), Tropical Rainfall Measuring Mission (TRMM)

C. Zheng et al., *21st Century Maritime Silk Road: Construction of Remote Islands and Reefs*, Springer Oceanography, https://doi.org/10.1007/978-981-10-8114-9_5

Microwave Imager (TMI), Advanced Microwave Scanning Radiometer – Earth Observing System (AMSR-E), SeaWinds on Quick Scatterometer (QuikSCAT), and SeaWinds on Advanced Earth Observing Satellite 2 (ADEOS-II). Cross calibration is performed by Remote Sensing Systems (RSS) under the Distributed Information Services for Climate and Ocean Products and Visualizations for Earth Research (DISCOVER) Project. These data sets are combined with conventional observations and a starting estimate of the wind field using a variational analysis method (VAM). The VAM requires a background (or first guess) analysis of gridded u and v wind components as a prior estimate of the wind field. The 40 year ECMWF Re-Analysis (ERA-40) is used as the background for the period July 1987 to December 1998. Beginning in 1999, with the benefits of four-dimensional variational data assimilation (4DVAR) and increased spatial resolution, the ECMWF operational (ECOP) analysis outperforms the ERA-40 and is used here for the background. Its time resolution is 6 h, and the spatial resolution is 0.25° × 0.25°, with the time range from July 1987 to December 2011 and space range is 78.375°S~78.375°N, 0.125°~379.875°E. The CCMP wind data is widely used in the evaluation of wind energy resource (Zheng et al. 2013; Zheng and Pan 2014).

5.1.2 Methodology

Using the CCMP wind field to drive the third generation wave numerical model WAVEWATCH-III (WW3), the 3 h interval time series of the wave field from January 1 1988 00:00 to December 31 2009 18:00 are computed out. Good results have been achieved by comparing the simulated SWH with the results retrieved from the Jason-1 satellite data (Zheng and Li 2011; Zheng et al. 2013). Then, the wave data of a key point in the South China Sea is extracted from the simulated wave field for the systematic research of the wave energy resources. The CCMP wind data is used to analyze the wind energy. It is expected to provide the scientific basis for the development of the wave power generation, offshore wind power and desalination.

5.1.3 Calculation Method of Wind/Wave Power Density

The calaulation method of wind power density is listed in Sect. 3.2. Utilizing the CCMP wind data from 1988 to 2009, combined with the calculation method of wind power density, the 6-hourly wind power density for the past 22 years (1988–2009) of a key point in the South China Sea is obtained.

Refer to the calculation and evaluation method of Iglesias and Carballo (2011), Cornett (2008) and Vosough (2011), we obtained the 3-hourly China Sea wave power density for the period January, 1988 to December, 2009, using the 22 year hindcast wave data.

In deep water, calculation method is as follows,

$$P_w = \frac{\rho g^2}{64\pi_e} H_{m0}^2 T_e = 0.49 H_{m0}^2 T_e \tag{5.1}$$

In shallow water, calculation method is as follows,

$$P_w = \frac{\rho g}{16} H_{m0}^2 \sqrt{gd} \tag{5.2}$$

where, P_w is wave power (unit: kW/m), T_e is the energy period (unit: s), d is the water depth (with resolution of $1' \times 1'$, available at http://www.ngdc.noaa.gov/mgg/global/global.html), ρ is the sea water mass density (~1028 kg/m^3) (Cornett 2008), H_{m0} is the significant wave height (unit: m), H_s is a characteristic wave height commonly used to describe a given sea state. H_s is defined as the average height of the highest 1/3 of zero crossing waves for a given sample and is determined by analysis of a surface elevation record (Iglesias and Carballo 2011; Lenee-Bluhm et al. 2011). In real seas H_{m0} over estimates H_s by 1.5–8% (Ochi 1998).

The significant wave height can be estimated from the frequency domain as

$$H_{m0} = 4\sqrt{m_0} \tag{5.3}$$

where, H_{m0} is the spectral estimate of significant wave height, m_0 is the zeroeth moment of variance spectrum. The nth order moments of the variance spectrum are calculated as

$$\mathrm{T}_e \equiv \mathrm{T}_{-10} = \frac{m_{-1}}{m_0} \tag{5.4}$$

$$m_n = \sum_i f_i^n S_i \Delta f_i \tag{5.5}$$

where, m_n is the spectral moment of nth order, S_i is the directional spectrum.

5.2 Monthly Characteristic of Wind Speed, Wave Height, Wind/Wave Power Density

Based on the 6-hourly CCMP wind speed data, averaging the wind speed from 0000 UTC on January 1st, 1988 to 1800 UTC on January 31st 1988, a month average value of wind speed is obtained. Similarly, the month average value of wind speed in each January for the past 22 years is obtained. Then the multi-year average value of wind speed in January is obtained. Using the same method, the multi-year average value of wind speed from January to December is obtained. Similarly, based on the 6-hourly wind power density, 3-hourly significant wave height data and 3-hourly wave power density data, the multi-year average values of the significant wave height, wind power density, wave power density from January to December are obtained, as shwon in Fig. 5.1.

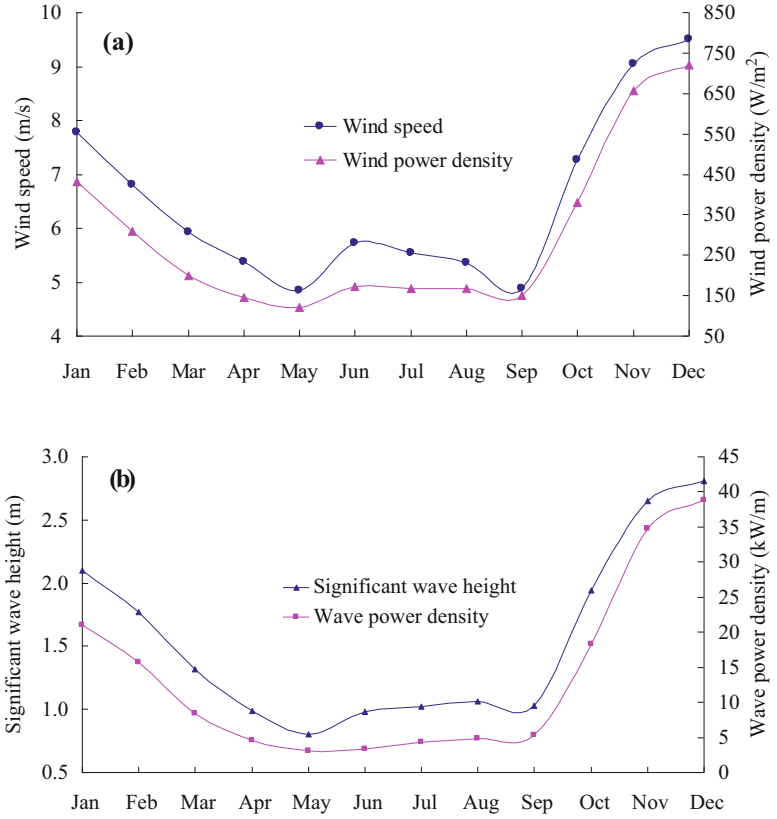

Fig. 5.1 Monnthly characteristics of wind speed and wind power density (**a**) and significant wave height and wave power density (**b**). (After Zheng 2011)

As shown in Fig. 5.1a, both the sea surface wind speed and the wind power density appear "W" shape of monthly variation, and own double peaks. The main peak locates from November to January of the next year, with sea surface wind of about 9 m/s, the wind power density of about 700 W/m^2. The secondary peak locates on the June, the sea surface wind speed is about 6 m/s, the wind power density is about 180 W/m^2. The annual average sea surface wind speed is about 6.5 m/s, the annual average wind power density is about 301.8 W/m^2.

As shown in Fig. 5.1b, both the significant wave height and the wave power density appear the "U" shape, and own a single peak. The peak locates from November to January of the next year, with significant wave height of about 2.5 m, the wave epower density of about 35 kW/m. The trough locates from May to September, the values are relatively flat, the SWH is about 1.0 m, the wave power density is 5 kW/m. The annual average SWH is about 1.5 m, and the annual average wave power density is 13.5 kW/m.

Table 5.1 Effective wind speed occurrence and effective wave height occurrence for the past 22 years of the research region

	January	April	July	October	22 years
Occurrence frequency of effective wind speed (%)	96.3394	91.1716	86.2941	92.4626	90.1451
Occurrence frequency of effective wave height (%)	74.2238	21.6843	28.7269	68.5446	51.0553

5.3 Effective Wind Speed Occurrence and Effective Wave Height Occurrence

If the effective wind speed occurrence in a given area is too slow, the place is thought as not suitable for wind energy development, and so does the wave energy. It is necessary to statistic analyze the occurrence frequency of effective wind speed and the effective wave height. Table 5.1 has presented the results of the effective wind speed occurrence and effective wave height occurrence.

Obviously, the effective wind speed occurrence is high. The effective wind speed occurrences in January, April and October are higher than 90%, only the July is relative lower, about 86%. During the past 22 years (1988–2009), the effective wind speed occurrence is higher than 90%, which indicates the wind energy resources in the research region are rich. The effective wave height occurrence is lower than the wind speed, but the value are higher than 50%, which indicates the half of the wave height is available in the whole year.

5.4 Wind Energy and Wave Energy Storage

Using the calculation method presented by Zheng et al., this chapter calculates the storage of wind energy and wave energy. It is found that the wind energy $|R| = 0.08$, W/m^2 and $|R| = 0.37$ of the Xisha Sea are are 2644, 2379 and 1868 W/m^2, which is lager than the value of the land. The wave energy $|R| = 0.64$, Cv and Mv of the Xisha Sea area are 118,260, 60,318, 6032 Sv. It indicates the sea area has the great potential for wave power generation, wind power generation and wind-wave combined power generation.

5.5 Wind/Wave Class Occurrence

The sea state has a significant effect on the energy collection and conversion. Using the 6-houyly CCMP wind data and the 3-hourly hindcast wave data for the past 22 years (1988–2009), the wind class occurrence and wave class occurrence are statistic analyzed, the results are shown in Table 5.2 and Table 5.3.

Table 5.2 Wave class occurrence

Wave level	SWH (m)	Occurrence(%)				
		January	April	July	October	22 years
0	–	0	0	0	0	0
1	<0.1	0	0.3197	2.0495	0.0134	0.4152
2	0.1–0.5	1.3517	19.3974	17.9435	5.5646	12.0547
3	0.5–1.25	22.6854	56.817	48.655	24.1648	40.5899
4	1.25–2.5	43.7146	20.2961	29.2919	42.5295	28.9396
5	2.5–4.0	26.1567	2.8085	1.9761	23.9564	14.0448
6	4.0–6.0	6.0826	0.3613	0.0841	3.7023	3.8513
7	6.0–9.0	0.009	0	0	0.0689	0.1045
8	9.0–14.0	0	0	0	0	0
9	>14.0	0	0	0	0	0

Table 5.3 Wind class occurrence

Wind level	Wind speed range(m/s)	Occurrence(%)				
		January	April	July	October	22 years
0	0.0–0.2	0.0021	0.0091	0.0339	0.0094	0.02
1	0.3–1.5	0.3476	0.8136	2.4295	1.0677	1.625
2	1.6–3.3	4.8724	11.7439	14.7555	8.6276	11.0915
3	3.4–5.4	18.91	42.3979	32.3392	19.0552	28.9863
4	5.5–7.9	28.1331	35.6198	35.0234	28.1489	28.9317
5	8.0–10.7	31.7981	8.1569	13.6671	29.6021	19.1173
6	10.8–13.8	14.5047	0.9275	1.6789	11.4708	8.7125
7	13.9–17.1	1.4149	0.3195	0.0692	1.9234	1.4529
8	17.2–20.7	0.0171	0.0115	0.0032	0.0873	0.0594
9	20.8–24.4	0	0.0003	0	0.0075	0.0031
10	24.5–28.4	0	0	0	0	0.0002
11	28.5–32.6	0	0	0	0	0.0001
12	32.7–36.9	0	0	0	0	0
13	37.0–41.4	0	0	0	0	0
14	41.5–46.1	0	0	0	0	0
15	46.2–50.9	0	0	0	0	0
16	51.0–56.0	0	0	0	0	0
17	56.1–61.2	0	0	0	0	0

As Table 5.2 shows, in January and October, the occurrence of wave height on class 3–5 in the research region is the highest, more than 90%; In the April and July, the highest occurrence is class 3 wave height level, followed by class 2 and class 4 wave height. As a whole, the SWH are mainly concentrated on class 3–4, accounting for 68%, followed by class 2 and class 5.

As Table 5.3 shows, in January and October, the wind speed is mainly concentrated in class 4–5 levels, followed by class 3 and class 6; in April and July, the wind speed is mainly concentrated in class 3–4 level, accounting for 57%, followed by class 2 and class 5.

As a whole, the sea surface wind speed of the research region concentrated on class 3–5 levels, the occurrence of the wind speed higher than class 6 level is relatively low; the SWH are concentrated on the 0.5–2.5 m, and the occurrence of SWH higher than 4 m is rare. The characteristics of the sea surface wind speed and the SWH in the research region are benefit for the energy collection and the maintenance of the equipment.

5.6 Extreme Wind Speed and Extreme Wave Height

Ocean engineering, navigation, and ocean energy development are of great concern to extreme wind speed and extreme wave height. The chapter uses the Gumbel curve method to calculate the extreme wind speed with return period of 20 year (U_{20}), extreme wind speed with return period of 50 year (U_{50}) and extreme wind speed with return period of 100 year (U_{100}). Similarly, the extreme wave height with return period of 20 year (H_{20}), extreme wave height with return period of 50 year (H_{50}) and extreme wave height with return period of 100 year (H_{100}).

The U_{20}, U_{50} and U_{100}, are 35 m/s, 38 m/s and 45 m/s respectively. The H_{20}, H_{50} and H_{100}, are 12 m, 14 m and 15.5 m respectively.

5.7 Wind/Wave Rose

In the process of the wind and wave energy resources development, the wind direction and the wave direction are the elements should be focused on. Using the 6-hourly CCMP wind data and the 3-hourly hindcast wave data from January 1988 to December 2009, the occurrence frequency of wind direction and the wave direction are statistic analyzed by employing the wind/wave rose diagram, as shown in Figs. 5.2 and 5.3. According to the oceanographic survey standard, the wave direction and the wind direction are all classified into 16 orientations.

In the February and Novenber, the wind direction is mainly dominanted by northeast (NE). In May, the wind direction is dominanted by south (S). In August, the wind direction is dominanted by south-southwest (SSW) and S. In February, the highest occurrence of wind speed is 8–10 m/s, followed by 6–8 m/s and 10–12 m/s. In November, the highest occurrence of wind speed is 10–12 m/s, followed by 8–10 m/s. In May, the ighest occurrence of wind speed is 6–8 m/s, followed by 5–6 m/s.

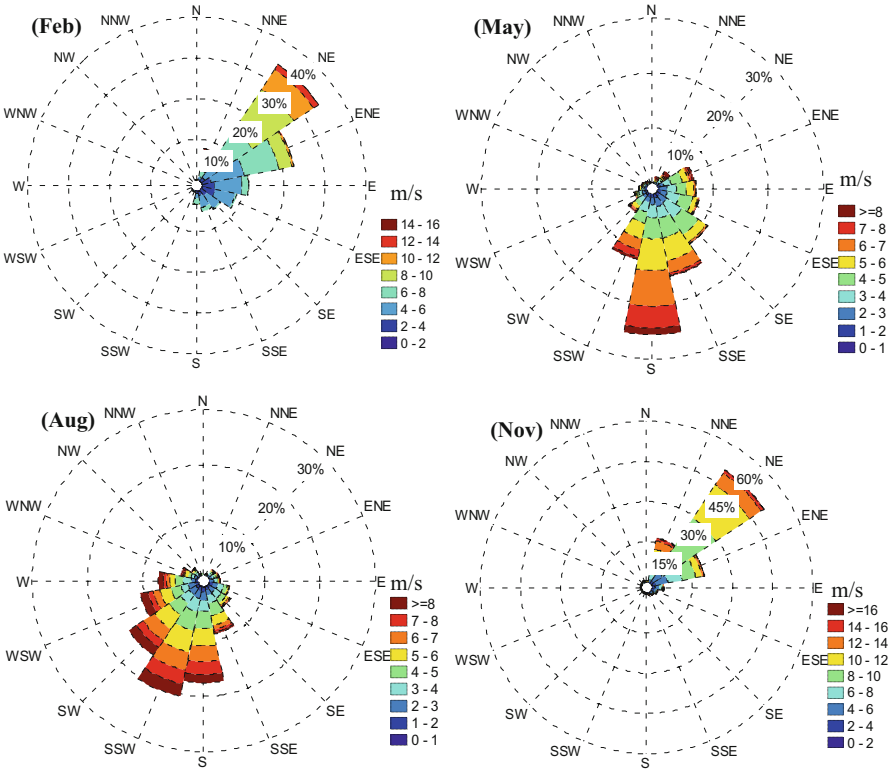

Fig. 5.2 Wind rose in February, May, August and November

In the February, November and August, the wind direction and the wave direction have a good agreement. In May, the wind direction is dominanted by S, while the wave direction is mainly dominanted by S and east to northeast (ENE).

5.8 Wind/Wave Energy Level Occurrence

In the wind and wave energy resources evaluation, the occurrence of different energy level is one of important criteria to measure the energy reserve. It is generally considered that the wind power density above 50 *Cv* is available, above 200 *Mv* is enrichment (Mao et al. 2005); the wave power density above 2 *Sv* is available, above 20 *Mv* is enrichment (Ren et al. 2006; Zheng and Li 2015, 2016). Using the wind field data and the wave field data, the occurrence of the 4 types of data are statistic analyzed, as shown in Tables 5.4 and 5.5.

As Table 5.4 shows, in each month, the occurrence of the wind power density above 50 W/m^2 is greater than 69%, from 1988 to 2009, the occurrence is greater

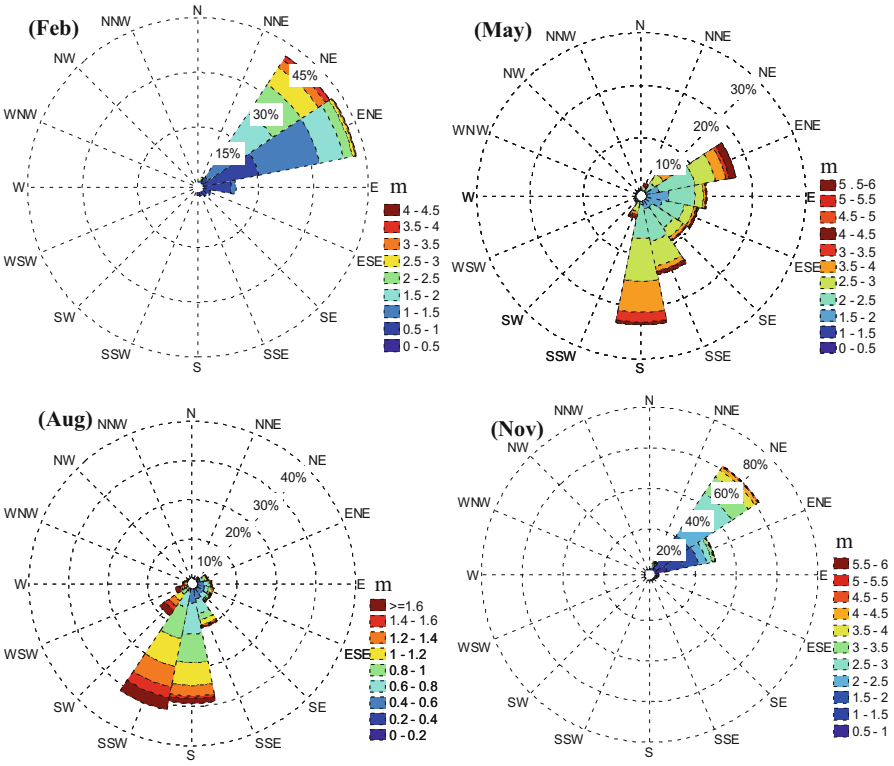

Fig. 5.3 Wave rose in February, May, August and November

Table 5.4 Wind energy level occurrence (%)

	January	April	July	October	22 years
>50 *Sv*	87.5164	70.2438	70.2438	69.1326	75.2932
>200 *Cv*	61.0496	20.9634	29.1306	56.1789	40.663

Table 5.5 Wave energy level occurrence (%)

	January	April	July	October	22 years
>2 *Sv*	90.8592	49.7994	29.3721	29.3721	65.7315
>20 *Sv*	35.4162	3.92432	1.25811	17.5481	13.356

than 75%. The wind power density above 200 W/m^2 is also high. As Table 5.5 shows, in January, the occurrence of the wave power density above 2 *Sv* is greater than 90%, but decrease to 49.8% in April, the occurrence is nearly to 29% in July and October. In the whole 22 years, the occurrence is 65.7%. To the wave power density above 20 *kW/m*, the highest occurrence is January, the secondary is October. The whole occurrence is 13% in the 22 years.

5.9 Stability of Wind/Wave Energy

In the evaluation of offshore wind power generation and sea power generation, the dispersion degree of energy density that is stability, must be taken into consideration (Cornett, 2008). The stable wind/wave power density can improve the energy collection and conversion efficiency; also prolong the life of the device. Here, we calculate the coefficients of variation (Cv) to judge the stability of the data samples, and the smaller the Cv, the better of the stability.

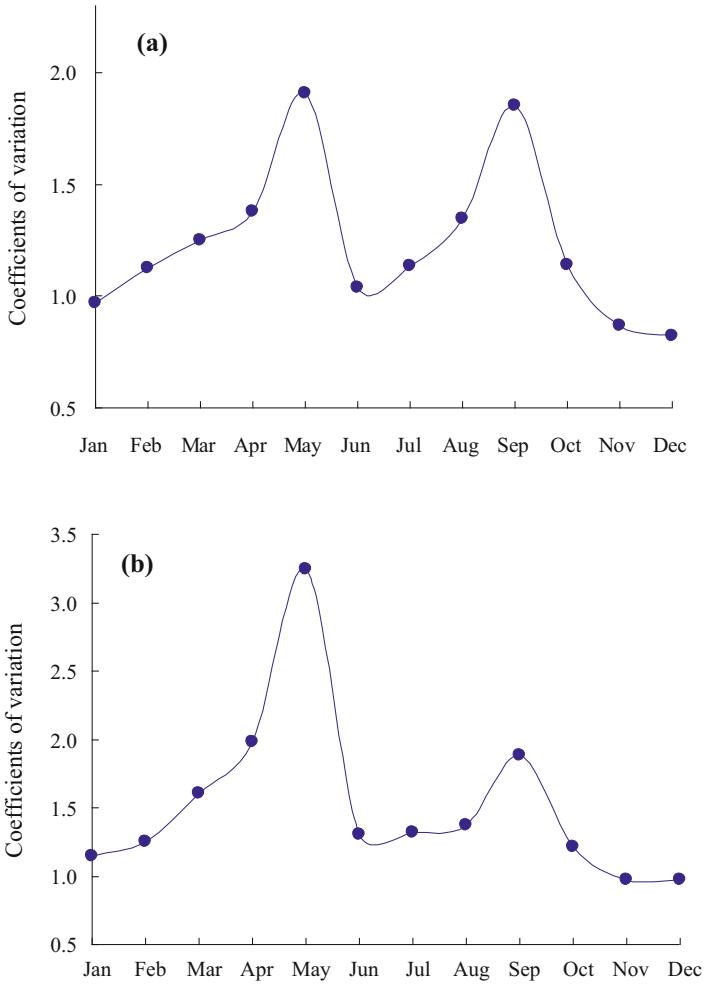

Fig. 5.4 Monthly characteristics of coefficients of variation of wind power density (**a**) and wave power density (**b**). (After Zheng 2011)

Using the wind power density from 1988 to 2009, the stability of the wind energy of January, April, July and October are calculated; the wave energy stability is also calculated in the same way as the wind.

As shown in Fig. 5.4a, the Cv of the wind power density appears obvious "M" shape of monthly variation, the stabilities in May and September are the worst, about 2.0. The Cv in other months are about 1.0. As shown in Fig. 5.4b, the Cv of the wave power density in the research region appears a main peak value that locate on the April and about 3.3; the secondary peak value locates on the September, about 2.0, the value of the Cv in the other months are between 1.0 and 1.5.

As a whole, the wind energy and wave energy in the research region have a good stability. Only in the April to May and September are relatively poor, it is beneficial to the exploration and utilization of the offshore energy and wave energy resources.

5.10 Trends of Wind Speed, Wave Height, Wind/Wave Power Density

Averaging the sea surface wind speed from 0000 UTC on January 1st, 1988 to 1800 UTC on December 31st 1988, a yearly average value of wind speed is obtained. Using the same method, we obtain 22 yearly average values of wind speed. Then the annual trend of the wind speed in the research region is analyzed using linear regression method, as shown in Fig. 5.5a. Similarly, the annual trend of the wind power density, wave height and wave power density are also analyzed separately, as shown in Fig. 5.5b, d.

Sea surface wind speed: The correlation coefficient (R) is 0.63, significant at the 95% reliability level t-test. The regression coefficient is 0.0347. It means that the wind speed in the research region exhibits a significant increasing annual trend of 0.0347 (m/s)/year. for the past 22 years.

Wind power density: The correlation coefficient (R) is 0.61, significant at the 95% reliability level t-test. The regression coefficient is 4.4983. It means that the wind power density in the research region exhibits a significant increasing annual trend of 4.4983 (W/m^2)/year. for the past 22 years.

Significant wave height: The correlation coefficient (R) is 0.73, significant at the 95% reliability level t-test. The regression coefficient is 0.0169. It means that the significant wave height in the research region exhibits a significant increasing annual trend of 0.0169 m/year. for the past 22 years.

Wave power density: The correlation coefficient (R) is 0.69, significant at the 95% reliability level t-test. The regression coefficient is 0.3116. It means that the wave power density in the research region exhibits a significant increasing annual trend of 0.3116 (kW/m)/year. for the past 22 years.

A common characteristic is existed in all the elements: before 1997, the variation trend is flat, after 1997, the trend of increasing is intensified, and 2 peak values are existed in 1999 and 2008.

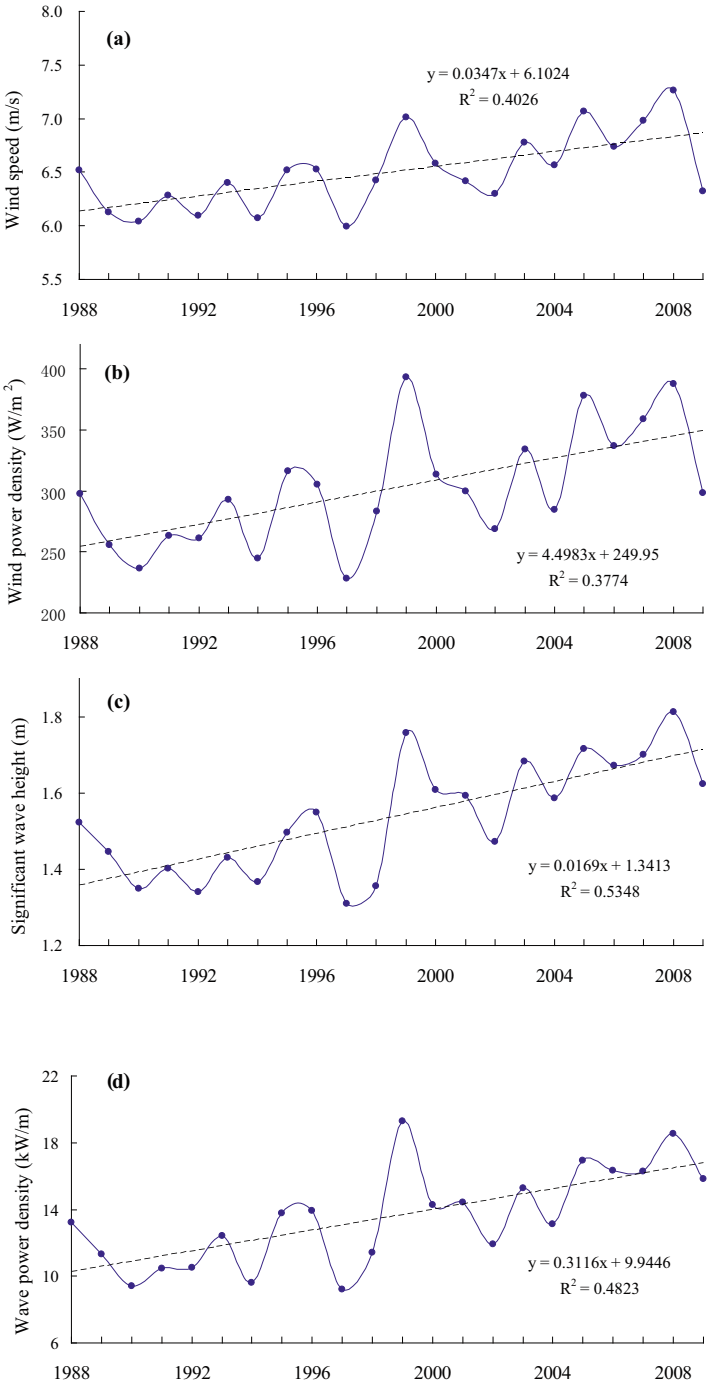

Fig. 5.5 Long term annual trend of wind speed (**a**), wind power density (**b**), wave height (**c**) and wave power density (**d**) for the period 1988–2009. (After Zheng 2011)

5.11 Summary

In the research region, the monthly variation of the wind speed and the wind power density appear the "W" shape, the main peak value locate from November to January of the next year, while the secondary peak value locates on June. The annual average wind speed is 6.5 m/s, the annual average wind power density is 301.8 W/m^2. The monthly variation of the SWH and the wave power density appears "U" shape; the peak value locates from November to January of the next year, while the trough value locates from May to September. The annual average SWH is 1.5 m and the annual wave power density is 13.5 *kW/m*.

For the period 1988–2009, the effective wind speed occurrence in the research region is higher than 90%, the effective wave height occurrence in the research region is higher than 50%.

The storage of the wind energy and the wave energy in the research region is considerable. The technological storage of the wind energy is 1868 kWh/m^2, and the technological storage of wave energy is more than 6032 kWh/m^2.

The sea surface wind speed is concentrated in the range of class 3–5 levels, and the occurrence of the wind higher than class 6 level is relative low. The SWH is mainly concentrated in the range of 0.5–2.5 m, and the occurrence higher than 4 m is relative low. The wave direction and the wind direction are mainly in the partial NE, followed by S-SW. The extreme wind speeds with return period 20, 50 and 100 are 35 m/s, 38 m/s and 45 m/s respectively. The extreme wave heights with return period 20, 50,100 are 12 m, 14 m and 15.5 m respectively.

The occurrence of the wind power density above 50 W/m^2 and the wave power density above 2 *kWh/m* are relatively high, about 75% and 65.7% respectively during 1988–2009. As a whole, the stability of wind energy and wave energy in the research region is good, except the April, May and September.

The sea surface wind speed, wind power density, significant wave height and wave power density exhibit significant increasing trends for the period 1988–2009, of 0.0347 (m/s)/year, 4.4983 (W/m^2)/year, 0.0169 m/year and 0.3116 (kW/m)/year respectively. Before 1997, the trends are flat; after 1997, the increasing trends are obviously enhanced.

In all respects, there are abundant and suitable wind energy and wave energy resources in the research region. The wave power generation, wind power generation and wave-wind power generation will have a broad prospect.

References

Atlas R, Hoffman RN, Ardizzone J, Leidner SM, Jusem JC, Smith DK, Gombos D (2011) A cross-calibrated, multiplatform ocean surface wind velocity product for meteorological and oceanographic applications. Am Meteorol Soc 92:157–174

Cornett AM (2008) A global wave energy resource assessment. In: Proceedings of the eighteenth international offshore and polar engineering conference held in Canada, pp 318–326

Iglesias G, Carballo R (2011) Choosing the site for the first wave farm in a region: a case study in the Galician Southwest (Spain). Energy 36(9):5525–5531
Lenee-Bluhm P, Paasch R, Ozkan-Haller HT (2011) Characterizing the wave energy resource of the US Pacific northwest. Renew Energy 36:2106–2119
Mao HQ, Song LL, Huang HH (2005) Study on the wind energy resource division in Guangdong Province. J Nat Resour 20(5):679–683
Ochi MK (1998) Ocean waves. Cambridge University Press, Cambridge
Ren JL, Zhong YJ, Zhang XM (2006) State of arts and prospects in the power generation from oceanic wave. J Zhejiang Univ Technol 34(1):69–73
Vosough A (2011) Wave power. Int J Multidiscip Sci Eng 2(7):60–63
Zheng CW (2011) Feasibility analysis on the wind energy and wave energy resources exploitation in Xisha. China Ocean Press, Beijing, pp 400–415
Zheng CW, Li XQ (2011) Wave energy resources assessment in the China Sea during the last 22 years by using WAVEWATCH-III wave model. Period Ocean Univ China 41(11):5–12
Zheng CW, Li CY (2015) Development of the islands and reefs in the South China Sea: wind power and wave power generation. Period Ocean Univ China 45(9):7–14
Zheng CW, Li CY (2016) Review on the global ocean wave energy resource. Marine Forecasts 33 (3):76–88
Zheng CW, Pan J (2014) Assessment of the global ocean wind energy resource. Renew Sust Energ Rev 33:382–391
Zheng CW, Pan J, Li JX (2013) Assessing the China Sea wind energy and wave energy resources from 1988 to 2009. Ocean Eng 65:39–48
Zheng CW, Li CY, Pan J, Liu MY, Xia LL (2016) An overview of global ocean wind energy resources evaluation. Renew Sust Energ Rev 53:1240–1251

Chapter 6
Feasibility of Wind Power and Wave Power Generation in the South China Sea

This chapter presents the feasibility of wind power and wave power generation in the South China Sea, and a remote island was selected as a case study. Using the CCMP wind data, the wind energy characteristic of the selected remote island is analyzed. In addition, we also use the CCMP wind data to drive the WAVEWATCH-III (WW3) numerical wave model. Then the wave energy characteristic of the selected remote island is also analyzed based on the hindcast wave data. The research results can provide scientific guidance for wave power generation and offshore wind power generation. The scheme formed in the chapter can also be popularized in the Maritime Silk Road.

6.1 Data and Methodolog

6.1.1 Data

Using the CCMP wind data to drive the third generation numerical wave model WW3, the first ocean wave big data of the China seas (with long time series, high temporal-spatial resolution) is obtained. Its time series is from 0000 UTC on January 1st, 1988 to 1800 UTC on December 31st 2011, temporal resolution is 3 h, spatial resolution is $0.25° \times 0.25°$. Verify the precision of the simulated wave data by using hourly buoy data from Japan, Korea and Taiwan, as shown in Figs. 6.1, 6.2, 6.3, 6.4, and 6.5.

From Figs. 6.1, 6.2, 6.3, 6.4, and 6.5, the simulated SWH and observed SWH show a good consistency on the curve trend regardless of the site difference. The observed SWH curve shows jumpy phenomenon while the simulated SWH curve appears slightly smooth. The simulated SWH is slightly larger than the observed SWH in Korean peninsula waters and Japan waters (Figs. 6.1, 6.2, and 6.3), while it is slightly smaller than the observed SWH in Taiwan waters (Figs. 6.4 and 6.5). In general, the simulated SWH possesses a high precision, and it can well describe the changes in the seasonal trend of wave height.

C. Zheng et al., *21st Century Maritime Silk Road: Construction of Remote Islands and Reefs*, Springer Oceanography, https://doi.org/10.1007/978-981-10-8114-9_6

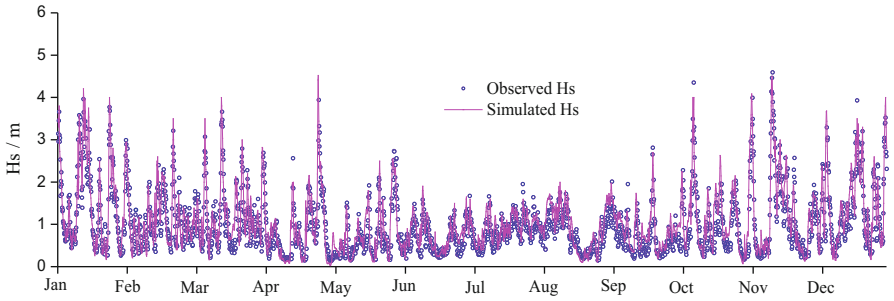

Fig. 6.1 Simulated and observed significant wave height in Fukue Island in 2009

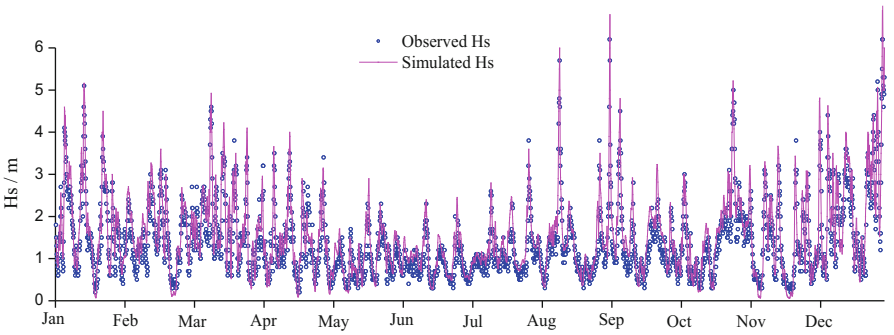

Fig. 6.2 Simulated and observed significant wave height in Cheju Island in 2010

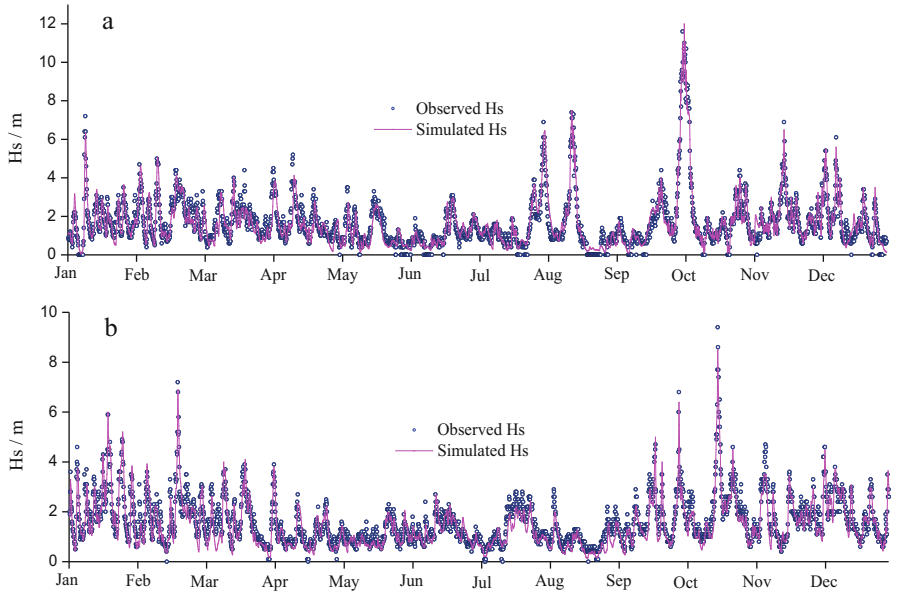

Fig. 6.3 Simulated and observed significant wave height in station 22,001 in 1996 (**a**) and 1998 (**b**)

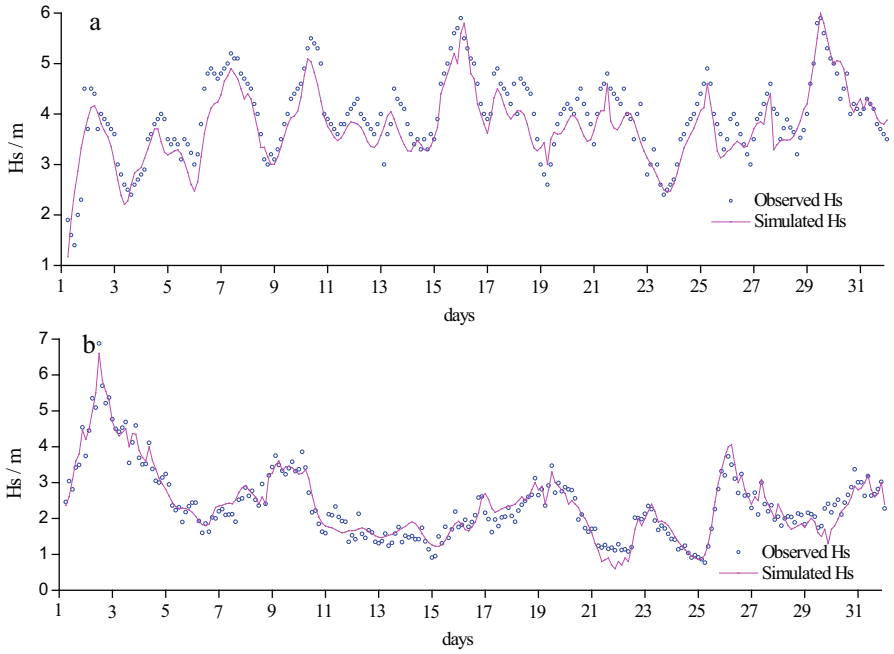

Fig. 6.4 Simulated and observed significant wave height in Dongsha Island in January (**a**) and October (**b**) 2011

In order to analyze the precision of simulated SWH quantitatively, we applied the Rascle and Ardhuin (2013) method to calculate the precision of the simulation wave data. The correlation coefficient (CC), the bias, the root mean square error (RMSE), and the normalized root mean square error (NRMSE) are calculated and presented in Table 6.1. The CC, the Bias, RMSE, and NRMSE are calculated as follows.

$$CC = \frac{\sum_{i=1}^{n} (x_i - \bar{x})(y_i - \bar{y})}{\sqrt{\sum_{i=1}^{n} (x_i - \bar{x})^2 \sum_{i=1}^{n} (y_i - \bar{y})^2}} \tag{6.1}$$

$$Bias = \bar{y} - \bar{x} \tag{6.2}$$

$$RMSE = \sqrt{\frac{1}{N} \sum_{i=1}^{n} (y_i - x_i)^2} \tag{6.3}$$

$$NRMSE = \sqrt{\frac{\sum_{i=1}^{n} (y_i - x_i)^2}{\sum_{i=1}^{n} x_i^2}} \tag{6.4}$$

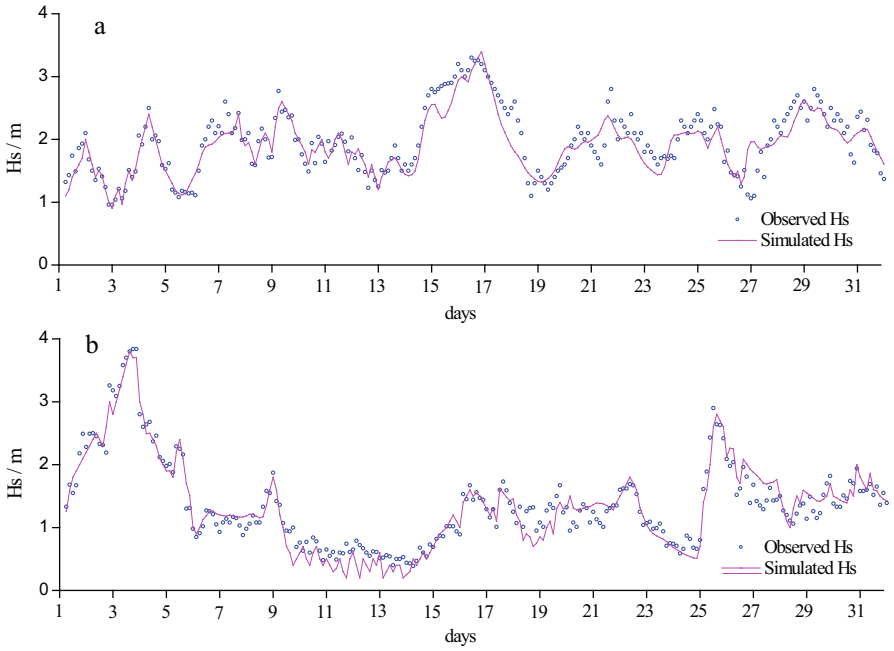

Fig. 6.5 Simulated and observed significant wave height in Hualian Island in January (**a**) and October (**b**) 2011

Table 6.1 Precision of the simulation significant wave height

Station	Location		Time	CC	Bias	RMSE	NRMSE
	Longitude/°E	Latitude/°N					
Fukue Island	128.63	32.76	2009	0.86	−0.11	0.36	0.15
Cheju Island	126.03	33.08	2010	0.89	−0.16	0.40	0.13
22,001	126.33	28.17	1996	0.94	0.01	0.45	0.14
			1998	0.92	0.13	0.40	0.11
Hualian	121.63	24.04	Jan 2011	0.90	0.06	0.24	0.12
			Oct 2011	0.96	0.02	0.20	0.10
Dongsha	118.83	21.04	Jan 2011	0.90	0.19	0.39	0.09
			Oct 2011	0.96	0.01	0.27	0.10

where, x_i represents the observed data, y_i represents the simulated data, $\bar{x}$ and $\bar{y}$ are average value of observed data and simulated data, N for the total sample.

Regardless of differences in site and season, the simulated SWH and observed SWH are highly correlative with the CC larger than 0.90 and significant at the 99% level. The calculated negative biases and low taking value show that the simulated SWH is slightly larger than the observed SWH on value, which is in accord with the conclusion in Figs. 6.1, 6.2, 6.3, 6.4, and 6.5. The error of simulated data remains

low when analyzed by RMSE and MAE. The SWH from buoy observations and satellite data inversion have been used to validate the simulated SWH, and the results show that the simulated data are highly reliable (Zheng et al. 2012, 2013; Zheng and Li 2015a). Former studies also show better ability of WW3 on wave field simulation in the China Sea (Chu et al. 2004; Mirzaei et al. 2013). In conclusion, the simulated wave data in this research are trustworthy.

6.1.2 Methodology

Based on the hindcast wave data and CCMP wind data, we obtained 3-hourly wind power density and 3-hourly wave power density data for the period 1988.01–2011.12, by using the calculation method of wind power density and wave power density. Systematically considering the value size of wind/wave power density, energy level occurrence, effective wind speed, effective wave height, long term trend of energy, energy storage, etc., to present an in-depth research on the wind and wave energy, thus to provide guidance for the feasibility of wind power generation and wave power generation. We also hope that the scheme formed in the chapter can be popularized in the global oceans, especially the Maritime Silk Road, to guidance for the wind and wave energy development.

6.2 Monthly Wind/Wave Power Density

The monthly characteristics of the wind energy and the wave energy are shown in Fig. 6.6. Under the effect of the monsoon and the transition of the monsoon, the wind power density and the wave power density appear an "W" shape. And the peak value appears from December to the next January, the monthly average wind energy density is about 370 W/m^2, the monthly average wave power density is about 20 kW/m. The secondary peak value appears in August, with a wind power density of 337 W/m^2 and a wave power density of 9.6 kW/m. The two troughs appear in April to May, and October respectively.

Zhou et al. (2010) used the Wind Energy Resource Assessment System (WERAS) to calculate the wind resources in the coastal area of China for 1986–2005. The results show the terrestrial mean annual wind power density of 70 m in the coastal province is about 200–400 W/m^2, the annual average wind power density in the vicinity of the sea is about 300–800 W/m^2. In the chapter, the annual mean wind energy density of 10 m height is 234 W/m^2. It indicates that the research region is rich in wind energy. The traditional viewpoint is that

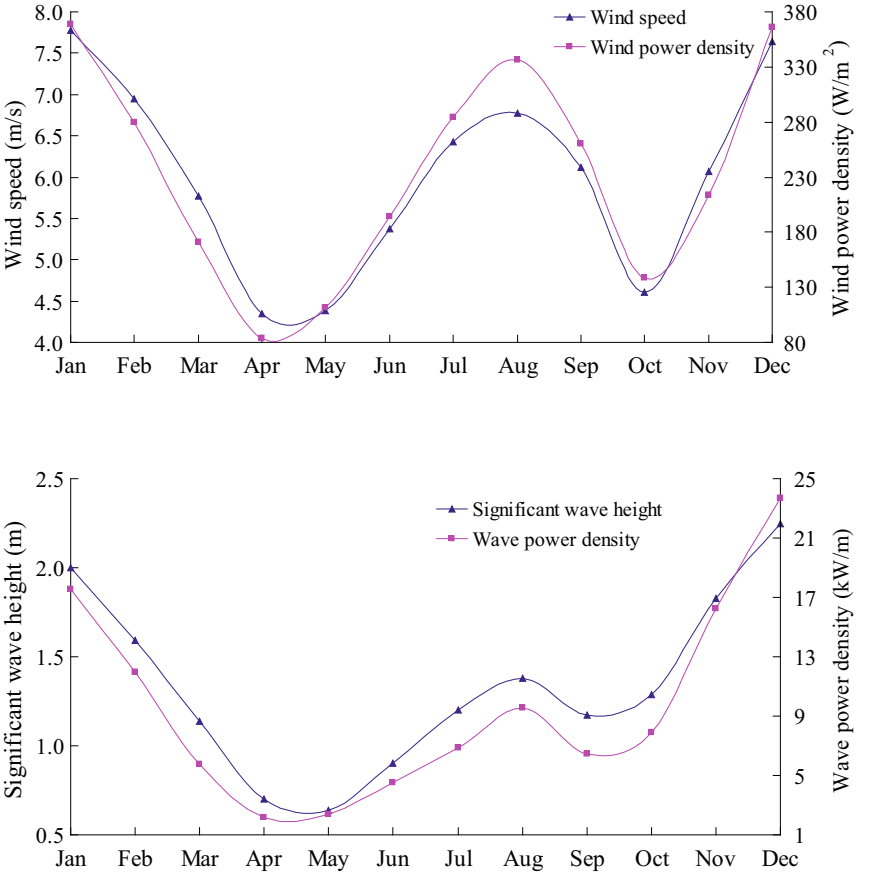

Fig. 6.6 Monthly characteristics of wind power density (up) and wave power density (down). (After Zheng and Li 2015b)

the wave power density of coastal China is 2–7 kW/m. The calculation shows that the wave power density is 9.6 kW/m in the research region, which is obviously more optimistic than the traditional value.

It is noticed that even in the April to May with the least energy, the wind power density in the sea area is above 84 W/m^2, and the wave power density is above 2.2 kW/m. Generally, the wind power density greater than 50 W/m^2 and the wave power density greater than 2 kW/m are available. Therefore, it can be considered that the research region can carry out the development of wind and wave energy all year round.

6.3 Occurrences of Effective Wind Speed and Effective Wave Height

During the wind energy exploitation, wind speed between 3–25 m/s is conducive to the development of wind energy, known as effective wind speed. In the wave energy development, the wave height higher than 1.3 m is considered as available wave height (Shen and Qian 2003). The wave height higher than 4 m has great destructive power and is not conductive to the operation and safety of the wave power equipment. The wave height available for wave development is limited between 1.3–4.0 m, known as the effective wave height. The occurrences of the effective wind speed and effective wave height are the important indexes to evaluate the avaiable degree of wind energy and wave energy respectively. In the chapter, the occurrences of effective wind speed and effective wave height are statistically calculated, as shown in Fig. 6.7.

The occurrence of the effective wind speed in each month of the research region is above 65%. Especially from November to March of the next year, the occurrence is even up to 90%, which is very beneficial to the development of wind energy resources. The occurrence of effective wave height is lower than that of effective wind speed. But it is only from April to June that the occurrence is below 50%, and in the remaining months, the occurrence of effective wave height can be greater than 50%.

Zheng and Li pointed out that the gale occurrrence and rough sea occurrences in the research region are low, which is beneficial to prolong the life of the wind energy

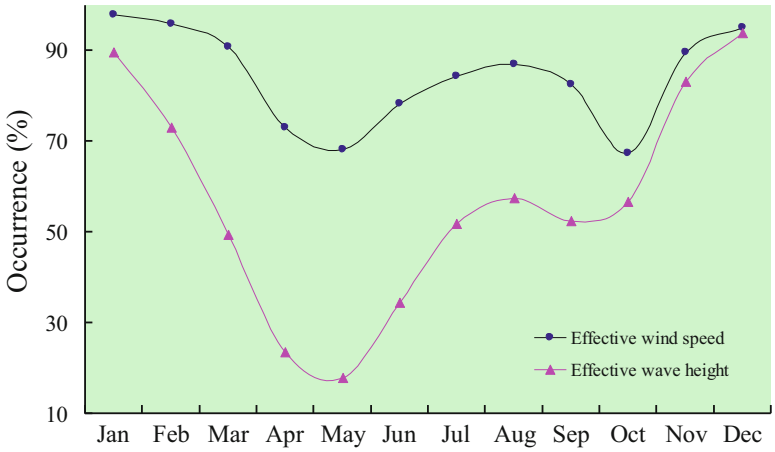

Fig. 6.7 Monthly characteristics of effective wind speed occurrence and effective wave height occurrence. (After Zheng and Li 2015b)

and wave energy devices. In addition, the wind direction and wave direction of the research region are dominated by the northeast in the winter and autumn, and mainly dominated by south-southwest direction in summer. The wind direction and wave direction are regular. All of these are beneficial to the exploitation and utilization of wave energy resources.

6.4 Energy Level Occurrence

Energy level occurrence is one of the important criteria to measure the abundance of resources. Generally, when the wind power density greater than 50 W/m^2 is considered to be effective utilized, and the wind power density greater than 200 W/m^2 is abundant (Mao et al. 2005); when the wave power density above 2 kW/m is effective utilized, and the value greater than 20 kW/m is abundant (Ren et al. 2006; Zheng and Li 2015b, 2016). The chapter has statistically analyzed the occurrence of the wind power density level greater than 50 W/m^2, 100 W/m^2 and 200 W/m^2 separately, and the occurrence of the wave power density greater than 2 kW/m, 10 kW/m and 20 kW/m separately. The wind power density and wave power under extreme wind and wave are excluded. The results are shown in Fig. 6.8.

As shown in Fig. 6.8a, the occurrence of the wind power density greater than 50 W/m^2 from November to April of the next year, June to September are greater than 50%, only in May and October the values are slightly lower than 50%. The occurrence of wind power density above 100 W/m^2 is greater than 50% in the months of November to March of the following year, July to September. As shown in Fig. 6.8b, the occurrence of the wave power density greater than 2 kW/m are greater than 50% in the months of November to March of following year, August to September. So, the development of wave energy resources can be carried out more than half of the year. Solar energy is limited by day and weather; the available time is less than 50%. Comparatively speaking, the wind energy and wave energy in theresearch region are more optimistic.

6.5 Wind and Wave Energy Rose

In the development of wind and wave energy, the energy direction is very important. If there is one or two energy direction prevailing all the year round, it is very helpful to improve the collection and conversion efficiency of energy. Based on the 6-hourly wind power density data for the past 24 years, we contoured the wind energy rose diagram (combination occurrence of wind energy direction and wind energy value size), as shown in Fig. 6.9a. Based on the 3-hourly wave power density data for the past 24 years, we contoured the wave energy rose diagram (combination occurrence of wave energy direction and wave energy value size), as shown in Fig. 6.9b.

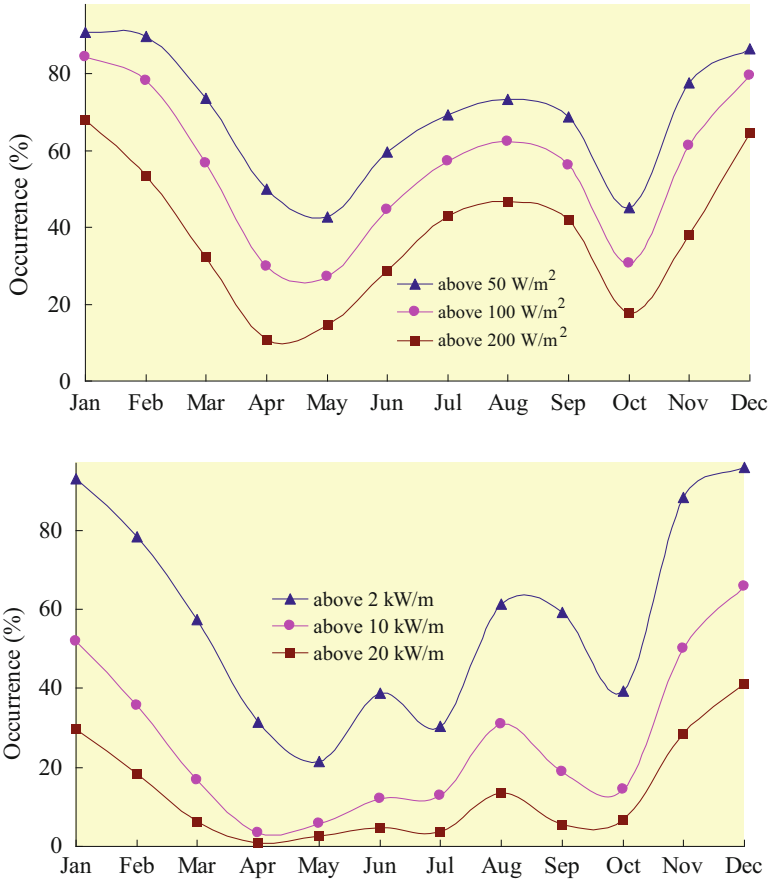

Fig. 6.8 Monthly characteristics of wind energy level occurrence (up) and wave energy level occurrence (down). (After Zheng and Li 2015b)

Wind energy rose: the highest occurrence of wind energy direction is east-northeast (ENE) and northeast (NE), followed by southwest (SW) and west-southwest (WSW). The highest occurrence of wind energy value size is 100–300 W/m^2. The wind power density greater than 1000 W/m^2 mainly comes from WSW, followed by SW. And the contribution is low in other direction.

Wave energy rose: the highest occurrence of wave energy direction is north-northeast (NNE) and WSW, while the contribution of the other direction is small. It is mainly attributed to the strong cold air in winter and strong southwest monsoon in summer. The highest occurrence of the wave power density is 0–5 kW/m, followed by 5–10 kW/m. In the NNE direction, the wave power density of 10–15, 20–30 and >40 kW/m is also very high.

In this chapter, we only contoured the annual wind energy rose and annual wave energy rose. In the future work, it is necessary to contour the wind/wave energy rose in each month, to provide detail scientific guidance for the energy development.

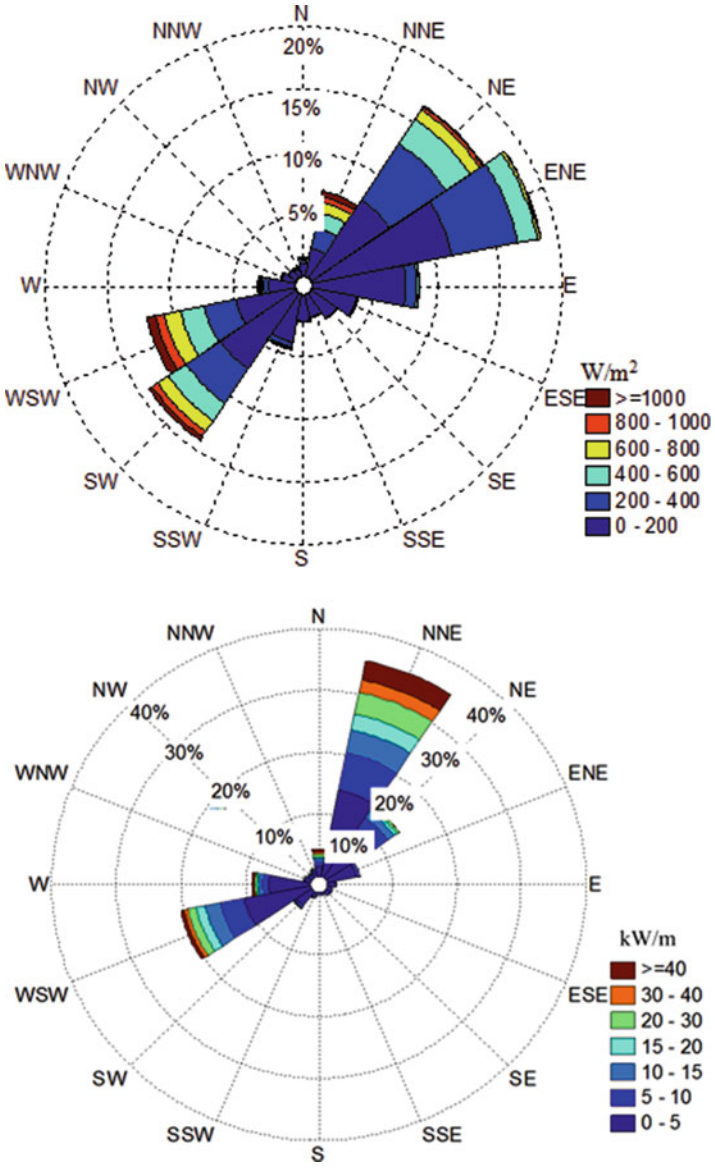

Fig. 6.9 Wind energy rose (up) and wave energy rose (down). (After Zheng and Li 2015b)

6.6 Contribution of Different Sea States to the Total Wave Energy

From the calculation of wave power density, it can be seen that the wave energy mainly depends on the wave height and wave period (Iglesias and Carballo 2010, 2011). In the chapter, the contribution of different sea states to wave energy is calculated, which can be used as a reference for improving the energy capture capability of power plants. The contribution of different sea states to the total wave energy in the research region is shown in Fig. 6.10. As shown in Fig. 6.10, the sea states with wave height 2–3 m and wave period 6–7 s contributes most to the total wave energy, and the contribution rate is about 14.6%. The secondary sea states is the situation that wave height is 2–3 m and wave period is 7–8 s, the contribution rate is about 11.1%. In addition, the contribution rate of the sea states with wave height 1–2 m, and wave period 5–6 s is about 9.1%; the contribution rate of the sea states with wave height 3–4 m, wave period 8–9 s is 8.1%.

In this chapter, we only analyzed the contribution of different sea states to wave energy in the whole year. In the future work, it is necessary to analyze the contribution of different sea states to wave energy in each month, to provide detail scientific guidance for the energy development.

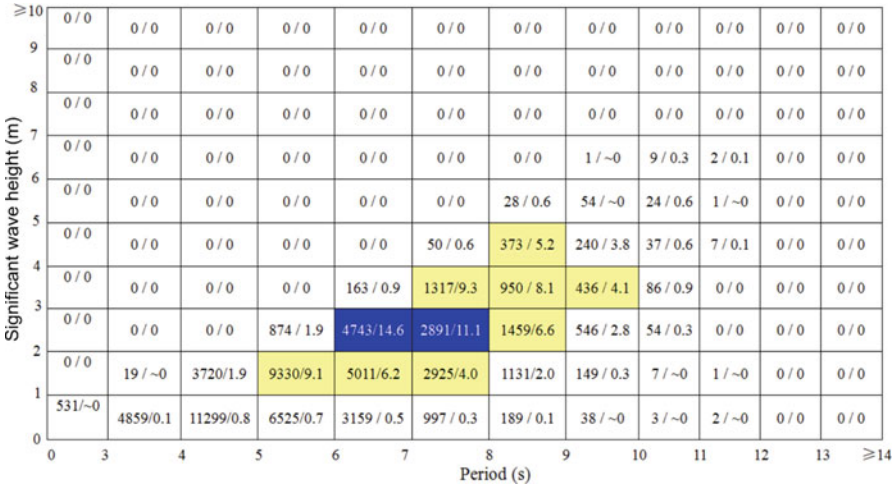

Fig. 6.10 Contribution of different sea states to the total wave energy. (After Zheng and Li 2015b) Note: A/B, A is the number of hours of occurrence for the period 2003–2010, B is the contribution of the sea state to the total incident energy, as a percentage.

6.7 Storage of Wind and Wave Energy Resource

To analyze the storage of wind/wave energy in detail, we calculated the per unit area total storage, effective storage, and exploitable storage of global ocean wind/wave energy, as shown in Table 6.2. The calculation method is below:

$$E_{PT} = \bar{P}^* H \tag{6.5}$$

$$E_{PE} = \bar{P}^* H_E \tag{6.6}$$

$$E_{PD} = E_{PE}{}^* C_e \tag{6.7}$$

where E_{PT} is the total storage of wind/wave energy, $\bar{P}$ is the annual average wind/wave power density, and H = 365d × 24 h = 8760 h. In Eq. (6.6), E_{PE} is the effective storage of wind/wave energy and H_E is the annual total number of hours of effective wind speed (or the annual total number of hours of effective wave height). In Eq. (6.7), E_{PD} is the technological development volume of wind/wave energy resources. When about wind energy development, Ce = 0.785; i.e., the actual swept area of the wind turbine blades is 0.785, meaning that for a diameter of 1 m, the swept area of the wind turbine is calculated from 0.52 × p, which equals 0.785 m2. When about wave energy development, Ce is usually about 10~30%. Using the most conservative algorithm, here we take the Ce as 10%.

The total storage of the wind energy resources in the research region is 2050 (kW·h)/m^2, the effective storage is 1722 (kW·h)/m^2. The total storage of wave energy resources are 84,079 (kW·h)/m, and the effective storage is 66,336 (kW·h)/m. Gong et al. (2006) point out the annual effective wind energy storage of Liaobing and Mingyang at the 50 m high are 2763 (kW·h)/m^2 and 1478 (kW·h)/m^2 respectively, which more than 1 times greater than the height of 10 m (that is, the annual effective wind energy storage of Liaobing and Mingyang at 10 m height is <1500 (kW·h)/m^2). The annual effective time is more than 6000 h, and it has the resource condition to establish large scale wind farm. Comparing to the Liaobing and Mingyang, the wind energy storage of the research region is more abundant, and the annual effective utilization time of the research region is more than 80%.

Table 6.2 Wind energy and wave energy storage of the research region

	Total storage	effective storage	exploitable storage
Wind energy unit: (kW·h)/m^2	2050	1722	1352
Wave energy unit: (kW·h)/m	84,079	66,336	6634

6.8 Long Term Trend of Wind and Wave Energy

The long term trend of wind/wave energy will affect the future development and utilization. Do average of wind power from 0000 UTC on January 1st, 1988 to 1800 UTC on December 31st 1988, a yearly average value of wind power density of the research region is obtained. Using the same method, we obtain 24 yearly average values of wind power density. Then the annual variation of the wind power density is analyzed using linear regression method, as shown in Fig. 6.11a. Similarly, the annual variation of the wave power density is analyzed using linear regression method, as shown in Fig. 6.11b. As a whole, the wind power density has a short term decreasing trend for the period 1989–1998, but shows a significant increasing trend for the period 1998–2009. 2010 is an abnormal year, the wind energy have undergone dramatic changes. As shown in Fig. 6.11b, correlation coefficient (R) of the wave power density is 0.72, significant at the 99.9% level t-test ($|R| = 0.84 > r_{0.001} = 0.51$). The regression coefficient is 0.2539. It means that the

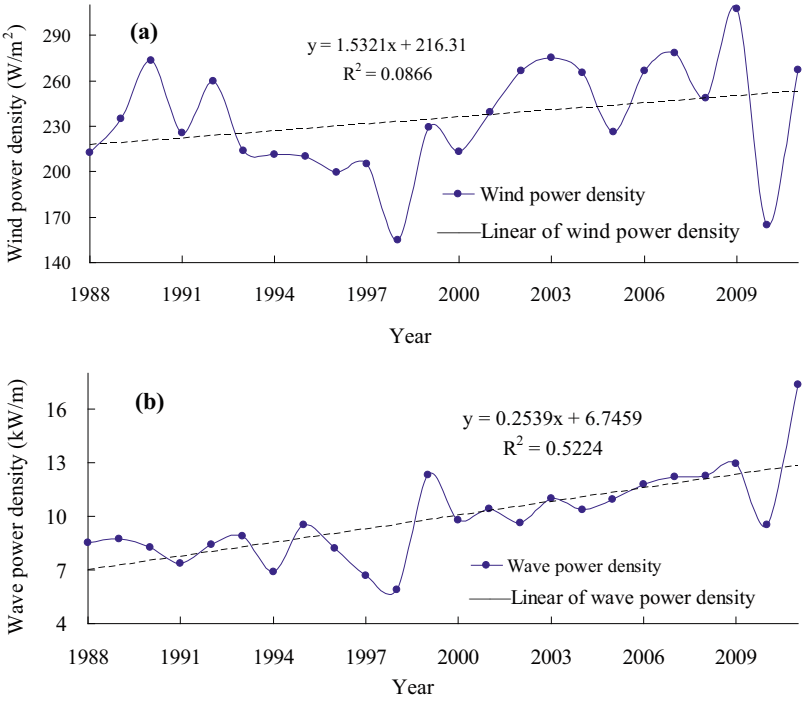

Fig. 6.11 Long term trends of wind power density (**a**) and wave power density (**b**). (After Zheng and Li 2015b)

wave power density exhibits a significant increasing trend of 0.25 (kW/m)/yr. in the research region for the past 24 years. And it reaches to the peak value in the year of 2011.

6.9 Stabillity of Wind and Wave Energy

The stability of resources will not only affect the energy acquisition, conversion efficiency, but also affect the life of equipment. The chapter use the 24 years wind power density and wave power density to calculate the coefficient of variation (*Cv*). The smaller the *Cv*, the better the stability.

The stability of wind energy and wave energy in November to April, and July to September are better than the rest of the months. This is because November to April next year, the research region is often attacked by the strong and regular cold air, the stability is very good. Similarly, the wind energy and wave energy is also good in July to September under the influence of stable southwest monsoon.

During the transition from the summer wind to winter monsoon, the stability of wind energy and wave energy doesn't show severe changes. However, during the transition from the winter monsoon to the summer monsoon, the stability of wind energy and wave energy show a dramatic change, and the *Cv* reaches its peak in May, that is the stability of the month is worst (Fig. 6.12).

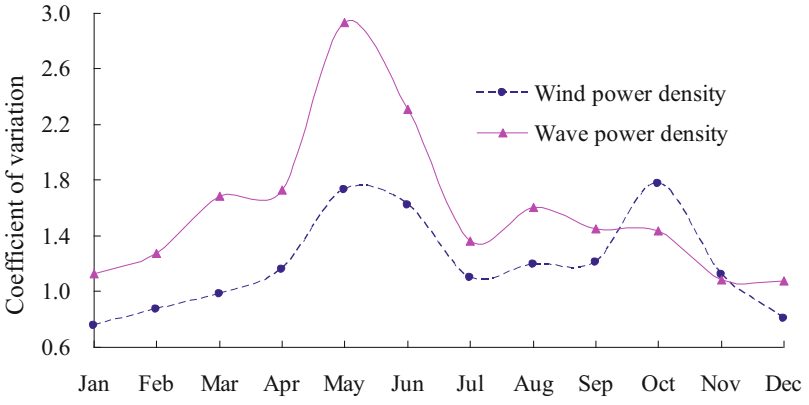

Fig. 6.12 Coefficient of variation of wind power density and wave power density. (After Zheng and Li 2015b)

6.10 Summary

In the chapter, the wind energy and wave energy resources in a remote island are systematically evaluated by using the CCMP wind field data and hindcast wave field data. It includes the monthly characteristicchange of wind/wave power density, the effective wind speed occurrence and effective wave height occurrence, the wind/wave energy level occurrence, the contribution of different sea states to total wave energy, the stability of wind/wave energy and long term trends of wind and wave energy, and energy storage. The results show:

Influenced by monsoon and monsoon transition, both monthly variation characteristics of the wind energy and wave energy appear "W" shape. The peak value appears from December to January of next year, of about 370 W/m^2 in wind power density and 20 kW/m in wave power density. The research region can carry out wind energy and wave energy development all year round, even in the relative poor month (April and May), the wind power density is above 84 W/m^2, and the wave power density is above 2.2 kW/m, and all of them are in the state of being available.

The effective wind speed occurrence, effective wave height occurrence and energy level occurrence are optimistic all year round: the effective wind speed occurrence is greater than 70% in each month, evenn up to 90% from November to March. Except April to June, the effective wave height occurrence is more than 50% for most of the year. And in most of the year, the occurrence of wind power density above 50 W/m^2 and the occurrence of wave power density above 2 kW/m are greater than 50%.

The wave energy of the research region is mainly contributed by the following sea states: wave height 2–3 m and wave period 6–7 s, contribution rate 14.6%; wave height 2–3 m and wave period 7–8 s, contribution rate 11.1%; wave height 1–2 m and wave period 5–6 s, contribution rate 9.1%; wave height 3–4 m and wave period 8–9 s, contribution rate 8.1%.

Then wind energy of the research region is mainly contributed by ENE, NE, SW and WSW, among which the occurrence of 100–300 W/m^2 is the highest. The high wind power density above 1000 W/m^2 is mainly contributed by WSW, followed by SW. The wave energy of the research region is mainly contributed by the waves of NNE and WSW. The highest occurrence of the wave power density is 0–5 kW/m, followed by 5–10 kW/m. In the NNE direction, the wave power density of 10–15, 20–30 and > 40 kW/m is also very high. The characteristic of wind rose is similar to the wave energy rose.

The total storage of wind energy resources of the research region is 2050 (kW·h)/m^2, and the effective storage is 1722 (kW·h)/m^2;. The total storage of wave energy resources is 84,079 (kW·h)/m, and the effective storage is 66,336 (kW·h)/m.

For the last 24 years, the long term trend of wind energy in the research region is not significant. And the wave power density exhibits a significant increasing trend of 0.25 (kW/m)/yr. in the research region for the past 24 years.

Under the influence of the strong, regular cold air and southwest monsoon, wind and wave energy of the research region show good stability in winter and summer.

During the transition from the summer wind to the winter monsoon, the stability of wind energy and wave energy do not appear violent changes. However, during the transition from winter to monsoon, the wind and wave energy in May are the worst for the whole year.

In addition, it is also found that the gale occurrence and rough sea occurrence are low in the research region, moreover, the wind direction and wave direction of the sea area are very regular. This is beneficial for the exploitation and utilization of wind energy and wave energy.

In summary, the research region contains abundant and suitable wind energy and wave energy resources, which should be paid attention to. After the formal expansion of wind power, wave power generation, desalination and other resources development work, it is necessary to carry out short term numerical forecasting, mid-long term prediction and weather warning for wind energy and wave energy development. The other energy sources, such as diesel power, the above parameters can be added in order to ensure uninterrupted supply of electricity when energy is insufficient.

References

Chu PC, Qi YQ, Chen YC, Shi P, Mao QW (2004) South China Sea wind-wave characteristics. Part I: validation of wavewatch-III using TOPEX/Poseidon data. J Atmos Ocean Technol 21:1718–1733

Gong Q, Yuan GE, Wang HY (2006) State and exploitation potentiality of wind energy resources in Liaoning littoral. Sci Geogr Sin 26(4):483–489

Iglesias G, Carballo R (2010) Offshore and inshore wave energy assessment: Asturias (N Spain). Energy 35(5):1964–1972

Iglesias G, Carballo R (2011) Choosing the site for the first wave farm in a region: a case study in the Galician Southwest (Spain). Energy 36(9):5525–5531

Mao HQ, Song LL, Huang HH (2005) Study on the wind energy resource division in Guangdong Province. J Nat Resour 20(5):679–683

Mirzaei A, Tangang F, Juneng L, Mustapha MA, Husain ML, Akhir MF (2013) Wave climate simulation for southern region of the South China Sea. Ocean Dyn 63(8):961–977

Rascle N, Ardhuin F (2013) A global wave parameter database for geophysical applications. Part 2: model validation with improved source term parameterization. Ocean Model 70:174–188

Ren JL, Zhong YJ, Zhang XM (2006) State of arts and prospects in the power generation from oceanic wave. J Zhengzhou Univ Technol 34(1):69–73

Shen SG, Qian XZ (2003) Resources ocean – develop and utilize the rich blue treasures. Haichao Press

Zheng C-W, Li C-Y (2015a) Variation of the wave energy and significant wave height in the China Sea and adjacent waters. Renew Sust Energ Rev 43:381–387

Zheng CW, Li CY (2015b) Development of the islands and reefs in the South China Sea: wind power and wave power generation. Periodic Ocean Univ China 45(9):7–14

Zheng CW, Li CY (2016) Review on the global ocean wave energy resource. Mar Forecast 33(3):76–88

Zheng CW, Zhuang H, Li X, Li XQ (2012) Wind energy and wave energy resources assessment in the East China Sea and South China Sea. Sci China Technol Sci 55(1):163–173
Zheng C-W, Pan J, Li J-X (2013) Assessing the China Sea wind energy and wave energy resources from 1988 to 2009. Ocean Eng 65:39–48
Zhou RW, He XF, Zhu R (2010) Numerical simulation of the development potential of wind energy resources over China's offshore areas. Resour Sci 32(8):1434–1443

Chapter 7
Wind Climate and Wave Climate in the Remote Island of the South China Sea

The marine environment is the primary consideration of marine construction (Li 2000; Li and Mu 2001a, b; Li et al. 2003, 2004a, b, 2008a, b, 2016; Zheng et al. 2013a, b, 2014a, b, 2014c, 2015; Zheng and Li 2015a, b, 2017; Reza et al. 2017). It has a great influence on the ocean navigation, development and utilization of marine resources, carrier aircraft landing, the use of weapons, maintenance of maritime rights and interests and so on. On December, 1944, the US Third fleet were assembling near to the central Mindoro, and preparing to attack the Japanese occupation Luzon. However, due to the location and path of typhoon inaccurate, the fleet is attacked by the typhoon, which directly led to the sinking of 3 destroyers, seriously damaging of 2 aircraft carrier, 146 airplanes were thrown into the sea, nearly 800 people died. There are so many examples caused by the bad marine environment. So the important influence of marine environment can be seen.

The Maritime Silk Road belongs to the tropical cyclone prone seas, and is in the monsoon transformation zone. The islands and reefs are numerous and the wind and wave characteristics are complex. An internsive study of the wind climate and wave climate of the Maritime Silk Road is a prerequisite for the efficient and safety development and utilization of the ocean and for disaster prevention and reduction.

Previous researchers have done a lot of statistical work on the characteristics of marine environment in the China seas. However, due to the scarcity of data, temporal-spatial resolution, precision and other issue, there are very few studies on the remote islands and reefs. The chapter takes an important remote island as the object of researching. Using the CCMP wind data with high accuracy and high resolution to drive the WW3 wave model, thus to obtain the wave filed in the China seas. Then the wind climate and wave climate of the important remote island were analyzed, based on the CCMP wind data and hindcast wave data, in hope of providing reference for the ocean navigation, development and utilization of marine resources, ocean engineering, disaster prevention and reduction, and so on.

C. Zheng et al., *21st Century Maritime Silk Road: Construction of Remote Islands and Reefs*, Springer Oceanography, https://doi.org/10.1007/978-981-10-8114-9_7

7.1 Data and Methodolog

Using the CCMP wind data to drive the third generation wave numerical model WAVEWATCH- III (WW3), the 3-hourly interval time and 0.25° × 0.25° special resolution series of the wave field from January 1 1988 00:00 to December 31 2011 18:00 are computed out. Good results have been achieved by comparing the simulated SWH with the satellite data and the buoy observation data of Korea, Japan and Taiwan. Based on the 6-hourly wind data and hindcast wave data for the period 1988–2011, the wind climate and wave climate of the research region is analyzed, systematically including the monthly variation of wind speed and significnt wave height, wind class occurrence, wave class occurrence, wind direction occurrence, wave direction occurrence, extreme wind speed and wave height, long term trend of wind speed and wave height.

7.2 Strong Wind/Wave Direction Occurrence

The wind direction and wave direction have a significant effect on ocean engineering, marine new energy development, and so on. Based on the 3-hourly wind speed and wind direction data, the wind rose (combination occurrence of wind direction and wind speed) is contoured, as shown in Fig. 7.1(left). Similarly, the wave rose (combination occurrence of wave direction and wave speed) is contoured, using the 3-hourly hindcast wave speed and wave direction data, as shown in Fig. 7.1(right).

In Februry, the northeast (NE) and east-northeast (ENE) wind accounted for an absolute dominant position. The highest occurrence wind speed is the 6–8 m/s NE and ENE wind, followed by the 8–10 m/s NE and ENE wind. Strong wind above 10 m/s mainly comes from the NE and north-northeast (NNE) directions. The wave rose is in an overall agreement with the wind rose. But the wave direction of the month is dominated by NE, followed by NNE, and in thees two directions, the occurrence of wave height between 1.2–2.4 m is the highest. Strong waves over 3 m mainly come from NNE.

In May, during the monsoon transition, it is obvious that the northeast monsoon has not yet completely subsided, while the southwest monsoon has not yet prevailed. The most frequent wind directions are ENE, east (E), NE, southwest (SW) and west-southwest (WSW). Strong winds over 10 m/s come from SW and WSW. The most frequent wave direction is WSW, followed by ENE. The wave height above 1.6 m mainly comes from WSW. In the month, it needs to take precautions against the strong winds from the WSW.

In August, under the influence of strong southwest monsoon, the winds from SW and WSW are absolutely dominated, among them, the occurrence of 8–10 and 6–8 m/s is the highest. Strong winds above 12 m/s mainly come from WSW. The wave is dominated by WSW, with occurrence as high as 75%. The month needs to focus on strong winds from WSW and strong waves from the WSW.

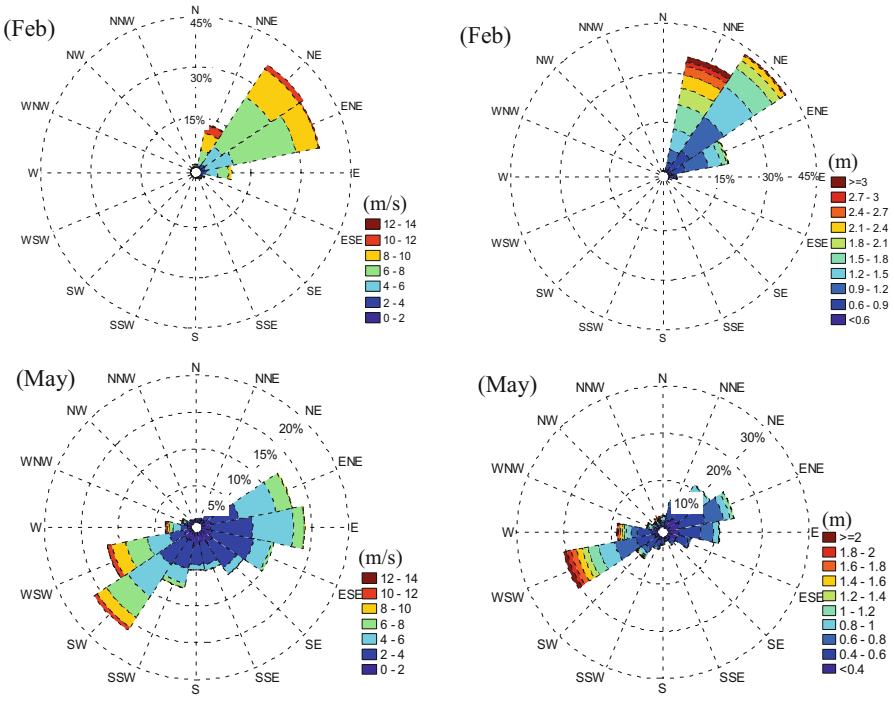

Fig. 7.1 Wind rose (left) and wave rose (right) in February, May, August and November. (After Zheng and Li 2015a)

In November, the southwest monsoon has been changed to northeast monsoon. The NE and ENE are the dominant wind direction. The occurrence of 6–8 m/s is the highest. Strong winds above 10 m/s mainly come from NNE. There is an obvious difference with the wind direction, the wave direction is dominated by NNE, nearly 55%. Big waves over 2 m mainly come from NNE.

7.3 Wind/Wave Class Occurrence

Based on the 3-hourly wind speed and wave height data, the wind class occurrence and wave class occurrence are statistically analyzed, as shown in Tables 7.1 and 7.2. The wind class scale is based on the Beaufort scale, and the wave class scale is based on the standard announced by the National Bureau of Oceanography (Shi et al. 2000).

Wind class occurrence: as a whole, the gale occurrence (wind speed above 10.8 m/s) is low. Under the influence of the southwest monsoon and typhoon, the gale occurrence in summer is higher than that in other seasons. Under the influence of the frequent and strong cold air, the gale occurrence in winter is the secondary situation. There is hardly any wind above class 7 all year round. In January

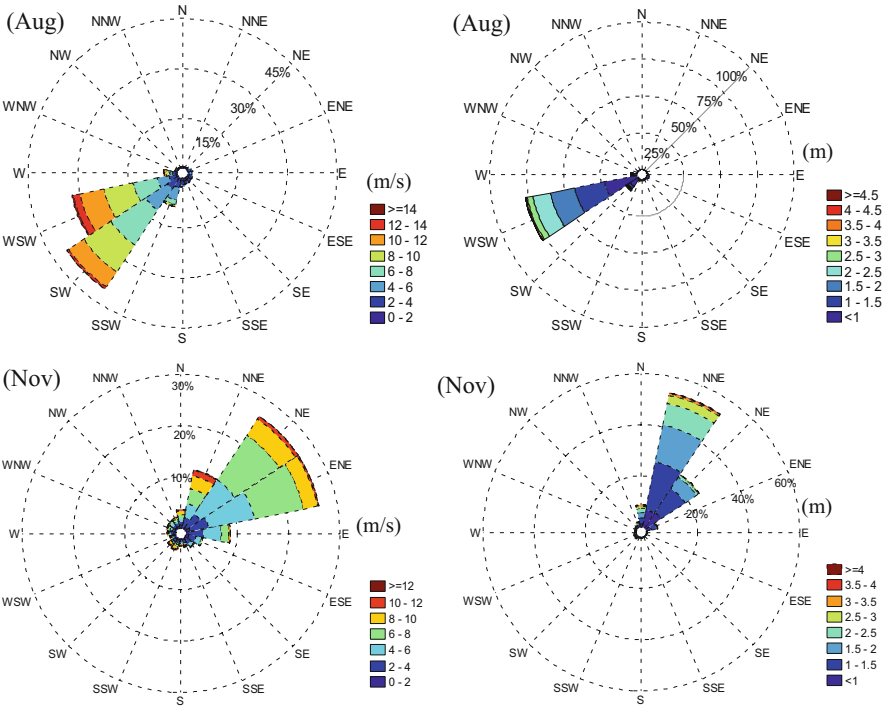

Fig. 7.1 (continued)

Table 7.1 Wind class occurrence of the research region (%)

Wind class	Wind speed scale (m/s)	January	April	July	October
0	0.0–0.2	0.00	0.12	0.02	0.04
1	0.3–1.5	0.06	5.38	3.79	8.44
2	1.6–3.3	2.58	26.40	14.58	29.39
3	3.4–5.4	10.04	39.06	22.52	30.60
4	5.5–7.9	41.27	25.75	25.37	19.71
5	8.0–10.7	39.06	3.27	26.29	8.44
≥6	≥10.8	7.00	0.02	7.44	3.39

Table 7.2 Wave class occurrence of the research region (%)

Wave class	Wave height scale (m)	January	April	July	October
0	–	0.00	0.00	0.00	0.00
1	<0.1	0.00	5.19	5.44	0.31
2	0.1–0.5	1.74	38.23	21.69	12.19
3	0.5–1.25	18.65	44.29	30.35	45.94
4	1.25–2.5	54.37	11.98	33.56	34.72
≥5	≥2.5	25.24	0.31	8.97	6.83

(on behalf of winter, same as below), the class 4 and class 5 wind play the dominant role, followed by class 3. In April (on behalf of the spring, same as below), class 3 wind plays the dominant role, followed by class 2 and class 4. In July (on behalf of the summer, same as below), class 3, class 4 and class 5 wind play the dominant role, followed by class 2. In October (on behalf of the autumn, same as below), class 2 and class 3 wind play the dominant role, followed by class 4.

Wave class occurrence: as a whole, the occurrence of wave height above 4.0 m is low. The relative highest occurrence of wave height above 4.0 m occurred in January, which should be attributed to the frequent and strong cold airs in winter. After entering the South China Sea, the intensity of the cold air has weakened, but it will cause the cold swell, which result in a higher occurrence of wave height above 4.0 m than the rest of the seasons. In January, the class 4 wave dominated, followed by class 3 and class 5 waves. In April, the class 2 and class 3 waves dominated, followed by class 4. In July and October, the class 3 and class 4 wave dominated, followed by class 2.

7.4 Monthly Variation of Wind Speed and Wave Height

The Monthly average significant wave height (SWH) and sea surface wind speed are presented in Fig. 7.2. On the whole, the SWH and the sea surface wind speed of the study area show "W" shape in the monthly variation. And the curve of SWH is similar to that of sea surface wind speed, which should be attributed to that the China seas is on the edge of the ocean, and the wind sea dominate the mixed waves. It is noticed that the monthly variation of wind speed in the study area is more apparent than that of SWH. The response of the ocean to the wind requires a process which is accompanied by energy decaying, and the effect of the swell can't be neglected, so the monthly amplitude of wave height is obviously smaller than that of wind speeds.

The peak value of the wind speed and SWH appear from December to January of the following year. The monthly mean wind speed is about 7.7 m/s, and the monthly mean average SWH is about 2.4 m. The secondary peak appears in August, with monthly mean wind speed of 6.8 m/s and monthly mean SWH of 1.4 m. It is formed in the effect of summer southwest monsoon. The trough value appears on the April to May and October, it can be attributed to the transition of the monsoon.

7.5 Daily Variation of Wind Speed and Wave Height

Based on the 3-hourly wind speed and wave height data, the multi-year average sea surface wind speed and SWH on 00:00, 03:00, 06:00, 09:00, 12:00, 15:00, 18:00, 21:00 values for the past 24 years (1988–2014) are obtained. The characteristics of

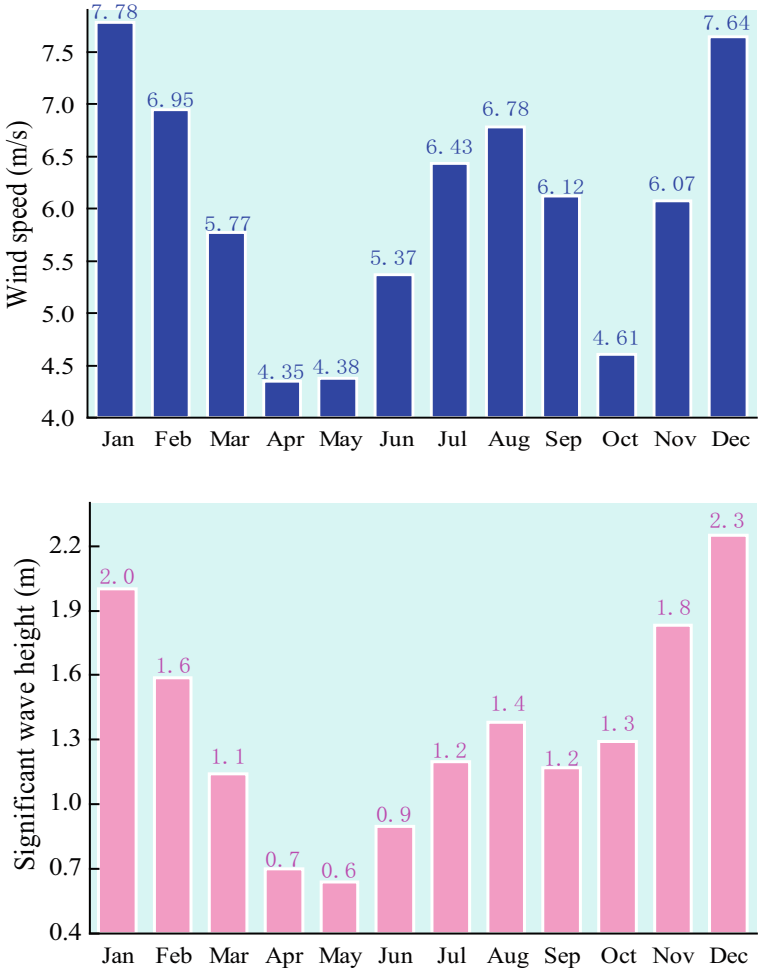

Fig. 7.2 Monthly characteristics of wind speed (up) and significant wave height (down). (After Zheng and Li 2015a)

daily variation are analyzed to provide the reference for wind and wave generator, air-sea interaction research, ocean engineering, and so on.

As shown in Fig. 7.3, the wind speed shows "W" shape of daily variation. The peak value appears at 00:00, the secondary appears at 12:00, the first trough at 06:00, and the 18:00 is the secondary trough. Obviously, there is a hysteresis effect of wave height than the wind speed. The SWH peak value appears on 03:00, while the first trough appears in 09:00. The diurnal variation of SWH basically presents a single peak daily variation.

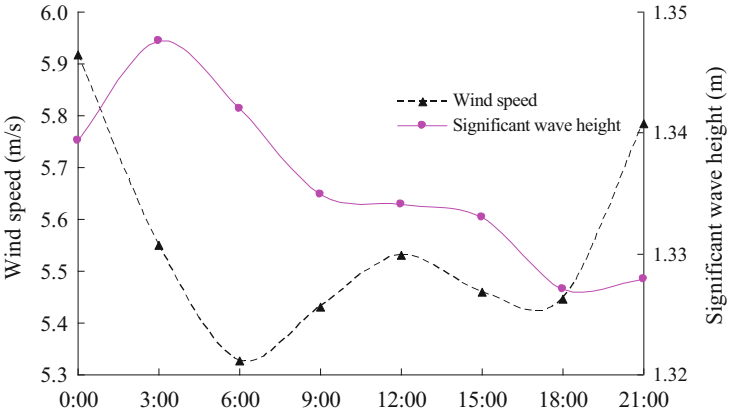

Fig. 7.3 Daily variations of wind speed and significnat wave height. (After Zheng and Li 2015a)

7.6 Long Term Trend of Wind Speed and Wave Height

Do average of the sea surface wind speed from 0000 UTC on January 1st, 1988 to 1800 UTC on December 31st 1988, a yearly average value of wind speed of the research region is obtained. Using the same method, we obtain 24 yearly average values of wind speed. Then the annual variation of the wind speed is analyzed using linear regression method, as shown in Fig. 7.4a.

The correlation coefficient (R) of the wind speed is 0.25, does not pass the significant level. It means that the wind speed of the research region does not have a significant long term trend for the past 24 years. Based on the curve, from 1990 to 1998, the wind speed tend do decrease; and from 1998 to 2009, the wind speed appears to increase. The year of 1998 is the trough of the 24 years, and the yearly average wind speed is 5.2 m/s. The year of 2010 is an abnormal point.

As shown in Fig. 7.4b, the correlation coefficient (R) of the SWH is 0.68, significant at the 99% level t-test. The regression coefficient is 0.016. It means that the SWH exhibits a significant increasing trend of 0.016 m/yr. (1.6 cm/yr) in the research region for the past 24 years. In view of the curve, from 1988 to 1998, the SWH in the research region appears a slightly decrease trend; but from 1998 to 1999, the value rapidly increase; and from 1999 to 2009, the value tend to increase slowly. The year of 1998 is the trough of the 24 years, the yearly average SWH is about 1.0 m. And the year of 2010 is an abnormal point.

Comparing Fig. 7.4(a) and 7.4(b), it is not hard to find that the annual variation of sea surface wind speed is relatively more obvious, while the annual variation of SWH is relatively mild.

It is noticed that in view of the wind speed, the year of 1998 is the trough of the 24 years, but the value rapidly increase in 1999. Some studies have shown that a strong El Nino event has occurred in April 1997 to May 1998, and accompanied by the weakening of the East Asian monsoon. This should be the reason for the wind

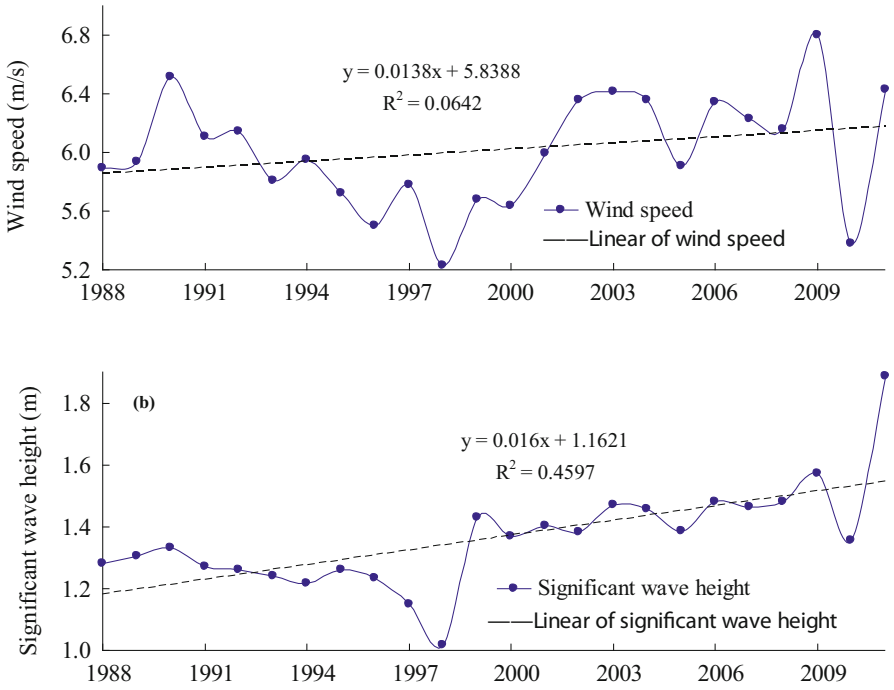

Fig. 7.4 Long term trends of wind speed (**a**) and significant wave height (**b**). (After Zheng and Li 2015a)

speed trough in 1998. From September 1998 to July 2000, a strong of La Nina event has happened, and accompanied by the strengthen of the East Asian monsoon. This should be the reason for the rapidly increase of the wind speed in 1999. The offshore of China is on the edge of the ocean, and wind wave occupy large component in the mixed waves. Therefore, the trend of the SWH has a good agreement with the sea surface wind speed as a whole.

7.7 Summary

Using the CCMP wind field data and hindcast wave field data, the wind climate and wave climate of a remote island in the South China Sea are analyzed, systematically including the monthly variation of wind speed and significnt wave height, wind class occurrence, wave class occurrence, wind direction occurrence, wave direction occurrence, extreme wind speed and wave height, long term trend of wind speed and wave height, in hope of providing scientific reference for the construction of remote islands and reefs. The results show that,

In January, NE direction wind situates the dominating position, while the wave direction is dominated by NNE, followed by the NE direction. In April, the most frequent wind direction are ENE, E and NE, and the most frequent wave direction is NE. In July, the wind direction is dominated by the SW and WSW direction, while the wave direction is WSW. In October, the wind with partial WSW and ENE directions has the highest occurrence, and the NNE wave plays the leading role. In January, the strong winds and waves of NNE are needed to guard against. In April, the strong wind from ENE is needed to guard against. In July, the strong WSW wind and wave are needed to guard against. In October, the WSW strong wind and wave are needed to guard against.

The gale occurrence (occurrence of wind speed >10.8 m/s) and occurrence of SWH >4 m in the research region is low. In spring, the class 3 wind is the main type; in summer, the class 3 and class 5 wind are the main type; in autumn, the class 2 and class 3 are the main type; in winter, the class 4 and class 5 wind are the main type. In spring, class 2 and class 3 waves are the main components; in summer and autumn, the class 3 and class 4 waves are the main components; in winter, the class 4 wave is the main component.

Under the influence of the monsoon and the transition of the monsoon, the sea surface wind speed and SWH appear "W" shape of monthly variation. The peak value appears from December to January of the following year, with the monthly average wind speed of 7.7 m/s and monthly average SWH of 2.4 m.

For the past 24 years (1988–2011), the sea surface wind speed in the research region has no significant long term trend, while the SWH significantly increased with an annual rate of 1.6 cm/yr.

References

Akpamar A, Komurcu MI (2013) Assessment of wave energy resource of the Black Sea based on 15-year numerical Hindcast data. Appl Energy 101:502–512

Li CY (2000) Introduction to climate dynamics. China Meteorological Press, Beijing

Li CY, Mu MQ (2001a) The dipole in the equatorial Indian Ocean and its impacts on climate. Chin J Atmos Sci 25(4):1–10

Li CY, Mu MQ (2001b) The influence of the Indian Ocean dipole on atmospheric circulation and climate. Adv Atmos Sci 18(5):1–16

Li CY, Sun SQ, Mu MQ (2001) Origin of the TBO-interaction between anomalous East-Asian winter monsoon and ENSO cycle. Adv Atmos Sci 18(4):554–566

Li CY, Long ZX, Mu MQ (2003) Atmospheric Intraseasonal oscillation and its important effect. Chin J Atmos Sci 27(4):1–16

Li CY, He JH, Zhu JH (2004a) A review of decadal/interdecadal climate variation studies in China. Adv Atmos Sci 21(3):1–10

Li CY, Wang ZT, Lin SZ (2004b) The relationship between East Asian summer monsoon activity and northward jump of the upper westerly jet location. Chin J Atmos Sci 28(5):1–9

Li CY, Mu M, Zhou GQ (2008a) Mechanism and prediction studies of the ENSO. Chin J Atmos Sci 32(4):761–781

Li CY, Gu W, Pan J (2008b) Mei-yu, Arctic oscillation and stratospheric circulation anomalies. Chin J Geophys 51(6):1–12

Li CY, Lin J, Yuan Y, Pan J, Jia XL, Chen X (2016) Frontier issues in current MJO studies. J Trop Meteorol 32(6):1–18

Reza TM, Mani FD, Ali DDM (2017) Response spectrum method for extreme wave loading with higher order components of drag force. J Mar Sci Appl 16(1):27–32

Roger B (2009) Wave energy forecasting accuracy as a function of forecast time horizon. EPRI-WP-013. October 31. Available at www.epri.com/oceanenergy/

Shi MC, Gao GP, Bao XW (2000) Ocean survey method. Qingdao Ocean University Press, Qingdao

Zheng CW, Li CY (2015a) Development of the islands and reefs in the South China Sea: wind climate and wave climate analysis. Period Ocean Univ China 45(9):1–6

Zheng CW, Li CY (2015b) Variation of the wave energy and significant wave height in the China Sea and adjacent waters. Renew Sust Energ Rev 43:381–387

Zheng CW, Li CY (2017) Analysis of temporal and spatial characteristics of waves in the Indian Ocean based on ERA-40 wave reanalysis. Appl Ocean Res 63:217–228

Zheng CW, Lin G, Shao LT (2013a) Frequency of Rough Sea and its long-term trend analysis in the China Sea from 1988 to 2010. J Xiamen Univ (Nat Sci) 52(3):395–399

Zheng CW, Pan J, Li JX (2013b) Assessing the China Sea wind energy and wave energy resources from 1988 to 2009. Ocean Eng 65:39–48

Zheng CW, Shao LT, Li G et al (2014a) Analysis of influence on the security of sea skimming caused by a typhoon wave. J Harbin Eng Univ 35(3):301–306

Zheng CW, Pan J, Huang G (2014b) Forecasting of the China Sea ditching probability using WW3 wave model. J Beijing Univ Aeronaut Astronaut 40(3):314–320

Zheng CW, Zhou L, Song S et al (2014c) Simulation of the wave field caused by 1307 Typhoon "Soulik". J Xiamen Univ (Nat Sci) 53(2):257–262

Zheng CW, Zhou L, Shi WL, Li X, Huang CF (2015) Decadal variability of global ocean significant wave height. J Ocean Univ China 14(5):778–782

Chapter 8
Wind-Sea, Swell and Mixed Wave Energy

The evaluation of wave energy in China started late, but it is developing rapidly. You and Ma (2003) believe that the South China Sea is the relative enrichment area of wave energy, Bohai Sea is poor, but even in poor seas, wave energy can also provide enough power to buoys. Chu (2004) pointed out in the wind area along the coast, the wave power density is relatively high. Ren et al. (2006) use the observation wave height to evaluate the wave energy of the Zhejiang Shengshan sea area. It is found the wave power density is about 0.5–8.8 kW/m, and the occurrence of the energy power above 2 kW/m is 60%, which is beneficial for the wave energy exploration. Wang and Lu (2009) used the observation wave data to calculate the theoretical coastal energy power of China is 7.0 × 107 kW, and pointed out that the high value area of the wave power density along the coast of China is located along the coast of Xisha Islans, north of the Haitan Island, Taiwan Island, central part of Zhejiang, Bohai Strait.

In 2010, we used the Simulating WAves Nearshore (SWAN) numerical wave model to realize the simulation analysis of the wave energy resources for the first time at home (Zheng et al. 2011a, b; Zheng and Li 2011). And the north of the South China Sea is selected as the case study. It is found that the north of the South China Sea contains abundant and suitable wave energy resources. In 2011, we used the CCMP wind field data to drive the third generation wave model WW3. The first wave big data covered the whole China seas and adjacent waters with long time series, high temporal-spatial resolution and high accuracy was obtained (Zheng and Li 2011). With this data, the detailed and systematic simulation analysis of wave energy resources of the China seas has been realized for the first time. In the evaluation of wave energy resources, it is generally considered that when the wave power density above 2 kW/m is available, and above 20 kW/m is considered as enrichment area of wave energy resources. This means that the occurrences of the wave power density of different classes are important criterion for measuring the extent and richness of wave energy resources. In the research, the occurrences of the wave energy density at different levels is defined as “energy level occurrence” (Zheng and Li 2011). This definition has also been widely recognized and applied

C. Zheng et al., *21st Century Maritime Silk Road: Construction of Remote Islands and Reefs*, Springer Oceanography, https://doi.org/10.1007/978-981-10-8114-9_8

(Wen et al. 2013; Jiang 2013; Wan et al. 2015). Considering the wave power density, energy level occurrence and the stability of wave power density, a systematic and precise assessment of wave energy resources in the China seas is implemented. The results show the wave power density of the China seas has obvious seasonal characteristics. Except the northern part of Bohai and the Yellow Sea, the annual average wave power density is more than 2 kW/m, belongs to avaiable degree. In the northern part of the South China Sea, the wave power density is relatively large in the four seasons, which is more optimistic than the traditional valuation of 2–7 kW/m. In 2013, Jiang (2013) used the SWAN model to simulate and analyze the wave energy resources of the Zhejiang sea area. Liang et al. (2013) used the SWAN model to analyze the wave energy resources climate characteristics from 1996 to 2011. It is found the maximum value of the wave power density is 296 kW/m, and the average value is 5.1 kW/m. In 2015, Liu et al. (2015) used the SWAN model to simulate the wave energy of the sea around Shandong. It is suggested that small and medium wave energy can be used in the sea area.

Until now, the research on wave energy in China seas is mainly focused on the mixed wave. The separately research on wind-sea or swell is very scarce. In the actual ocean, swell can be surprisingly destructive in the actual ocean; it can lead to phenomena such as hogging and sagging that can cause serious damage to ships. After being generated by a storm, swell can propagate long distances until it breaks and dissipates upon reaching a coast. These characteristics make swell an indicator of various atmospheric phenomena like tropical cyclones, distant storms, or even large-scale sea breeze such as that related to the monsoon. As a vast and reliable source of energy, swell has been the focus of increasing attention for power generation because of its potential contribution to alleviating energy and environmental problems. An Australian company, Oceanlin, has achieved better results by using swell power. This chapter uses the ERA-40 wave reanalysis data from ECMWF, which separates the wind wave and the swell, to analyze the features of the wind wave and swell in Xisha and Nansha Island sea area, and explore the energy characteristics around the important island and the wave power generation prospects.

8.1 Data and Methodology

8.1.1 Data

Based on the ERA-40 wave reanalysis data, the wind-sea energy, swell energy and mixed wave energy in an important remote island of the South China Sea was analyzed. The ERA-40 wave reanalysis data ranges from Sep 1st, 1957 to Aug 31st, 2002 with the time resolution of 6 h and spatial resolution of $1.5^\circ \times 1.5^\circ$, covers global ocean and separates the wind wave and swell from each other. ERA-40 wave reanalysis data is the first re-assimilation products coupled with wave (WAM) and the atmospheric general circulation model simulations, moreover, assimilated observations datas. Wave reanalysis data is divided into four different periods,

however, the problem of observational data in December 1991–1993 in May leads to the data assimilation time errors being relatively larger. In general, ERA-40 wave data with high precision (Hemer et al. 2007; Alvaro and Kay 2010; Alvaro et al. 2009; Bi et al. 2012; Zheng and Li 2017a, b; 2018) processes the longest time series so far, therefore the separation of the wind wave and swell should be the best choice.

8.1.2 Methodology

In this chapter, the ERA-40 wave reanalysis data which separate the wind-sea and swell over the past 45 years (1957.09–2002.08) derived from ECMWF are adopted. The sea surface wind speed, wind-sea wave height, swell wave height, wave class occurrence and wave direction occurrence in an important remote island of the South China Sea was analyzed. The seasonal variation and stability characteristics of wind-sea wave energy and swell wave energy are mainly discussed.

8.2 Monthly Characteristics of Wind Speed and Wave Height

The monthly variation of sea surface wind speed, wind-sea wave height, swell wave height and mixed wave height in the research region appear "W" form feature, as shown in Fig. 8.1. In winter, the wind speed and wave height are the highest, the secondary peak is summer, and the value of spring and autumn are the trough. The

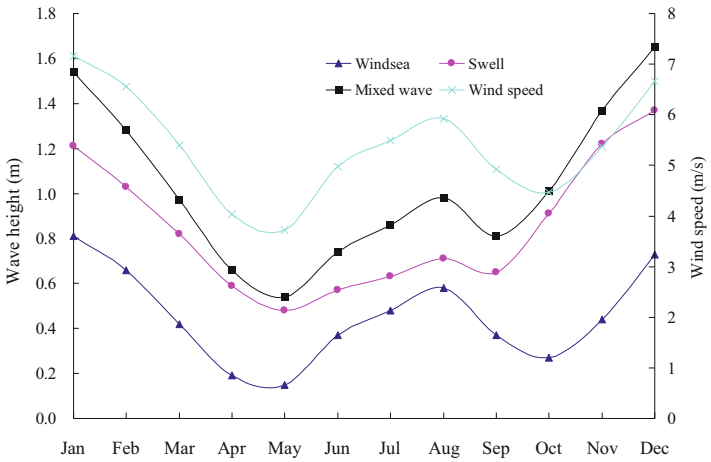

Fig. 8.1 Monthly characteristics of sea surface wind speed, wind-sea wave height, swell wave height and mixed wave height. (After Zheng et al. 2011b)

Table 8.1 Wave class occurrence (%)

Wave class	Wave height (m)	January	April	July	October
0	–	0	0	0	0
1	<0.1	0	0	0.38	0
2	0.1–0.5	0.76	30.21	27.37	11.55
3	0.5–1.25	30.76	49.27	37.72	51.44
4	1.25–2.5	45.03	4.12	17.29	18.75
5	2.5–4.0	6.78	0.06	0.9	1.79
≥6	≥4.0	0.32	0	0	0.13

monthly variation of wind-sea wave height is almost the same as that of sea surface wind speed. The monthly variation of swell wave height is consistent with that of mixing wave height.

8.3 Wave Class Occurrence

In this paper, the wave class occurrence is statistically analyzed by using ERA-40 reanalysis data which span from 00:00 September 1, 1957 to 18:00 August 31, 2002. The standards for wave classification are published be the State Oceanic Administration (Shi et al. 2000).

As shown in Table 8.1, in January, the significant wave height of the research region is mainly concentrated in class 3–5, where the class 4 is the highest, about over 45%. In April, the significant wave height is mainly concentrated in class 2–3. In July, the significant wave height is mainly concentrated in class 2–4. In October, the significant wave height is mainly concentrated in class 3, the occurrence is about 51%, followed by class 2 and class 4. Generally speaking, the significant wave height in the research region is mainly between 0.5 and 2.5 m. The occurrence of class 5 or above is low.

8.4 Occurrence of Wave Direction

Referring to the marine survey standard, the wave direction is divided into 16 directions (Shi et al. 2000). The occurrence of wave direction in the research region is statistically analyzed, as shown in Fig. 8.2.

In January, the wind-sea direction is dominated by the NE direction; the swell wave direction is dominated by the NE-NNE direction. In April, the main wind-sea wave direction is S; the main swell direction is NE. Obviously, the angle between the wind-sea wave direction and swell wave direction is larger than 90 degree. In July, the wind-sea wave direction is dominated by the S-SW; the

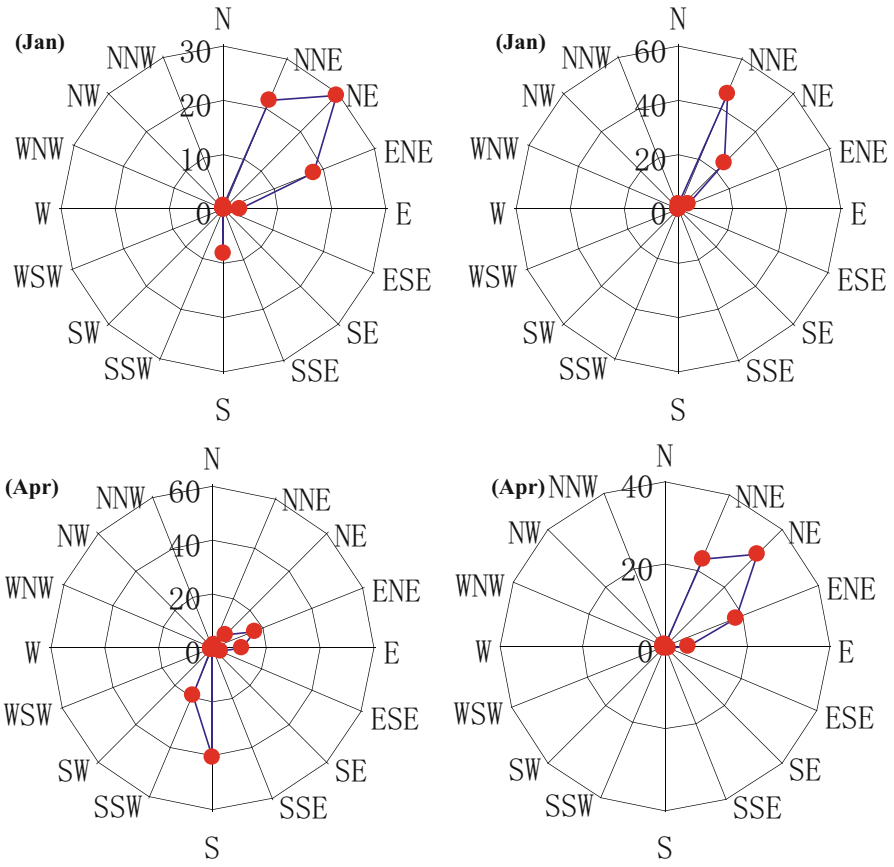

Fig. 8.2 Occurrences of wind-sea wave direction (left) and swell wave direction (right) in January, April, July and October. (After Zheng et al. 2011b)

swell wave direction is mainly WSW. In October, the wind-sea wave direction is dominated by S. The swell direction is dominated by NE.

As a whole, the wind-sea wave direction and swell wave direction have a good agreement in monsoonseason. But during the monsoon transition season, such as April and October, the wind-sea wave direction is dominated by partial S, while the swell wave direction is dominated by partial NE.

8.5 Monthly Characteristics of the Wave Power Density

Based on the 6-hourly wind-sea wave height and wave period data, using the calculation method of wave power density in section "5.1.4 Calculation Method of Wave Power Density", the 6-hourly wind-sea wave power density for the period

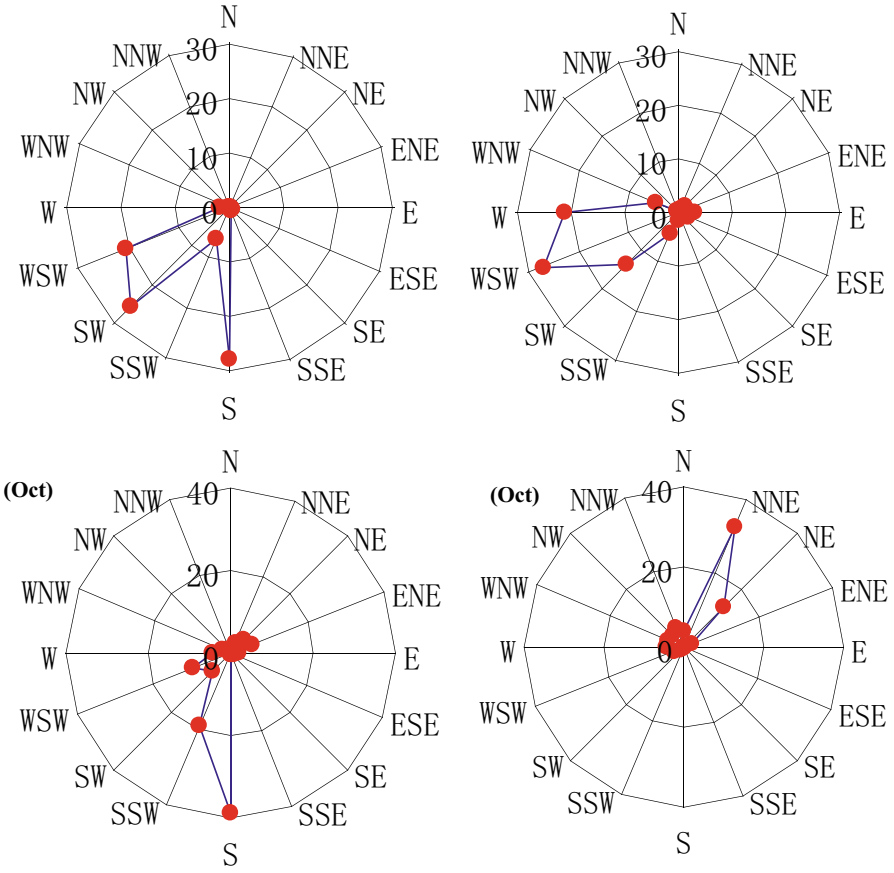

Fig. 8.2 (continued)

1957.09–2002.08 is obtained. Similarly, the 6-hourly swell wave power density and 6-hourly mixed wave power density for the period 1957.09–2002.08 are obtained.

Averaging the wind-sea wave power density from 0000 UTC on January 1st, 1958 to 1800 UTC on January 31st 1958, a month average value of wind-sea wave power density is obtained. Similarly, the month average value of wind-sea wave power density in each January for the past 45 years (1957.09–2002.08) is obtained. Then the multi-year average value of wind-sea wave power density in January is obtained. Using the same method, the multi-year average value of wind-sea wave power density from January to December is obtained. Similarly, the multi-year average values of swell wave power density and mixed wave power density from January to December are obtained. The monthly characteristics of the wind-sea, swell and mixed wave power density are presented in Fig. 8.3.

The swell energy (swell wave power density) in the research region is obviously larger than the wind-sea wave energy (wind-sea wave power density). The mixed

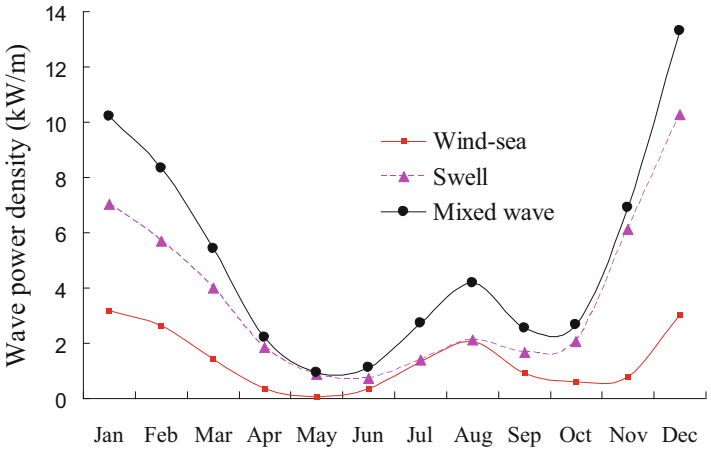

Fig. 8.3 Monthly characteristics of wind-sea and swell wave power density. (After Zheng et al. 2011b)

wave energy (mixed wave power density) is larger in November to the following March, of about 5–13 kW/m; lower in April to June, of about 1–2 kW/m. Due to the low latitude and small wind speed, the wind-sea wave power density of the research region from April to October is close to 0.

The annual average mixed wave power density in the research region is about 4.8 kW/m. The wave energy above 70% is swell energy, and the minimum value is more than 1 kW/m. Therefore, the integrated wave power generation device can be built.

8.6 Stability of Wind–Sea and Swell Energy

The development and utilization of wave energy are very concerned with the stability of energy, and the stable of wave power density is beneficial to the collection and transformation of energy. In the unstable conditions, it is not only detrimental to energy acquisition, but may damage the equipment. In this chapter, the stability of wind-sea and swell wave power density in South China Sea is judged by calculating the coefficient of variation (Cv). The smaller the Cv, the better stability. Using the 6-hourly wind-sea wave power density for the period 0000 UTC on January 1st, 1988 to 1800 UTC on January 31st 1958, the Cv in January 1958 is calculated. Similarly, the Cv in each January for the past 45 years (1957.09–2002.08) is calculated. Then the multi-year average Cv in January of wind-sea wave power density is obtained. Using the same method, the multi-year average Cv of wind-sea wave power density and swell wave power density in January, April, July and October were obtained, as shown in Figs. 8.4 and 8.5.

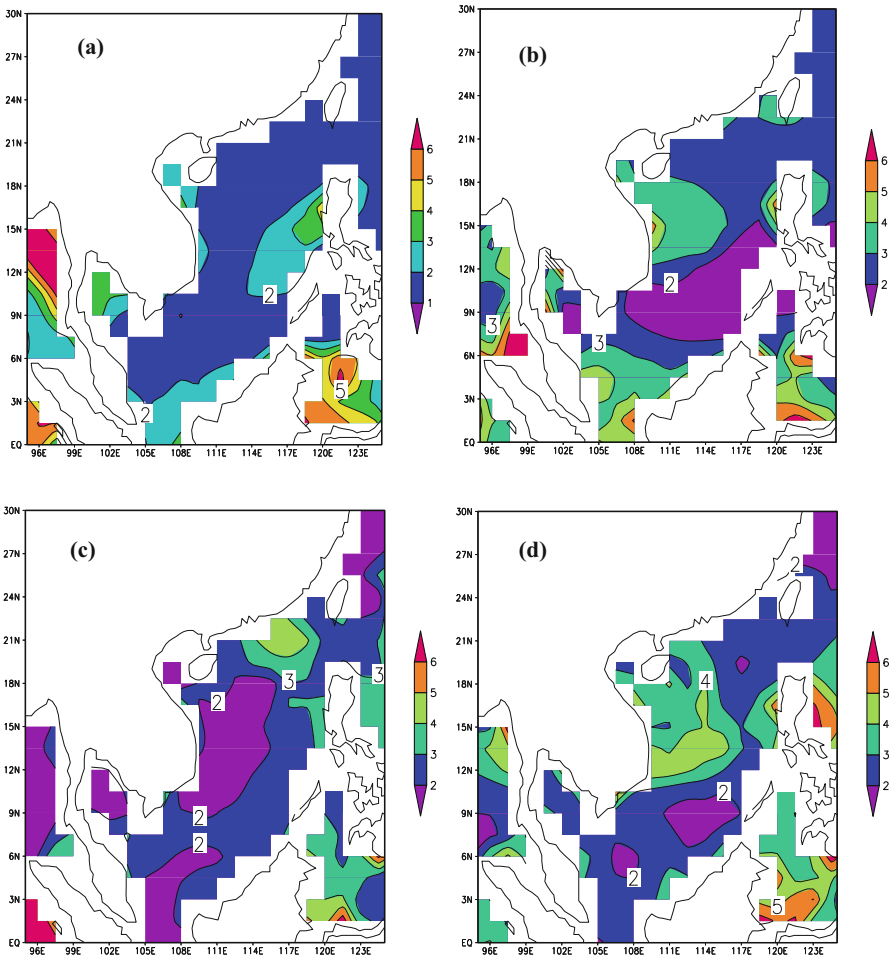

Fig. 8.4 Coefficient of variation of wind-sea wave power density in January (**a**), April (**b**), July (**c**) and October (**d**). (After Zheng et al. 2011b)

Obviously, in January, April, July and October, the coefficient of variation of the swell wave power density is smaller than that of the corresponding wind-sea wave power density. It indicates that the swell energy is more stable than that of the wind-sea.

The stability of wind-sea wave power density: the stability in January is better than in other months. Most of the Cv in South China Sea are below 2. The secondary months are the April and July, the worst stability in October (with Cv in most areas above 2). This may be related to the frequent typhoon activity in the

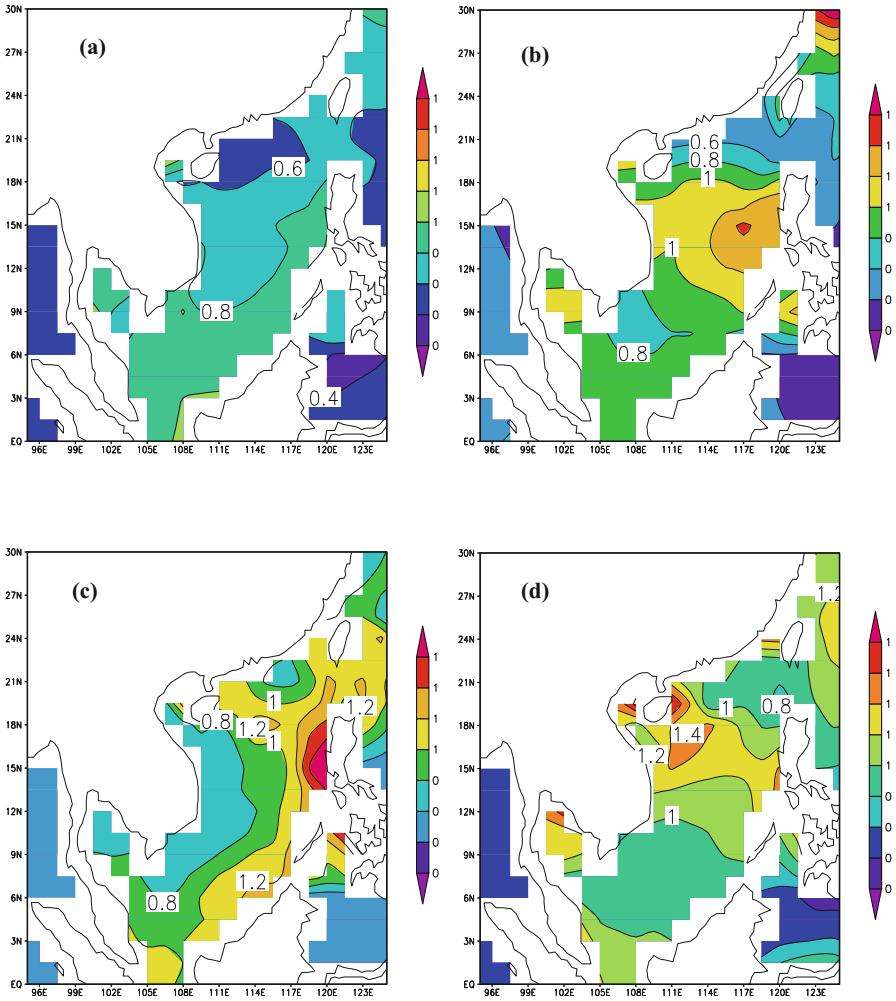

Fig. 8.5 Coefficient of variation of swell wave power density in January (**a**), April (**b**), July (**c**) and October (**d**). (After Zheng et al. 2011b)

South China Sea in October, and the cold air invasion at some time, resulting in the instability of the waves in the South China Sea.

The stability of swell wave power density: similar to the wind-sea, the best stability is January, followed by April and July, and the worst stability in October. Therefore, in South China Sea, under the control of strong winter wind, the wind wave and swell wave power density can be relatively stable. In autumn, the impact of typhoon and cold air on the South China Sea is relatively worst.

8.7 Summary and Prospect

The sea surface wind speed, wind-sea, swell and mixed wave height in the research region show the "W" form in the monthly variation characteristics. In winter, the wind speed and wave height are the largest, followed by the summer, and the two transition seasons (spring and autumn) are relatively weak. In the research region, the change of wind-sea wave height is determined by the change of sea surface wind speed, while the variation of mixed wave height (significant wave height) is mainly determined by the change of swell wave height.

The significant wave height in the research region is mainly between 0.5 and 2.5 m. The occurrence of class 5 wave is over 10% in January and October. Except spring, the wind-sea wave direction and swell wave direction have a good agreement. The wind-sea wave direction and swell wave direction is more consistent in monsoon season; but in monsoon transition season, the wind-sea wave direction is dominated by partial S, while the swell wave direction is dominated by partial NE.

In the South China Sea, the swell wave power density is more stable than that of the wind-sea wave power density. Both the stability of wind-sea and the swell wave power density are the best in January, and the stability is relatively poor in October. The annual average mixed wave power density is about 4.8 kW/m, and the swell wave power density is about 70%.

Due to the stability and huge energy storage of the swell, the research of swell power generation has been paid much attention internationally. For the lack of wave data that separate the swell and wind-sea, the research on the swell energy is scarce until now. In this chapter, we analyzed the wind-sea, swell and mixed wave energy of a remote island in the South China Sea for the first time at home and abroad, in hope of providing scientific guidance for the swell power generation. Here, we only analyzed partial of the swell parameters: the monthly characteristics of wind speed, monthly characteristics of wave height (wind-sea, swell and mixed wave), and monthly characteristics of wave power density (wind-sea, swell and mixed wave), stability of wind-sea energy and swell energy, wave class occurrence, occurrence of wave direction, and so on. In the future work, an in-depth research on the swell energy is needed. It is necessary to systematically considering the value size of swell wave power density, available rate of swell energy, swell energy level occurrence, long term trend of swell energy, swell energy storage, the coming direction of swell energy (swell energy rose), propagation characteristics of swell energy (propagation route, propagation speed, propagation terminal target), short-term forecasting and long-term prediction of swell energy, etc., to provide guidance for the swell power plant location, daily operation of swell power generation device, mid-long term development plan of swell energy.

In this chapter, the ERA-40 wave reanalysis from the ECMWF is used to analyze the characteristics of wind-sea energy, swell energy and mixed wave energy for the first time, which pointed out the direction for the research of swell energy. However, the spatial resolution of the ERA-40 wave reanalysis used in this book is relative low, which can not focus on the islands and reefs very well. In the future work, it is

necessary to use the new numerical wave model WW3 (Version 4.18 or an updated version) to obtain a high spatial resolution wave data that separate apart the the wind-sea and swell, thus to detailed analyze the characteristic of swell energy of the important remote islands and reefs.

References

Alvaro S, Kay S (2010) A global view on the wind sea and swell climate and variability from ERA-40. J Clim 23:1461–1479

Alvaro S, Kay S, Anna R (2009) Variability of Wind Sea and swell waves in the North Atlantic based on ERA-40 re-analysis. In: Proceedings of the 8th European wave and tidal energy conference, Uppsala, Sweden, pp 119–129

Bi F, Kejian WU, Yuming ZHANG (2012) The effect of stokes drift on Ekman transport in the open sea. Acta Oceanol Sin 31(6):12–18

Chu TJ (2004) Marine energy resources development and utilization. Chemical Industry Press, Beijing

Hemer MA, Church JA, Hunter JR (2007) Waves and climate change on the Australian coast. J Coast Res 50:432–437

Jiang T S. (2013) Wave numerical simulation and wave energy resource analysis in the waters of Zhejiang province. Master degree thesis of Zhejiang University of Technology

Liang BC, Fan F, Yin ZG, Shi HD, Lee DY (2013) Numerical modelling of the nearshore wave energy resources of Shandong peninsula, China. Renew Energy 57:330–338

Liu SH, Yang ZL, Yue XY (2015) Wave energy resource assessment in Shandong offshore. Acta Oceanol Sin 37(7):108–122

Ren JL, Zhong YJ, Zhang XM (2006) State of arts and prospects in the power generation from oceanic wave. J Zhejiang Univ Technol 34(1):69–73

Shi MC, Gao GP, Bao XW (2000) Ocean survey method. Qingdao Ocean University Press, Qingdao

Wan Y, Zhang J, Meng JM et al (2015) A wave energy resource assessment in the China's seas based on multi-satellite merged radar altimeter data. Acta Oceanol Sin 34(3):115–124

Wang CK, Lu W (2009) Marine energy resource analysis method and reserve assessment. China Ocean Press, Beijing

Wen B, Xue YG, Zhang FR (2013) Numerical simulation of wave energy resources in the China Sea. Mar Forecast 30(2):36–41

You YG, Ma YJ (2003) The sea energy source application in the sea environment. Meteorol Hydrol Mar Instrum 3:32–35

Zheng CW, Li XQ (2011) Wave energy resources assessment in the China Sea during the last 22 years by using WAVEWATCH-III wave model. Period Ocean Univ China 41(11):5–12

Zheng CW, Li CY (2017a) Analysis of temporal and spatial characteristics of waves in the Indian Ocean based on ERA-40 wave reanalysis. Appl Ocean Res 63:217–228

Zheng CW, Li CY (2017b) Propagation characteristic and intraseasonal oscillation of the swell energy of the Indian Ocean. Appl Energy 197:342–353

Zheng CW, Zheng YY, Chen HC (2011a) Research on wave energy resources in the northern South China Sea during recent 10 years using SWAN wave model. J Subtrop Res Environ 6(2):54–59

Zheng CW, Zhou L, Zhou LJ (2011b) Seasonal variation of wave and wave energy in Xisha and Nansha Sea area. Adv Mar Sci 29(4):419–426

Zheng CW, Li CY, Pan J (2018) Propagation route and speed of swell in the Indian Ocean. J Geophys Res Oceans 123:8–21. https://doi.org/10.1002/2016JC012585

Chapter 9
Wind Climate Under the Demand of Island Runway Design

Remote islands and reefs are the important support for human society to step into the deep sea, which can provide support for oceanic supply, maritime search and rescue, humanitarian aid, disaster prevention and mitigation. An understanding of the characteristics of the marine environment is key to safety in marine construction (Li 2000; Li and Mu 2001a, b; Li et al. 2001, 2003a, b, 2004a, b, 2008a, b, 2016). The runway is one of the most important parts of the remote islands and reefs construction, which has long been a worldwide problem. In the construction of runway design, the factors need to be considered include: geographical features, climate features, marine environmental characteristics, etc. Building the runway according to the terrain can save materials, shorten the construction period and reduce the difficulty of building, which has certain rationality. But in practice, the runway is mainly used to support the aircraft to take-off and landing. Whether the runway is benefit for aircraft rising or landing should be the highest standard of runway construction. Strong cross winds and gusts can easily cause the aircraft to slip out of the runway. The phenomenon is particularly evident in the island runway. This requires a detailed statistical analysis of wind climate characteristics under the demand of island runway construction.

Previous researchers have done much research and contribution to the wind characteristics of the global oceans. Li et al. (2003a, b) used the 46-year (1950–1995) meteorological ship data to analyze the average wind speed, and gale occurrence of the northern Indian Ocean. Zheng et al. (2015) used the ERA-interim reanalysis wind data from the European Centre for Medium-Range Weather Forecasts (ECMWF) to analyze the wind climate characteristics of the 21st Century Maritime Silk Road, mainly including the seasonal characteristics of the sea surface wind (wind direction and wind speed), (strong) wind direction occurrence, gale occurrence and gust occurrence, gust index, long term trend of the sea surface wind speed. Zheng et al. (2012) have analyzed the abrupt change of sea surface wind speed in northern Indian Ocean. It is found that the abrupt change of annual mean sea surface wind speed is similar to that in winter, and the mutation period is in early 1980s. Liu and He (2003) used the QuikSCAT wind data to analyze the gale

C. Zheng et al., *21st Century Maritime Silk Road: Construction of Remote Islands and Reefs*, Springer Oceanography, https://doi.org/10.1007/978-981-10-8114-9_9

occurrence in the South China Sea. It is found that there is northeast gale occurrence center in the Bashi Channel and the Taiwan Straits from October to March, in December, the maximum occurrence can even reach 20 d. In summer, from June to August, the occurrence of southwest gale increases from 6 d to 12 d. Zheng used the 10 years (August 1999 to July 2009) QuikSCAT/NCEP wind data to analyze the seasonal and regional differences of the gale occurrence in the global oceans.

But so far, there is little statistical analysis on the wind climate under the demand of runway design of remote islands and reefs. Based on the ERA-interim wind data from the ECMWF, this chapter assumed a remote island as a study case, to statistical analysis the wind climate characteristics under the demand of runway design, in hope of providing scientific and technological support and decision-making assistance for the runway design of remote islands and reefs.

9.1 Data and Methodolog

9.1.1 Data

The chapter uses the ERA-interim wind data (contain U and V components) and ERA-interim gust data to statistical analyze the wind climate characteristics under the demand of island runway construction. The ERA-Interim wind data is hosted at the ECMWF, which is a new production after the ERA-40 data. A high resolution meteorology model is applied to obtain this data (Dee et al. 2011; Song et al. 2015). There also exists a great improvement in the assimilation method and application of observation data. The temporal resolution covers 6-hourly, daily and monthly. In this study, the temporal resolution of 6-hourly is used. The spatial resolution covers $0.125° \times 0.125°$, $0.25° \times 0.25°$, $0.5° \times 0.5°$, $0.75° \times 0.75°$, $1.0° \times 1.0°$, . . ., $2.5° \times 2.5°$. In this study, the spatial resolution of $0.125° \times 0.125°$ is used. It covers the time range from January 1979 to December 2014 and a space range of 90°S to 90°N and 0.0°E to 359.875°E. The ERA-Interim wind data is proved to have a high precision by comparing with the observation data (Dee et al. 2011; Bao and Zhang 2013; Song et al. 2015), and can be available at http://data-portal.ecmwf.int/data/d/interim_daily/ (ECMWF 2011).

9.1.2 Methodology

The chapter selects a remote island as the assumed object of study. The topography of this island is near north-south, and some engineers have planned the reef runway as north-south direction, which is mainly based on the terrain. The idea and method can save the material, shorten the construction period and reduce the difficulty. However, in practice, the runway is mainly to safeguard the aircraft from take-off and landing, and the strong cross winds and gusts can easily cause the aircraft to slip

out of the runway. This requires fine statistical analysis of the wind characteristics of the island, so as to provide decision-making support for runway construction. In the chapter, ERA-interim 10 m sea surface wind field data and ERA-interim gust wind speed data from the ECMWF are used to statistical analyze the wind climate characteristics under the demand of island runway construction, mainly including the wind rose (combination occurrence of wind direction and wind speed), gale occurrence, occurrence of gust wind speed above 10.8 m/s, gust index and so on.

9.2 Wind Climate Analysis

This chapter use the ERA-interim 10 m sea surface wind field data and ERA-interim gust data from the ECMWF to analyze the wind climate, which is important in the take-off and landing of the aircraft, mainly including the wind rose (combination occurrence of wind direction and wind speed), gale occurrence, occurrence of gust wind speed above 10.8 m/s, gust index and so on.

9.2.1 Wind Rose

The cross wind is one of the important considerations in the planning of the island runway. Based on the 6-hourly wind speed and wind direction data, we contoured the wind rose diagram (combination occurrence of wind direction and wind speed), as shown in Fig. 9.1.

In February, under the effect of the cold air, the highest occurrences of wind direction are NE and ENE, about 36% and 34% respectively. The highest occurrence of wind speed is 6–8 m/s, followed by 8–10 m/s. The strong wind above 10 m/s mainly comes from NNE (7%) and NE (4%).

In May, during the transition of the winter wind to the summer wind, the wind direction is slightly disorder, and relatively high occurrence are SW, E, ENE and WSW. The overall wind speed in this season is low. And the wind speed above 8 m/s mainly comes from SW and WSW direction.

In August, the southwest monsoon has already in vogue. And SW wind direction and WSW wind direction occupy the dominate position, the occurrence is 40%, 33% respectively. The highest occurrence wind speed in the season is 8 m/s and above, followed by 6–8 m/s. The occurrence of strong wind over 10 m/s is obviously higher than that in other seasons. In the WSW and SW directions, the occurrences of the wind speed over 10 m/s are 12% and 6% respectively.

In November, the wind has transited from the summer type to the winter type. The highest occurrence direction is NE (27%) and ENE (26.5%). The highest occurrence

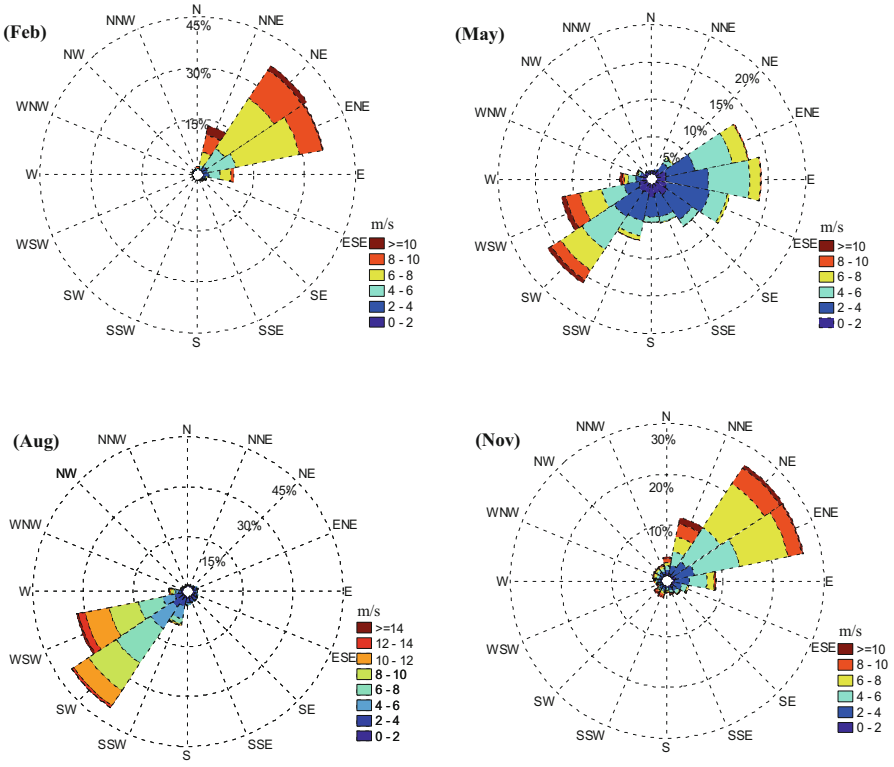

Fig. 9.1 Wind rose in the research region in February, May, August and November. (After Zheng et al. 2017)

wind speed is: 6–8 m/s NE wind (11%), 6–8 m/s ENE wind (11%), 4–6 m/s ENE wind (8%), 6–8 m/s NE wind (7%). The occurrence of wind speed above 8 m/s is relatively low, mainly comes from the NE, NNE, ENE.

In order to demonstrate whether the north-south runway is liable to suffer the cross winds, the paper present Fig. 9.2. Obviously, in February, the gale mainly comes from NNE and NE, which has a large angle with the runway. It means the take-off and landing of aircraft during this season are liable to suffer the cross wind. In August, the gale mainly comes from the SW and WSW, which also has a large angle with the reef runway and liable to threaten the take-off and landing of the aircraft.

It indicates that if the runway is constructed in accordance with the north-south plan (red rectangle in Fig. 9.2), aircrafts are vulnerable to cross winds during winter and summer. If Fig. 9.1 is used as a scientific basis, turn the runway a proper rotation and keep in line with the strong wind direction (green rectangle in Fig. 9.2). It will benefit for the take-off and landing of the aircraft.

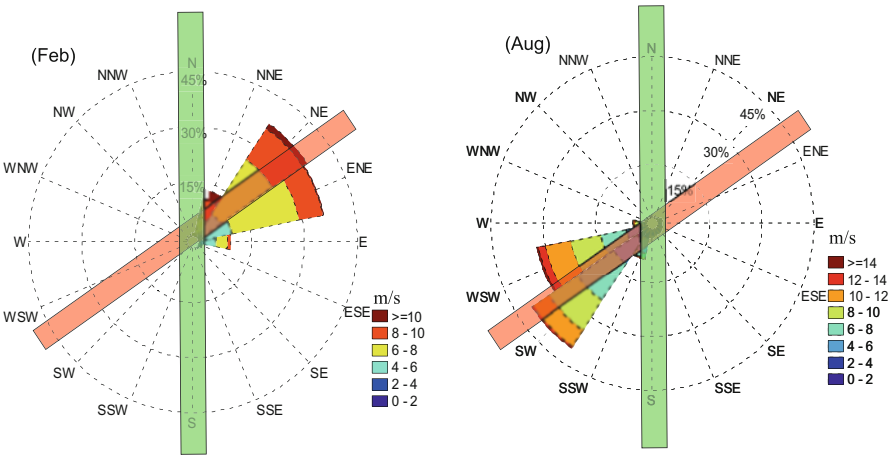

Fig. 9.2 The designed reef runway direction and the wind rose. (After Zheng et al. 2017)
Note: Green represents the designed reef runway direction according to the topography. Red represents the reef runway based on the wind rose.

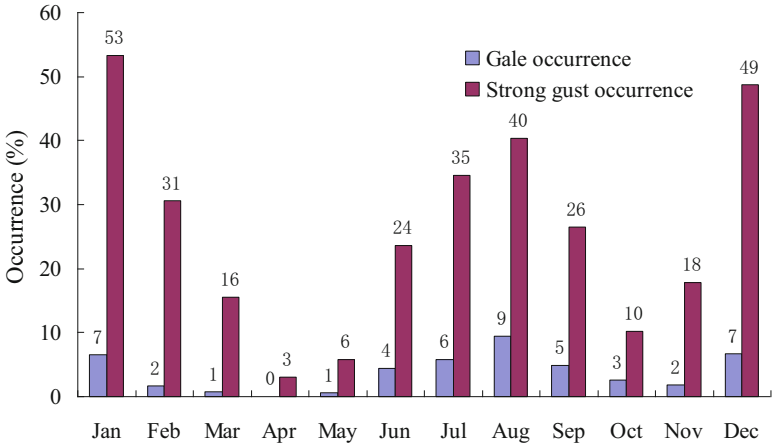

Fig. 9.3 Monthly characteristics of gale occurrence (occurrence of 10 min average wind speed above 10.8 m/s) and strong gust occurrence (occurrence of gust wind speed above 10.8 m/s). (After Zheng et al. 2017)

9.2.2 Gale Occurrence and Strong Gust Occurrence

The gale, especially the strong gust, has a significant effect on the take-off and landing of the aircraft (Zheng 2013). The chapter uses the ERA-interim wind data and ERA-interim gust data to statistically analyze the monthly occurrence of gale occurrence (occurrence of 10 min average wind speed >10.8 m/s), strong gust occurrence (occurrence of gust wind speed >10.8 m/s), as shown in Fig. 9.3.

The gale occurrence is low all year round, within 5%. Only in January, July to August and December, the gale occurrence is relatively high, but only 5–10%. The lower gale occurrence is optimistic for the takeoff and landing of the aircraft. However, the strong gust occurrence is greater than the gale occurrence. Over half of the year (December to February, June to September), the strong gust occurrence is higher than 20%, and in some seasons, even more than 50%. Obviously, although the gale occurrence is low, the strong gust occurrence will still have a great impact on the takeoff and landing of aircraft. This requires more attention to avoid the influence of strong gust during the runway design.

9.2.3 Gust Index

In the actual weather forecasting, the forecasting wind speed is usually the 10 min average wind speed. The Gust Index (GI) is defined as at a given time, the ratio of maximum gust wind speed to the corresponding 10 min average wind speed. The section use the 6-hourly wind field data and gust wind data from 1979 to 2014 to calculate the 6-hourly GI when the 10 min average wind speed is above 10.8 m/s. Based on the 6-hourly GI data, we calculate the monthly average GI, maximun GI and minmum GI from January to December, as shown in Fig. 9.4.

Figure 9.4a presents the average GI. The curve appears one main peak and one secondary peak characteristics. The main peak value appears in November and the secondary peak value appears in July. From January to June, the curve appears gentle, and fluctuates about 1.38.

Figure 9.4b presents the maximum GI. From January to November, the curve tends to gentle and flat, fluctuates from 1.6 to 2.6. The peak value appears in December, about 5.1.

Figure 9.4c presents the minimum GI. From January to June, the curve intensively fluctuates in 1.08–1.23. From July to December, the value tends to decrease. The peak value appears in April, and the trough value appears in November.

9.3 Summary and Prospect

The chapter use the ERA-interim wind data and ERA-interim gust data from ECMWF to statistically analyze the wind climate characteristics under the demand of island runway construction. The results show that, in February and November, the NE, ENE wind dominate the research region, and the occurrence of wind speed of 6–8 m/s is the highest; the wind with speed of above 8 m/s mainly comes from these two direction. In August, the SW and WSW are the dominating direction; the occurrence of wind speed above 8 m/s and above 10 m/s is apparently higher than the other seasons. In May, the wind speed is low. The gale occurrence is low all year round. However, the strong gust occurrence is high. For almost half of the year, the

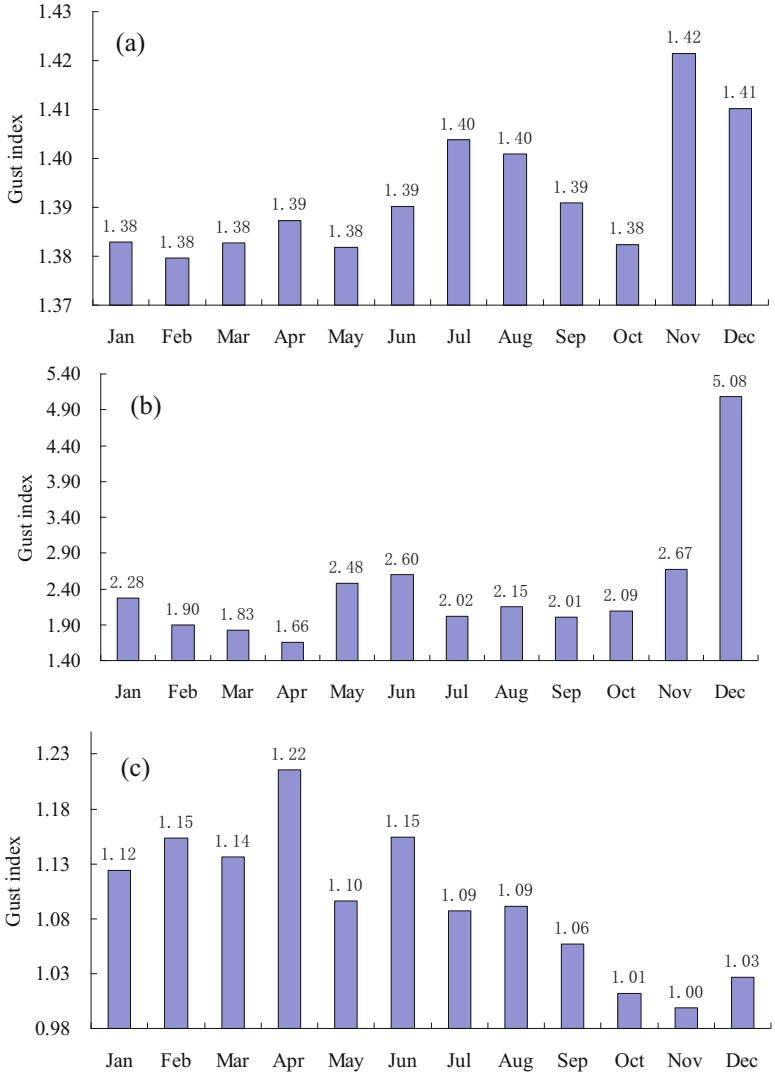

Fig. 9.4 Average (**a**), maximum (**b**), minimum value (**c**) of the gust index. (After Zheng et al. 2017)

strong gust occurrence is higher than 20%, in some seasons can reach 50%. The main peak of the average GI appears on November, about 1.42, the secondary peak value appears on July, about 1.40. From January to June, the curve tends to gentle and flat, fluctuate around 1.38. The maximum GI tends to gentle and flat from January to November, fluctuates in 1.6–2.6, in December the value reaches 5.1. The minimum GI intensively fluctuates from 1.08 to 1.23 in first half of the year, but in the next half of the year, the value tends to decreasing.

To sum up, the strong winds in the area mainly come from NE-SW toward and ENE-WSW toward, and the strong gust occurrence is relatively higher. If the runway is designed according to the topography from north to south. In winter and summer, the aircrafts will suffer crosswind threat. Based on the statistical results of the paper, designing the runway for ENE-WSW toward will be more conducive to reduce the impact of wind on the aircraft.

In this book, the resolution of the ERA-interim data is the highest spatial resolution covering a wide range of sea area, but there is still a big gap from the actual application. Therefore, in the real construction process of runway, the collection and arrangement of marine meteorological observation data is particularly important. Actively building the observation stations in a series of important islands and reefs is benefit for the construct the data foundation for marine engineering. In view of the wind data, it is necessary to obtain data of wind speed and wind direction at different heights, and to study the turbulence, gale direction frequency, gust occurrence and gust index more precisely. It provides more accurate scientific and technological support and decision-making support for the strategic support points construction.

Runway design is a complex and systematic work, this chapter mainly analyzed the effect of the wind speed at 10 m of sea surface on the design of the island runway. Besides the analysis of wind field near the ground, it is necessary to systematically and finely analyze the wind speed and wind direction characteristics at different heights, the influence of island geomorphology or future architecture on the mean wind field, the coordinated construction of runway and port. It is expected to provide more close to the actual demand, more scientific and reasonable program.

References

Bao XH, Zhang FQ (2013) Evaluation of NCEP–CFSR, NCEP–NCAR, ERA-Interim, and ERA-40 reanalysis datasets against independent sounding observations over the Tibetan Plateau. J Clim 26:206–214

Dee DP, Uppala SM, Simmons AJ et al (2011) The ERA-Interim reanalysis: configuration and performance of the data assimilation system. Q J R Meteorol Soc 137(656):553–597

ECMWF (2011) ERA-Interim wind data. http://data-portal.ecmwf.int/data/d/interim_daily/

Li CY (2000) Introduction to climate dynamics. China Meteorological Press, Beijing

Li CY, Mu MQ (2001a) The dipole in the equatorial Indian Ocean and its impacts on climate. Chin J Atmos Sci 25(4):1–10

Li CY, Mu MQ (2001b) The influence of the Indian Ocean dipole on atmospheric circulation and climate. Adv Atmos Sci 18(5):1–16

Li CY, Sun SQ, Mu MQ (2001) Origin of the TBO-interaction between anomalous East-Asian winter monsoon and ENSO cycle. Adv Atmos Sci 18(4):554–566

Li CY, Long ZX, Mu MQ (2003a) Atmospheric intraseasonal oscillation and its important effect. Chin J Atmos Sci 27(4):1–16

Li P, Zhang X, Yu MG (2003b) Analysis of climate characteristics in the northern Indian Ocean. Mar Forecast 20(3):25–30

Li CY, He JH, Zhu JH (2004a) A review of decadal/interdecadal climate variation studies in China. Adv Atmos Sci 21(3):1–10

Li CY, Wang ZT, Lin SZ (2004b) The relationship between east Asian summer monsoon activity and northward jump of the upper westerly jet location. Chin J Atmos Sci 28(5):1–9
Li CY, Mu M, Zhou GQ (2008a) Mechanism and prediction studies of the ENSO. Chin J Atmos Sci 32(4):761–781
Li CY, Gu W, Pan J (2008b) Mei-yu, Arctic oscillation and stratospheric circulation anomalies. Chin J Geophys 51(6):1–12
Li CY, Lin J, Yuan Y, Pan J, Jia XL, Chen X (2016) Frontier issues in current MJO studies. J Trop Meteorol 32(6):1–18
Liu CX, He CX (2003) The analysis on the statistical character of quikscat scatterometer winds and strong wind frequency using remote sensor data from QUIKSCAT. J Trop Meteorol 19 (Supply):107–117
Song LN, Liu ZL, Wang F (2015) Comparison of wind data from ERA-interim and buoys in the yellow and East China seas. Chin J Oceanol Limnol 33(1):282–288
Zheng CW (2013) Statistics of Gale frequency in global oceans. J Guangdong Ocean Univ 33 (6):77–81
Zheng YH, Zheng CW, Li XQ (2012) Study on the characteristics of sea surface wind and wave in North Indian Ocean in recent 45 years. Mari Sci 36(8):53–58
Zheng CW, Li XQ, Gao ZS et al (2015) Strategic of the 21st century Maritime Silk Road: wind climate analysis. Ocean Dev Manag 32(8):4–11
Zheng CW, Gao CZ, Zhang Z, Kong J, Wan Y (2017) Wind climate analysis under the demand of reef runway construction. Mar Forecast 34(4):52–57

Appendix

(1) Wind Energy Rose of the Gwadar Port

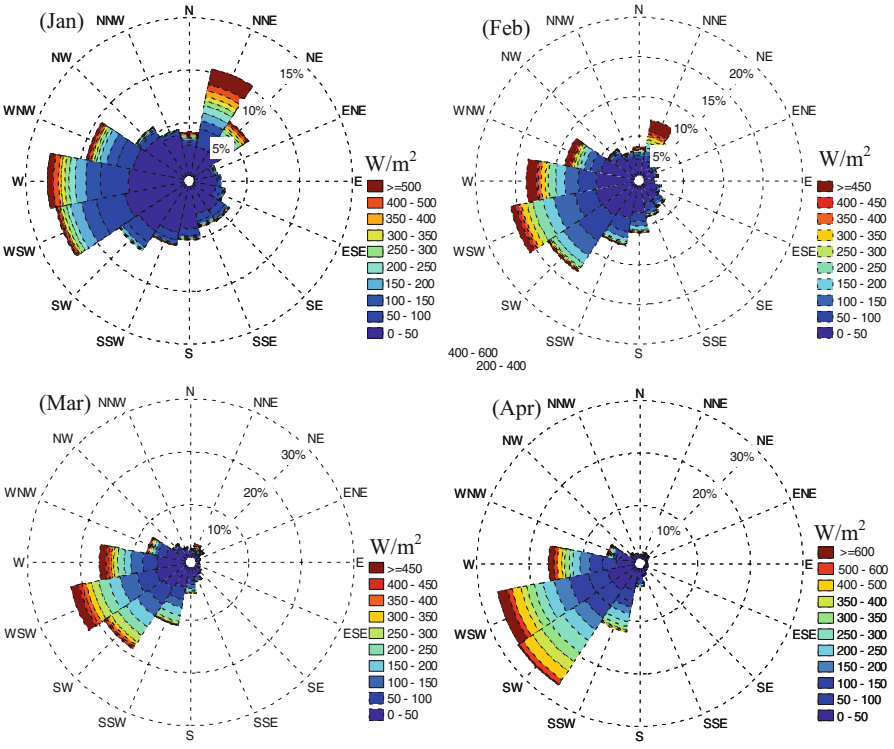

C. Zheng et al., *21st Century Maritime Silk Road: Construction of Remote Islands and Reefs*, Springer Oceanography, https://doi.org/10.1007/978-981-10-8114-9

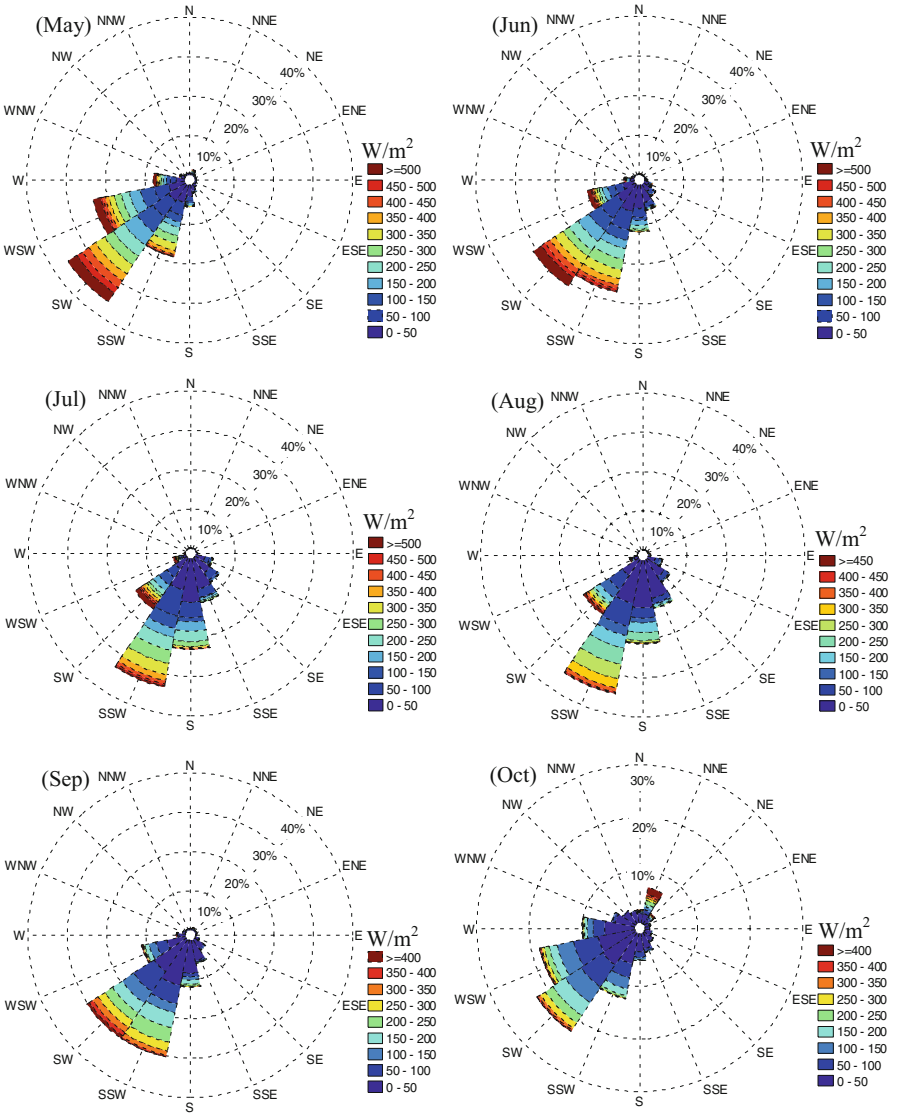
(May)
(Jun)
(Jul)
(Aug)
(Sep)
(Oct)
N
NNE
NE
ENE
E
ESE
SE
SSE
S
SSW
SW
WSW
W
WNW
NW
NNW
10%
20%
30%
40%
W/m2
>=500
450 - 500
400 - 450
350 - 400
300 - 350
250 - 300
200 - 250
150 - 200
100 - 150
50 - 100
0 - 50
>=450
>=400

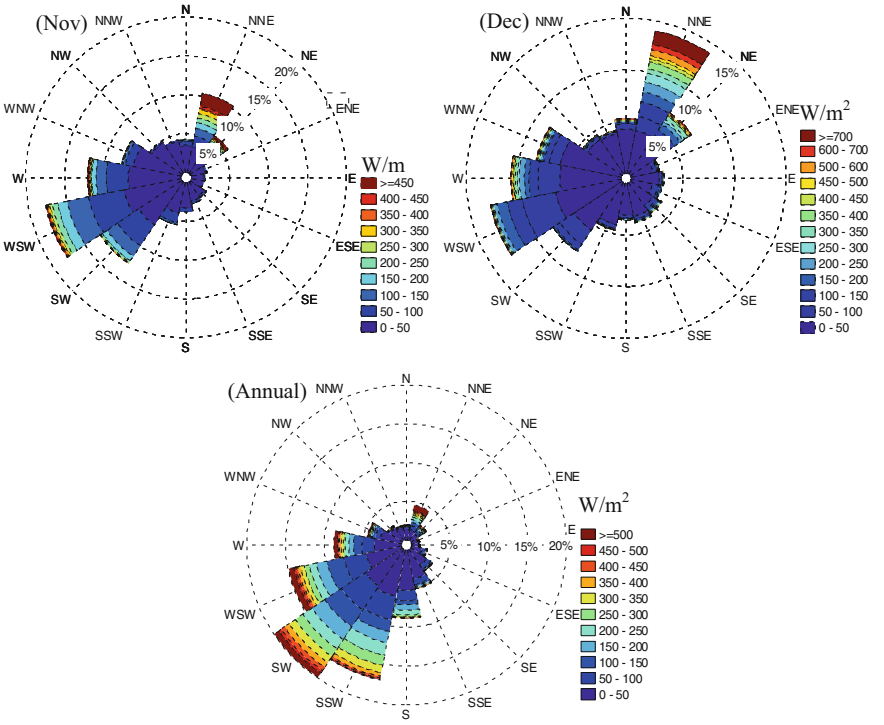
(Nov)
N
NNE
NE
ENE
E
ESE
SE
SSE
S
SSW
SW
WSW
W
WNW
NW
NNW
5%
10%
15%
20%
W/m
>=450
400 - 450
350 - 400
300 - 350
250 - 300
200 - 250
150 - 200
100 - 150
50 - 100
0 - 50
(Dec)
W/m2
>=700
600 - 700
500 - 600
450 - 500
400 - 450
350 - 400
300 - 350
250 - 300
200 - 250
150 - 200
100 - 150
50 - 100
0 - 50
(Annual)
W/m2
>=500
450 - 500
400 - 450
350 - 400
300 - 350
250 - 300
200 - 250
150 - 200
100 - 150
50 - 100
0 - 50

(2) Wind Rose of the Sri Lanka Waters

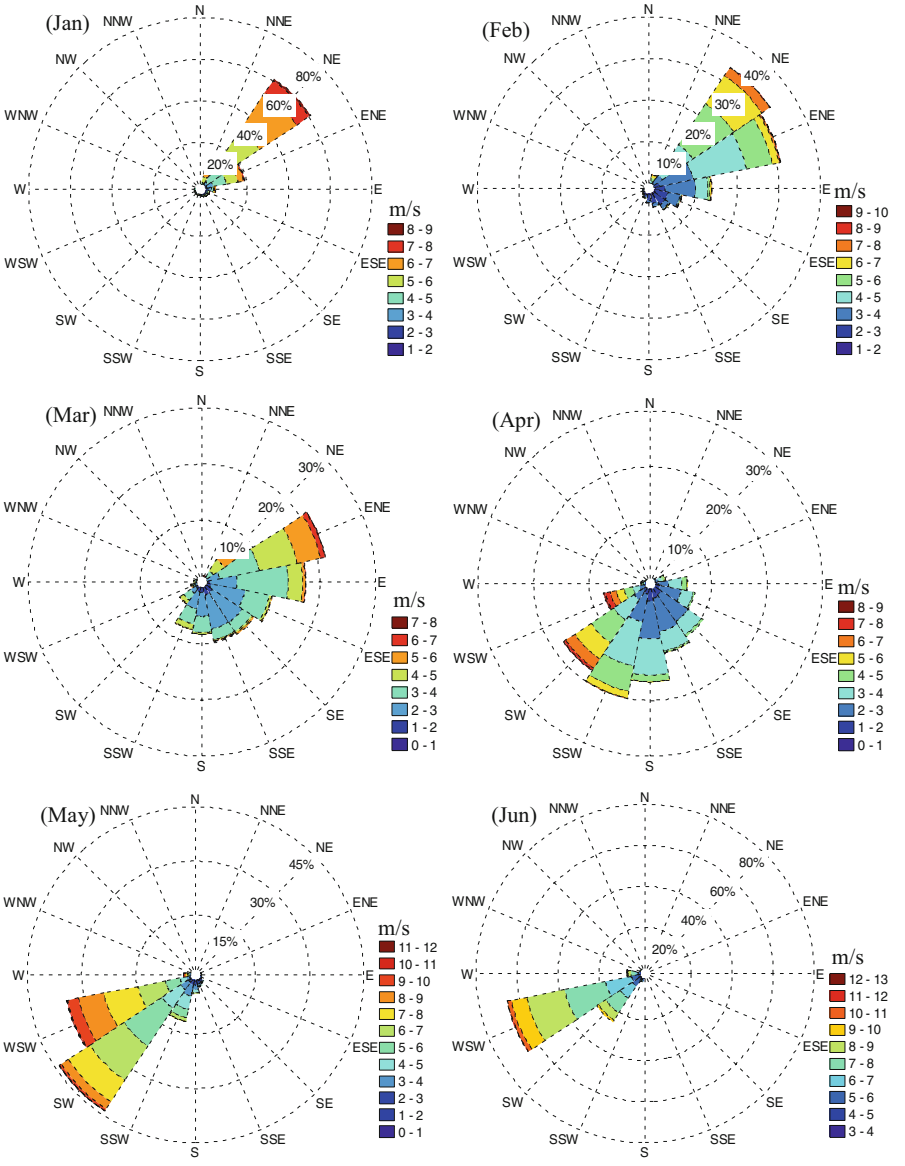

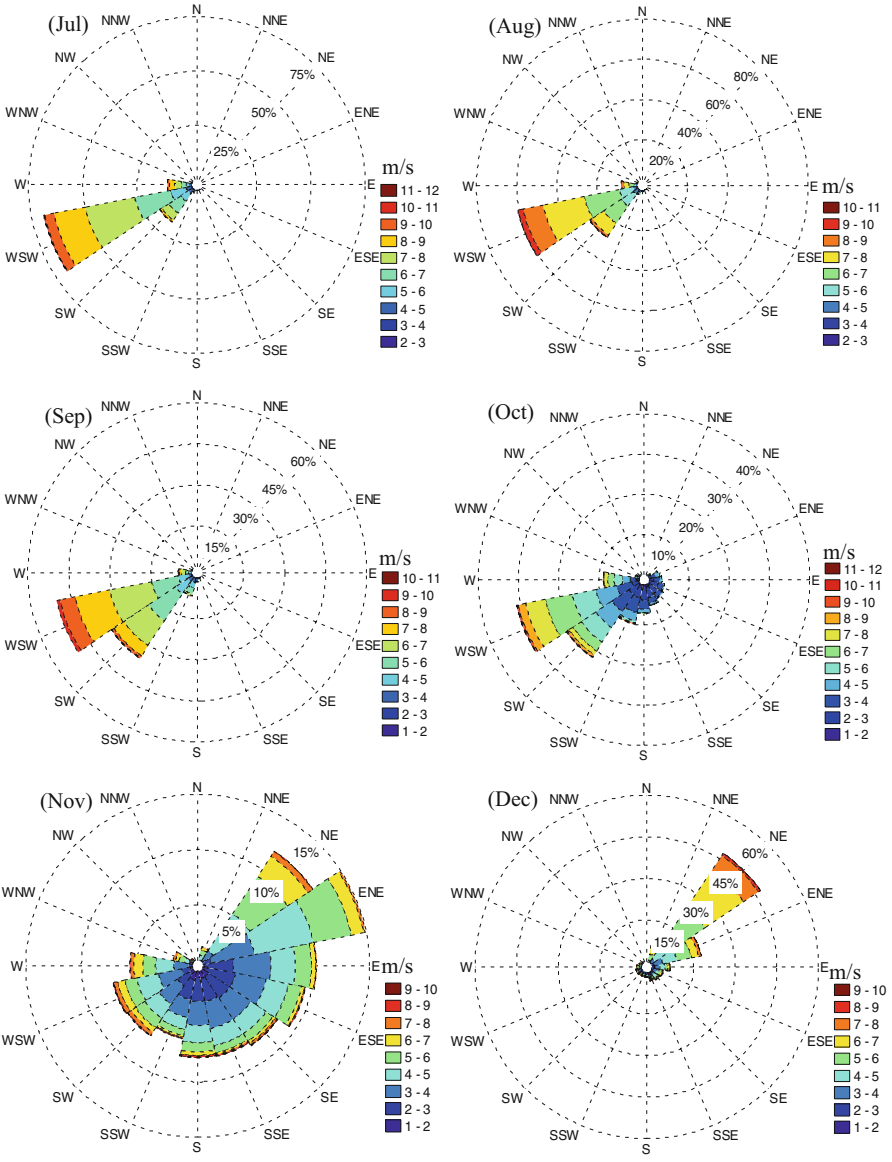
(Jul)
N
NNE
NE
ENE
E
ESE
SE
SSE
S
SSW
SW
WSW
W
WNW
NW
NNW
25%
50%
75%
m/s
11 - 12
10 - 11
9 - 10
8 - 9
7 - 8
6 - 7
5 - 6
4 - 5
3 - 4
2 - 3
(Aug)
20%
40%
60%
80%
m/s
10 - 11
9 - 10
8 - 9
7 - 8
6 - 7
5 - 6
4 - 5
3 - 4
2 - 3
(Sep)
15%
30%
45%
60%
m/s
10 - 11
9 - 10
8 - 9
7 - 8
6 - 7
5 - 6
4 - 5
3 - 4
2 - 3
1 - 2
(Oct)
10%
20%
30%
40%
m/s
11 - 12
10 - 11
9 - 10
8 - 9
7 - 8
6 - 7
5 - 6
4 - 5
3 - 4
2 - 3
1 - 2
(Nov)
5%
10%
15%
m/s
9 - 10
8 - 9
7 - 8
6 - 7
5 - 6
4 - 5
3 - 4
2 - 3
1 - 2
(Dec)
15%
30%
45%
60%
m/s
9 - 10
8 - 9
7 - 8
6 - 7
5 - 6
4 - 5
3 - 4
2 - 3
1 - 2

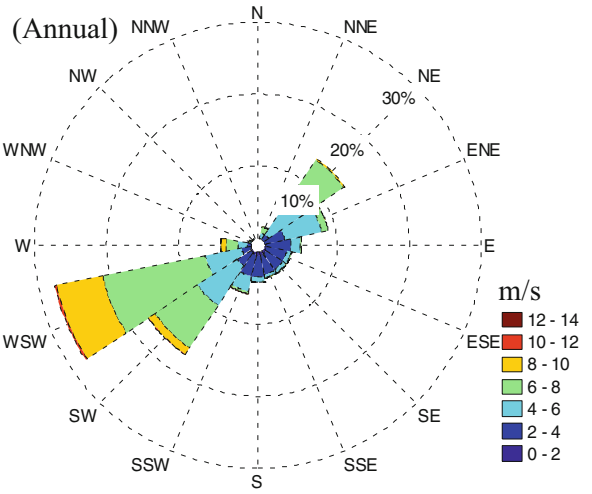
(Annual)
N
NNE
NE
ENE
E
ESE
SE
SSE
S
SSW
SW
WSW
W
WNW
NW
NNW
30%
20%
10%
m/s
12 - 14
10 - 12
8 - 10
6 - 8
4 - 6
2 - 4
0 - 2

(3) Wave Rose of the Sri Lanka Waters

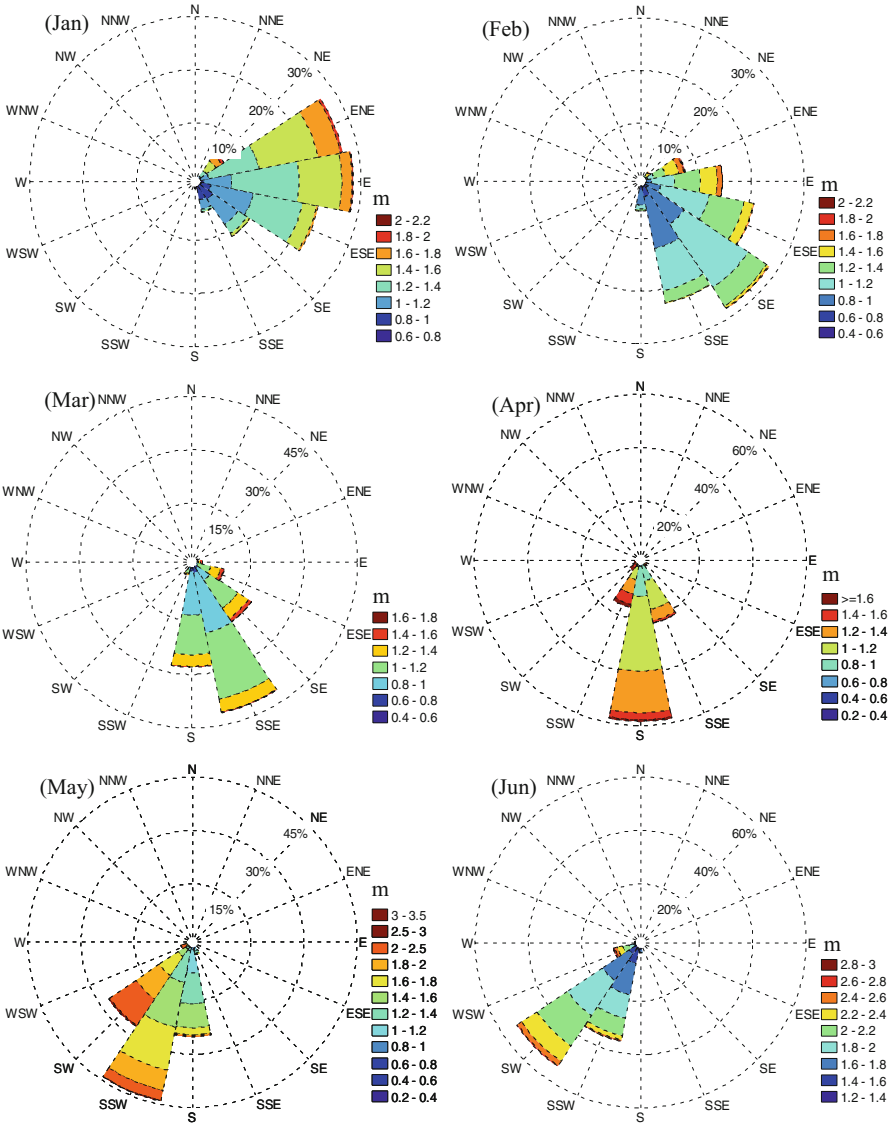

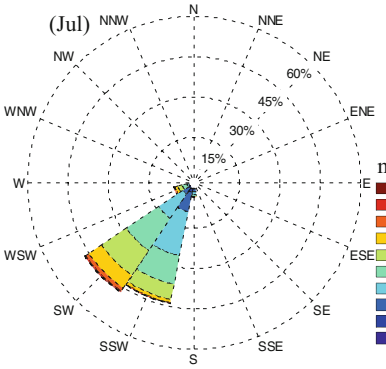
(Jul)
N
NNE
NE
ENE
E
ESE
SE
SSE
S
SSW
SW
WSW
W
WNW
NW
NNW
15%
30%
45%
60%
m
2.8 - 3
2.6 - 2.8
2.4 - 2.6
2.2 - 2.4
2 - 2.2
1.8 - 2
1.6 - 1.8
1.4 - 1.6
1.2 - 1.4
1 - 1.2

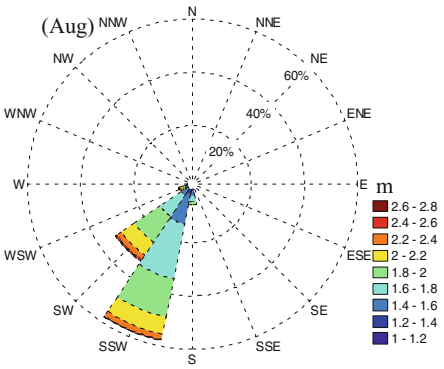
(Aug)
N
NNE
NE
ENE
E
ESE
SE
SSE
S
SSW
SW
WSW
W
WNW
NW
NNW
20%
40%
60%
m
2.6 - 2.8
2.4 - 2.6
2.2 - 2.4
2 - 2.2
1.8 - 2
1.6 - 1.8
1.4 - 1.6
1.2 - 1.4
1 - 1.2

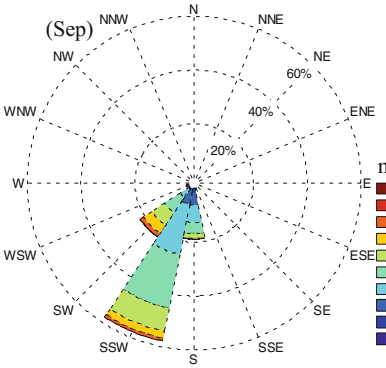
(Sep)
N
NNE
NE
ENE
E
ESE
SE
SSE
S
SSW
SW
WSW
W
WNW
NW
NNW
20%
40%
60%
m
2.6 - 2.8
2.4 - 2.6
2.2 - 2.4
2 - 2.2
1.8 - 2
1.6 - 1.8
1.4 - 1.6
1.2 - 1.4
1 - 1.2
0.8 - 1

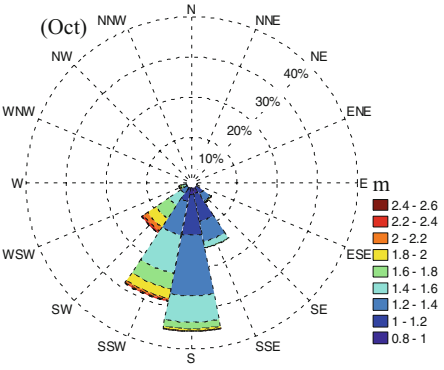
(Oct)
N
NNE
NE
ENE
E
ESE
SE
SSE
S
SSW
SW
WSW
W
WNW
NW
NNW
10%
20%
30%
40%
m
2.4 - 2.6
2.2 - 2.4
2 - 2.2
1.8 - 2
1.6 - 1.8
1.4 - 1.6
1.2 - 1.4
1 - 1.2
0.8 - 1

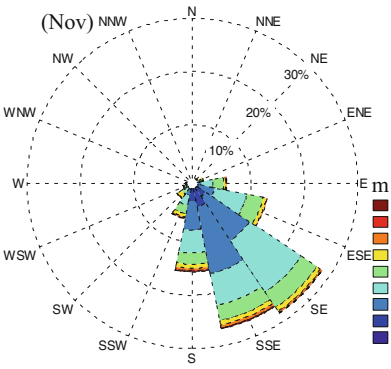
(Nov)
N
NNE
NE
ENE
E
ESE
SE
SSE
S
SSW
SW
WSW
W
WNW
NW
NNW
10%
20%
30%
m
2.2 - 2.4
2 - 2.2
1.8 - 2
1.6 - 1.8
1.4 - 1.6
1.2 - 1.4
1 - 1.2
0.8 - 1
0.6 - 0.8

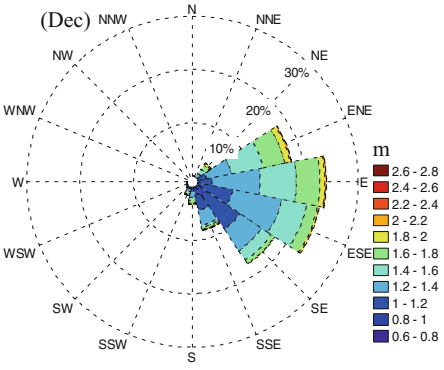
(Dec)
N
NNE
NE
ENE
E
ESE
SE
SSE
S
SSW
SW
WSW
W
WNW
NW
NNW
10%
20%
30%
m
2.6 - 2.8
2.4 - 2.6
2.2 - 2.4
2 - 2.2
1.8 - 2
1.6 - 1.8
1.4 - 1.6
1.2 - 1.4
1 - 1.2
0.8 - 1
0.6 - 0.8

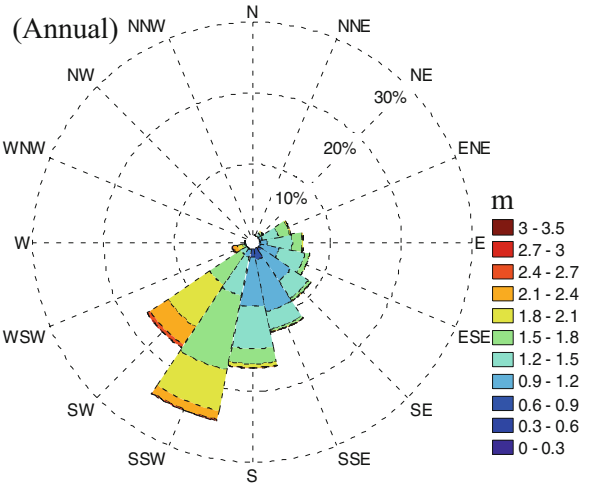
(Annual)
N
NNE
NE
ENE
E
ESE
SE
SSE
S
SSW
SW
WSW
W
WNW
NW
NNW
10%
20%
30%
m
3 - 3.5
2.7 - 3
2.4 - 2.7
2.1 - 2.4
1.8 - 2.1
1.5 - 1.8
1.2 - 1.5
0.9 - 1.2
0.6 - 0.9
0.3 - 0.6
0 - 0.3

(4) Wind Energy Rose of the Sri Lanka Waters

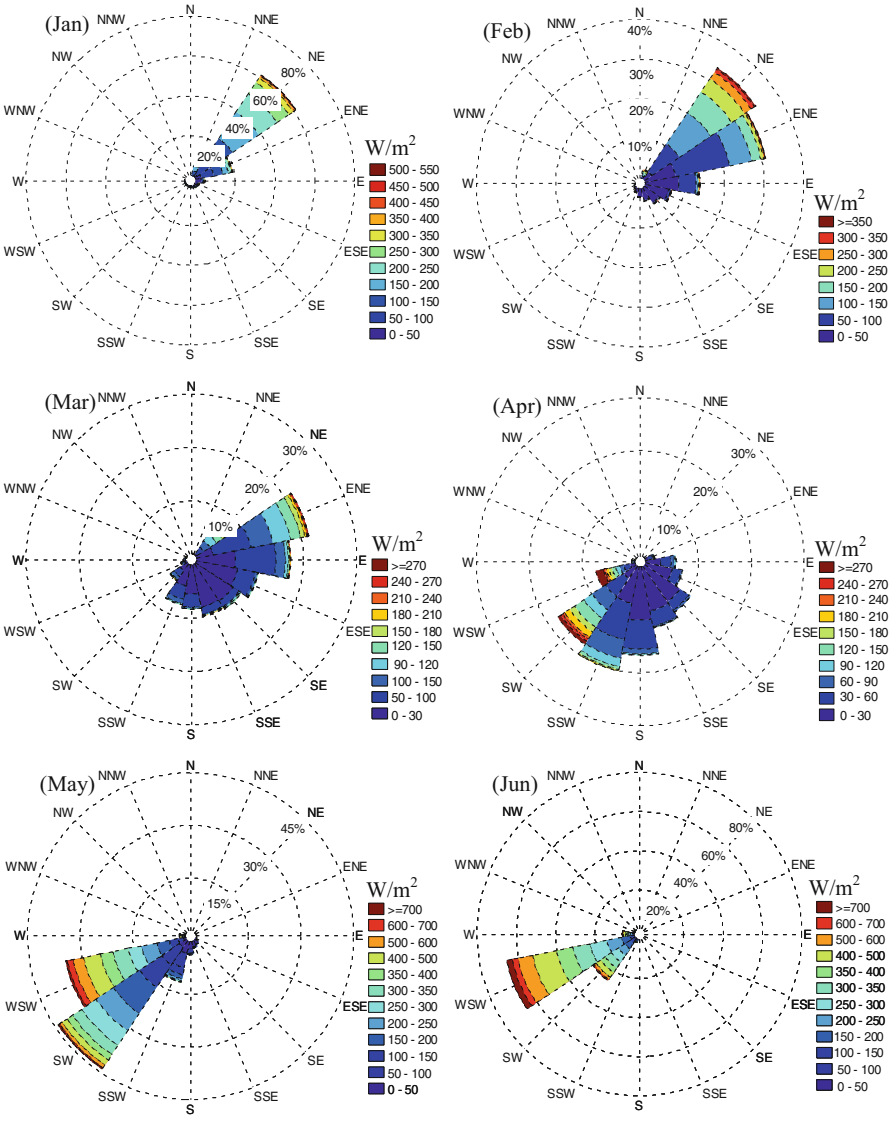

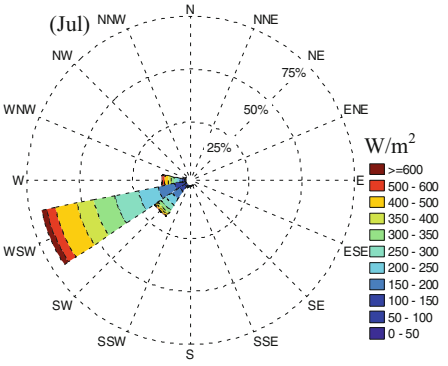
(Jul)
N
NNE
NE
ENE
E
ESE
SE
SSE
S
SSW
SW
WSW
W
WNW
NW
NNW
75%
50%
25%
W/m2
>=600
500 - 600
400 - 500
350 - 400
300 - 350
250 - 300
200 - 250
150 - 200
100 - 150
50 - 100
0 - 50

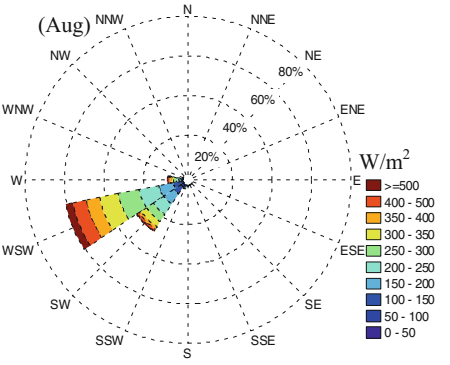
(Aug)
N
NNE
NE
ENE
E
ESE
SE
SSE
S
SSW
SW
WSW
W
WNW
NW
NNW
80%
60%
40%
20%
W/m2
>=500
400 - 500
350 - 400
300 - 350
250 - 300
200 - 250
150 - 200
100 - 150
50 - 100
0 - 50

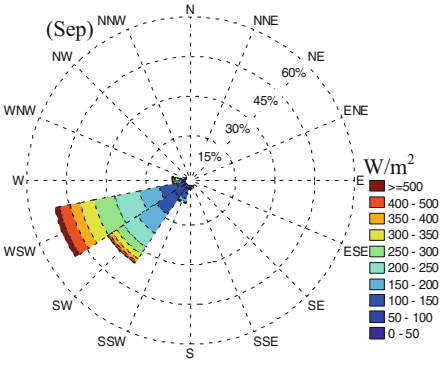
(Sep)
N
NNE
NE
ENE
E
ESE
SE
SSE
S
SSW
SW
WSW
W
WNW
NW
NNW
60%
45%
30%
15%
W/m2
>=500
400 - 500
350 - 400
300 - 350
250 - 300
200 - 250
150 - 200
100 - 150
50 - 100
0 - 50

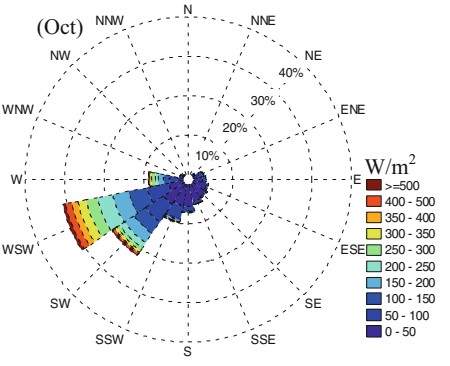
(Oct)
N
NNE
NE
ENE
E
ESE
SE
SSE
S
SSW
SW
WSW
W
WNW
NW
NNW
40%
30%
20%
10%
W/m2
>=500
400 - 500
350 - 400
300 - 350
250 - 300
200 - 250
150 - 200
100 - 150
50 - 100
0 - 50

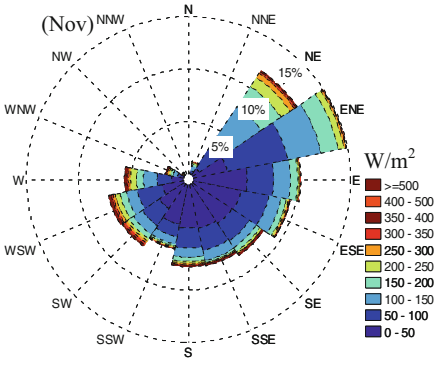
(Nov)
N
NNE
NE
ENE
E
ESE
SE
SSE
S
SSW
SW
WSW
W
WNW
NW
NNW
15%
10%
5%
W/m2
>=500
400 - 500
350 - 400
300 - 350
250 - 300
200 - 250
150 - 200
100 - 150
50 - 100
0 - 50

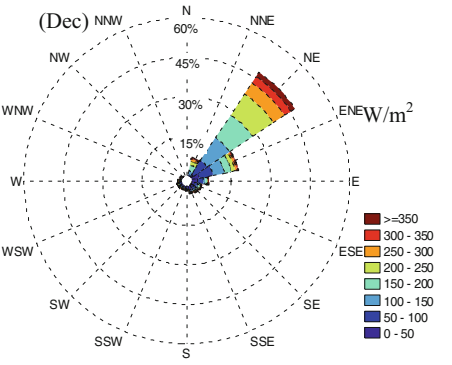
(Dec)
N
NNE
NE
ENE
E
ESE
SE
SSE
S
SSW
SW
WSW
W
WNW
NW
NNW
60%
45%
30%
15%
W/m2
>=350
300 - 350
250 - 300
200 - 250
150 - 200
100 - 150
50 - 100
0 - 50

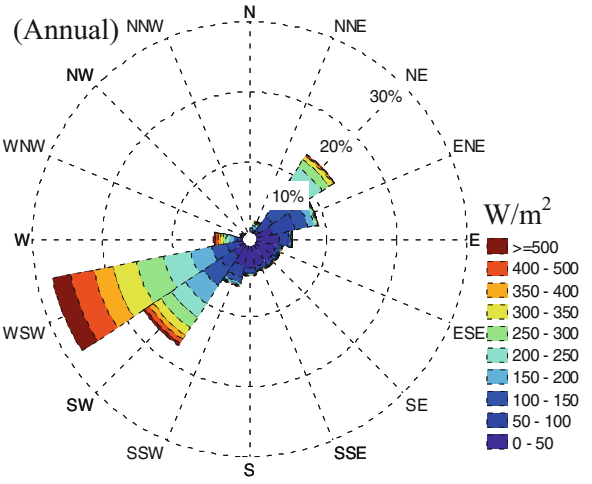
(Annual)
N
NNE
NE
ENE
E
ESE
SE
SSE
S
SSW
SW
WSW
W
WNW
NW
NNW
30%
20%
10%
W/m2
>=500
400 - 500
350 - 400
300 - 350
250 - 300
200 - 250
150 - 200
100 - 150
50 - 100
0 - 50

(5) Wave Energy Rose of the Sri Lanka Waters

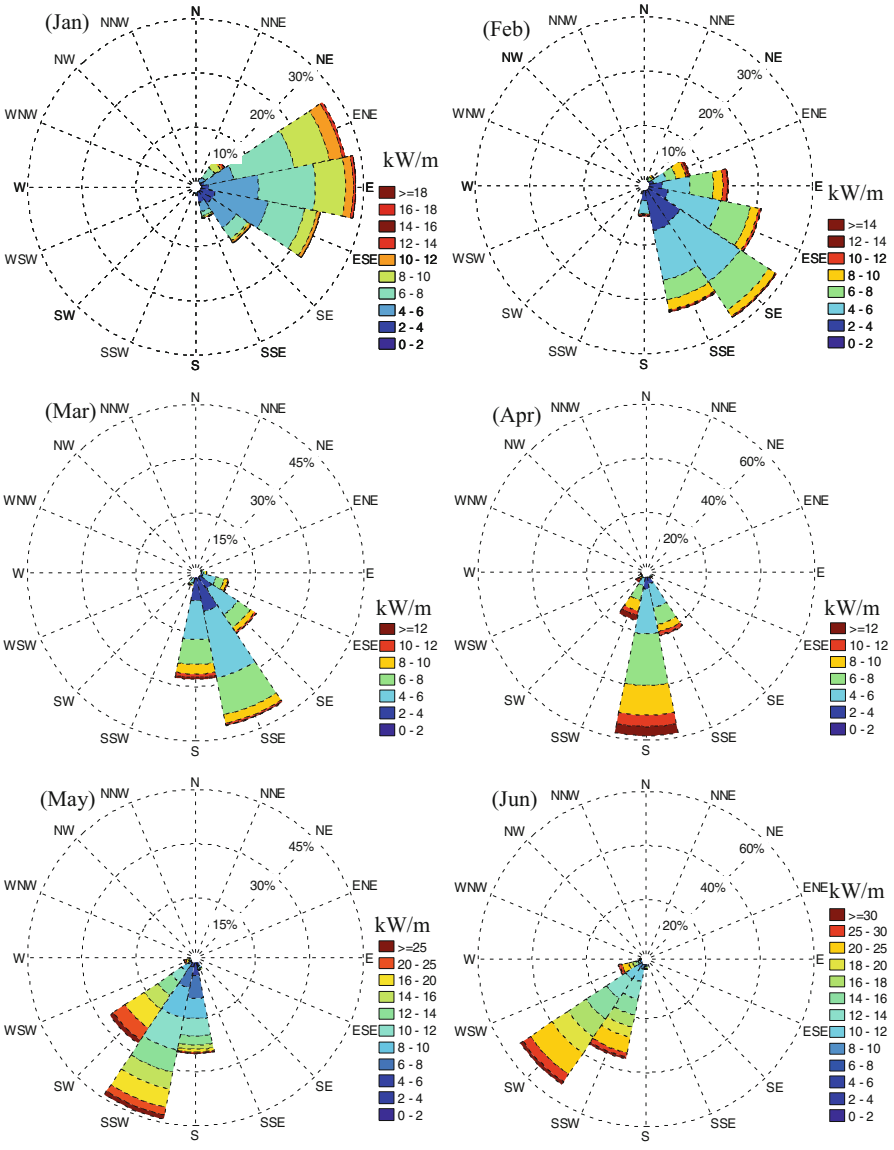

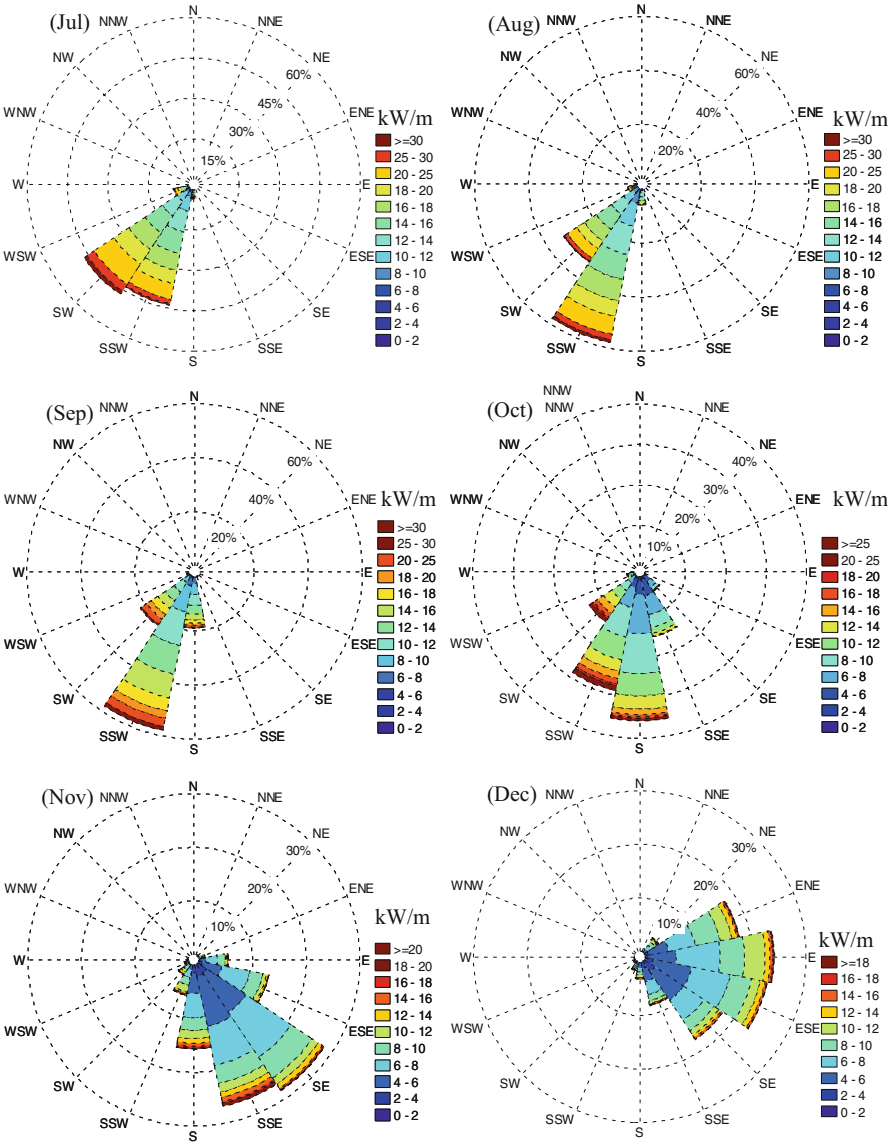
(Jul)
N
NNE
NE
ENE
E
ESE
SE
SSE
S
SSW
SW
WSW
W
WNW
NW
NNW
15%
30%
45%
60%
kW/m
>=30
25 - 30
20 - 25
18 - 20
16 - 18
14 - 16
12 - 14
10 - 12
8 - 10
6 - 8
4 - 6
2 - 4
0 - 2
(Aug)
20%
40%
(Sep)
(Oct)
>=25
(Nov)
>=20
(Dec)
>=18

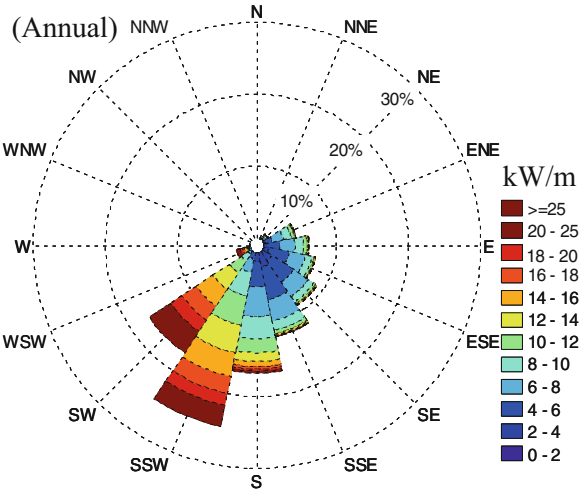
(Annual)
N
NNE
NE
ENE
E
ESE
SE
SSE
S
SSW
SW
WSW
W
WNW
NW
NNW
30%
20%
10%
kW/m
>=25
20 - 25
18 - 20
16 - 18
14 - 16
12 - 14
10 - 12
8 - 10
6 - 8
4 - 6
2 - 4
0 - 2